Can We Predict the Magnitude and Direction of Epistasis from Individual Allelic Effects?

Darcy Henderson

A thesis

Submitted to the School of Graduate Studies in Partial Fulfillment of the Requirements for the Degree Master of Science

McMaster University, Master of Science (2021), Hamilton, Ontario (Biology)

Title: Can We Predict the Magnitude and Direction of Epistasis from Individual Allelic Effects?

Author: Darcy Henderson, BSc Biotechnology and Molecular Bioscience, Rochester Institute of Technology

Supervisor: Dr. Ian Dworkin

Number of pages: 1-178

Abstract

Linking allelic variants to variation for complex traits has been a major focus in modern genetics. However, the ability to assess and predict how genetic factors influence complex traits (including human disease) requires an understanding of the specific genes that influence a trait, but also a broader understanding of the genetic architecture of complex traits. Epistatic interactions are crucial when mapping genotypic to phenotypic effects, as mutations in two (or more) genes can produce a phenotype that differs substantially from the expectation of the sum of individual effects. Epistatic interactions are both common and vary considerably in magnitude. Yet little current research focuses on identifying and predicting when mutations will have epistatic interactions and the extent of such effects. I examined the extent of epistatic interactions as a function of individual allelic effects (magnitudes) and wild-type genetic background using the *Drosophila melanogaster* wing as a model system. The aim of this research is to demonstrate whether individual mutational effects are predictive of the magnitude and direction of epistatic interactions. My results indicate 1) relationships between the average mutant effect and the resulting epistasis and 2) the genetic background can have a strong influence on epistasis.

Acknowledgments

Throughout the writing of this dissertation I have received enormous support and guidance.

I would first like to thank my supervisor, Dr. Ian Dworkin, for pushing me to think critically and teaching me a great deal about scientific research. His encouragement, patience and eagerness to help has been invaluable. He has shown me what a good researcher (and person) should be throughout this project. I would also like to express my deepest appreciation to my supervisory committee, Dr. Lesley MacNeil and Dr. Roger Jacobs, for offering their time and insightful perspectives.

I am grateful for my fellow Dworkin lab members Audrey, Caitlyn, Katie, Maria, and Sarah. I am thankful for the fun, emotional support and friendship. I would also like to extend my sincere thanks to Yun Bo Xi and Tyler Audet for their help with dissecting wings when I needed it the most.

Lastly, I would like to thank my family for their unwavering support and love. To my parents, I am profoundly grateful for the opportunities and experiences provided to me. I have always been pushed to be strong and go after things that inspire me. To Riley and the Kellies, I am appreciative of the warmth, kindness and constant laughs provided. To Eli, for always being an endless source of support and encouragement.

Contents

List of Figures

List of Tables

List of Abbreviations

aa – Additive by additive

ad – Additive by dominance

da – Dominance by additive

dd – Dominance by dominance

R – reference

a – Additive

d – Dominance

sd – scalloped

bx – beadex

bi - bifid

vg – vestigial

GWAS – genome-wide association study

QTL – quantitative trait locus

1. Introduction

1.1 Complex Traits are Complex

Complex trait variation is not explained by one or a small number of genetic variants, but rather a complex combination of genetic and environmental factors (Robinson, Wray, & Visscher, 2015). There is importance in understanding the genetic architecture of these traits to understand how variation at the genomic level is linked to phenotypic variation. While genome-wide association studies (GWAS) have allowed thousands of variants to be linked to traits (Robinson et al., 2015) , it still remains challenging and necessary to understand the genetic underpinnings of many complex traits. It is crucial to recognize that genetic architecture extends beyond just identifying single variants but additionally encompasses the number of variants influencing a phenotype, the magnitude of their effects on the phenotype, the population frequency of these variants, and notably the interactions among these variants with each other and their environment in terms of how they influence the phenotype (Timpson, Greenwood, Soranzo, & Lawson, 2017).

Evidence has shown that a particular "focal" mutation under study will not always have the same phenotypic effect in different individuals, and interactions between genetic variants modulate variation in penetrance and expressivity. A portion of this variation is explained by interactions between mutations and the genetic background in which they occur, also known as epistasis or genetic interaction (Domingo, Baeza-Centurion, & Lehner, 2019). It is apparent that the ability to assess and predict how

genetic factors influence complex traits requires an understanding of not only the specific loci that affect a trait but also an understanding of the genetic architecture of complex traits (Timpson et al., 2017).

This chapter will provide an overview of our current understanding of genetic interactions, specifically between two mutations (pairwise) and more (genetic background effects), the possible implications, and what our current knowledge tells us about the predictability of these interactions.

1.2 What is Epistasis?

Epistasis is a type of genetic interaction that has been used in many different contexts and to describe a variety of phenomenon since William Bateson originally defined the word in 1909 (Phillips, 1998). Do to the many distinct usages, there has been confusion by biologists from different disciplines as to what epistasis does in fact mean. William Bateson first defined the term after observing phenotypes from a series of dihybrid crosses and noting that the phenotypic ratios were altered from the expected 9:3:3:1 and, in some cases, novel phenotypes not seen in crosses with either individual single mutant were observed (Bateson, 1909). Bateson inferred that this was a result of a masking effect taking place where the allele of one gene prohibited the allele at another gene to manifest its phenotypic effect; much in the same way complete dominance involves masking of one allele by another. The mutation that “stopped” the phenotypic effect of other mutations was described as epistatic, and the mutations being blocked were said to be hypostatic. Qualitative, discrete differences in phenotypes illustrated that these mutations were interacting in some sense. In contrast, R.A Fisher defined a related term

"epistacy" in 1918 when he was able to show that one cannot always predict the quantitative phenotype of a particular two-locus genotype by merely adding the effect of the loci together (Fisher, 1918). Population geneticists quickly adopted the term epistasis to describe this phenomenon, and it became evident that many forms of genetic interaction can lead to epistatic "deviations". In the intervening years of study of genetics, epistasis has been used to describe three distinct things: functional relationships between genes, genetic ordering of pathways, and quantitative differences of allele-specific effects (Phillips, 2007). Making it necessary for researchers who work with epistasis to be incredibly clear (one hopes) in defining the type of gene interaction they are referring.

Phillips (2007) has condensed epistasis into three main categories to illustrate key differences between the various phenomena currently defined as epistasis. Functional epistasis describes the molecular interactions that proteins (and other genetic elements) have with one another. These interactions can occur within a single pathway or between proteins involved in a complex together. This type of epistasis describes a functional relationship that does not offer a direct genetic link. The term statistical epistasis is used when the average deviation of combinations of alleles at different loci is estimated over all other genotypes present in a population. This type of epistasis can be used to describe the deviation induced by substituting two alleles at different loci within a random individual within a population, after taking into account the expected effect of substituting each allele separately. Importantly measures of statistical epistasis are dependent on genotypic frequencies and thus is not simply a function of comparisons

among genotypes. Lastly, Compositional epistasis depicts the traditional Bateson definition of epistasis, which is the complete blocking of one allelic effect by an allele at another locus. For this type of interaction, one allele is substituted for another in a standard genetic background. Therefore, the effects of a specific genotype can be observed, and the influence that this specific genetic background has on these particular set of alleles. This can be expanded to include genetic interactions that include quantitative phenotypes and thus quantitative measures of interactions. This is also sometimes referred to as "physiological epistasis"(Cheverud & Routman, 1995). Additionally, this can be extended to include interactions beyond those shown with a double mutant homozygote. In my work, a compositional approach is used to observe the quantitative effects of allelic substitutions in two different wild-type genetic backgrounds.

Much like the definition of epistasis, terminology about epistasis can vary between scientific fields. Magnitude epistasis describes the situation where the phenotype associated with a double mutant deviates from the mutants' additive effects, but not in a way that will change the sign (or direction) of either allele's individual effect. For example, mutant X1 decreases wing size in *Drosophila* by 0.30mm, while mutation Y1 reduces wing size by an average effect of 0.20 mm. The double mutant X1Y1 is observed to have a wing size reduction of 0.40 mm, which is better (a smaller reduction) than the 0.50 mm reduction expected from the additive effects of the mutants. In this example, both mutant alleles have the same direction of effect, but the magnitude of these effects' changes when together. These interactions can be further classified into negative or positive epistatic interactions (Figure 1.1). When a double mutant has a less severe (or

more fit) phenotype than expected from the additive effects of the mutants individually it is referred to as *positive epistasis*. While *negative epistasis* defines an interaction when a double mutant's observed phenotype is more severe (or less fit) than what is expected. For *sign epistasis*, the sign (i.e. from deleterious to beneficial) of an individual alleles phenotypic effect changes in the presence another mutation. An example of sign epistasis when a mutation is beneficial individually, but it can act deleterious when in the presence of another mutation, and has been shown to be common among alleles that contribute to antibiotic resistance and their interactions with second site compensatory modifiers (Weinreich, Watson, & Chao, 2005).

Relative to haploid organisms, epistasis in diploids is further complicated by the presence of two alleles of each gene (and dominance between them). Therefore, epistasis can occur between loci and between the two copies of each locus in heterozygotes. In the absence of epistasis, mutations will act in an additive manner. Meaning that the estimates of additive and dominance effects for each locus are the same regardless of the genotype at a different locus. While in the presence of epistasis, both additive and dominance effects are dependent on the genotype of the interacting locus. Given this, genetic effects can be partitioned (and estimated) into eight different effects: additive and dominance effects for each locus and then additive-by-additive, dominance-by-additive, additive-by-dominance, and dominance-by-dominance epistasis (Figure 1.2).

Positive and Negative Genetic Interactions

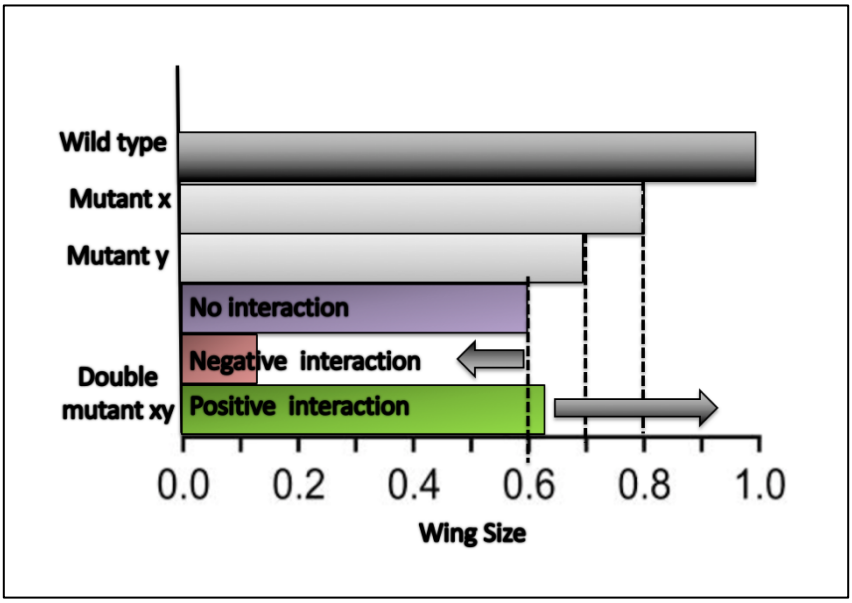

Figure 1.1: Types of genetic interactions. When mutant x and mutant y reduce wing size by 0.3mm and 0.20mm, the expected double mutant (xy) based on the additive effects of each individual mutant is a reduction of 0.50mm. A negative epistatic interaction occurs when the observed double mutant phenotype (wing size) is worse or smaller than expected (red). A positive epistatic interaction occurs when the double mutant phenotype is better or larger than expected (green). When the alleles act in a purely additive manner, there is no interaction (purple).

Four Different Types of Epistatic Interactions

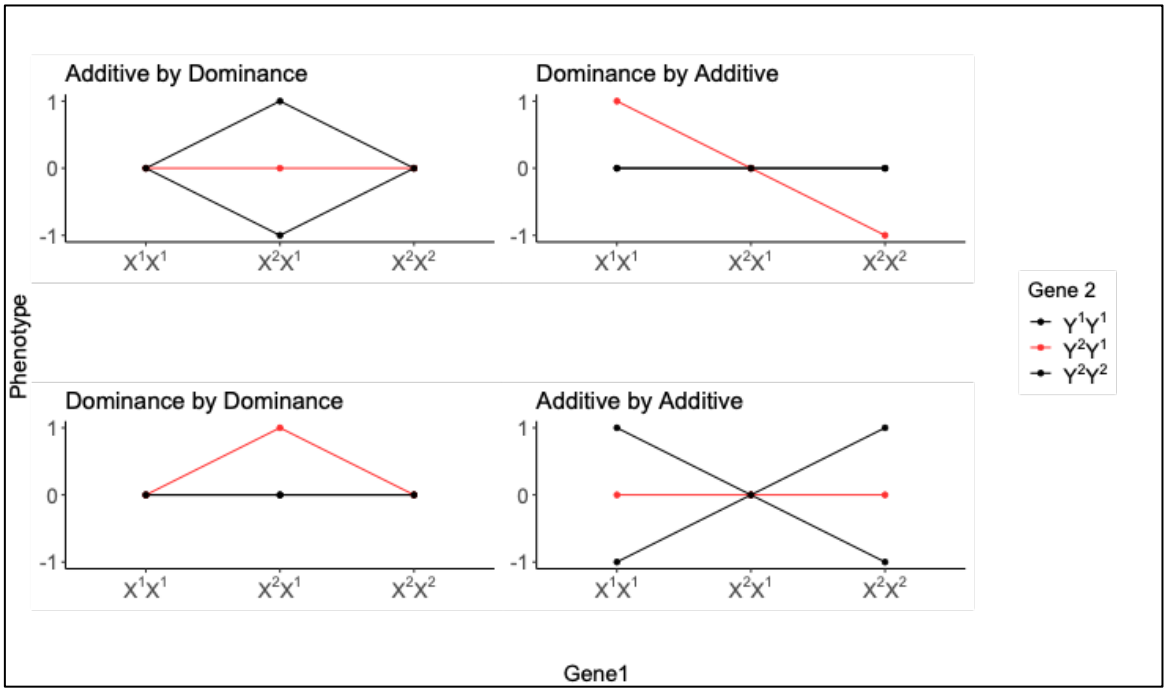

Figure 1.2: A graphical representation of some of the ways the different epistatic interactions can manifest. For additive-by-dominance, the additive effect of Y (black lines) is influenced by the dominance of X. For dominance-by-additive, the dominance effect of Y (red line) is impacted by the additive effect of X. For dominance-by-dominance, the dominance of Y (red line) is influenced by the dominance of X. Lastly, for additive-by-additive, the additive effect of Y (black lines) is influenced by the additive effect of X. Additive-by-additive can also manifest as changes in the same direction, but with differing slopes according to the genotype at gene 2.

1.3 The Prevalence and Relevance of (Pairwise) Epistasis

Research using natural, engineered and selected mutations has shown that epistasis is extremely common. Work by Costanzo et al. (2016) illustrated the abundance of epistatic interactions in *Saccharomyces cerevisiae* when examining temperature sensitive mutant alleles, carrying mutations that generally alter coding regions of genes. These temperature sensitive mutants were screened at a temperature where cells were viable but partially compromised for gene function and associated with a reduced growth rate. 23 million double mutants were constructed and 550,000 negative and 350,00 positive genetic interactions were identified. Elena and Lenski (1997) constructed 27 recombinant genotypes in *Escherichia coli,* and observed that 52% of random pairs of mutations tested showed epistasis for fitness. Similarly, Yamamoto et al. (2007), generated 105 double heterozygotes carrying p[GT1] transposon insertions in *Drosophila melanogaster.* 36% of the double heterozygotes had significant effects on startle-induced locomotor behaviour. Also in *Drosophila melanogaster*, 27% of random pairs tested for epistasis showed significant epistatic effects of quantitative traits affecting metabolism (Clark & Wang, 1997). Interestingly, these epistatic effects were large, but the individual mutations did not always have substantial individual (marginal) effects, exemplifying the importance of looking at the combined effects of mutations not just assessing them individually.

Modifier screens can identify second site mutations that modify the phenotypic outcome of a focal mutation. The starting material is a strain whose genetic composition causes a phenotypic defect. Second site mutations are then introduced (via crosses or

direct mutagenesis) and progeny are examined to determine if they enhance or suppress the starting phenotype (Jorgensen & Mango, 2002). A modifier screen was performed by Verheyen et al. (1996) to isolate modifiers of the eye phenotype caused by the expression of Notch in *Drosophila*. 137,000 individuals were screened, and 290 dominant modifiers were recovered. Many new alleles were recovered in previously identified genes in the Notch pathway, while new alleles of known genes not directly implicated in Notch signalling previously were also isolated. These results (as well as others) suggest that modifier screens are a successful tool used to identify missing components of genetic pathways (Johnston, 2002; Jorgensen & Mango, 2002). Modifier alleles may not have a phenotypic effect by themselves but can modify the phenotypes of other alleles. For example, Rutledge et al. (1988) examined the effects of 6 allele specific modifier genes on the expression of 18 modifiable alleles at 11 loci in *Drosophila melanogaster*. The 6 allele specific modifier genes had no visible mutant phenotype on their own, but a screen of 40,000 individuals illustrated the each of the 6 allele specific modifiers enhanced some phenotypes, suppressed others, and had no noticeable effect on others.

Genetic interactions have also been shown to be an important consideration when evaluating disease risk as mutations can affect the severity of a disease phenotype. In some rare cases, individuals have been reported where a single large effect mutation associated with severe disease outcomes showed no clinically relevant phenotypic effects. For example, individuals that are homozygous for a mutant allele in *DFNB26* have complete hearing loss. Yet, individuals in one family were carrying two copies of this deleterious allele have been identified with full hearing. These individuals were found to

have a secondary mutation, *DFNM1*, which protects against hearing loss (Riazuddin et al., 2000). Similarly, a screen of 874 genes in 589,306 genomes identified 13 adults with mutations associated with 8 severe Mendelian conditions, with no reported manifestation of the indicated disease (Chen et al. 2016). Suppression interactions are also of key importance in understanding how genetic differences can affect complex disease phenotypes, such as cancer progression. The growth defect caused by the absence of the tumor suppressor gene *BRCA1* in humans can be suppressed by the loss of either *53BP1* or *REV7* (Bouwman et al., 2010; Xu et al., 2015) It has also been shown that a cancer causing mutation can interact strongly with many mutations, having little effect individually, but lethal when combined (Ashworth, Lord, & Reis-filho, 2011). Epistasis has also been shown to be involved with other complex diseases, including cardiovascular disease (Y. Li, Cho, Wang, Canela-Xandra, & Luo, n.d.), diabetes (Wiltshire et al., 2006), autism (Mitra, Yeh, & Tsang, 2017), cleft lip and palate (Vieira, 2008), schizophrenia and other neurological disorders (Combarros, Cortina-borja, Smith, & Lehmann, 2009), and different types of cancer (X. Wang, Fu, Mcnerney, & White, 2014).

Based on the ease of isolating these interactions in model organisms and examples illustrated in disease severity, it seems probable that epistatic interactions are common, and important determinants for variation for complex traits. This is supported by research showing that epistatic interactions contribute to natural variation of traits and can explain significant proportions of otherwise unattributed variance within populations (Caicedo, Stinchcombe, Olsen, Schmitt, & Purugganan, 2004; Gaertner, Parmenter, Rockman, Kruglyak, & Phillips, 2012; Jarvis & Cheverud, 2011). Yet, the relative importance of

these non-additive interactions to the genetic contributions to complex traits and diseases remains controversial (Monnahan & Kelly, 2015).

1.4 The Genotype-Phenotype Map and Epistasis

The effects of epistasis can differ significantly in both magnitude and sign, but what remains unclear is why such a range is observed. Fundamentally, the work summarized in this dissertation is meant to address this question. Understanding what causes variation in epistatic interactions is essential to predict phenotypic effects from genotypic variation. In some cases, epistatic effects are highly specific to the alleles involved in the interaction and arise through the distinctive effects of particular combinations of mutations (Diss and Lehner, 2018). In such occurrences, resulting interactions may depend not only on the effect size (magnitude) of the mutations involved but also specifics of the alleles or genes involved. These specifics include, the three-dimension structure of proteins (Melamed, Young, Gamble, Miller, & Fields, 2013), and changes in physical interaction affinity and specificity (Ortlund, Bridgham, Redinbo, & Thornton, 2007). This is illustrated when observing the consequences for two mutations in human protooncogenes FOS and JUN on the formation of the AP-1 transcription factor complex (Melamed et al. 2013). The Glu residue in position 3g of Fos establishes a salt-bridge with the Arg residue in position 4e of Jun. Individual mutations Glu3gLys and Arg4eGlu destabilize the interaction between Fos and Jun by replacing the salt-bridge by repulsive electro-static interactions. However, when these two mutations are combined,

they are able to compensate each other by recreating the salt-bridge (Melamed et al. 2013).

In other cases, genetic interactions may emerge from the quantitative nonlinearity between gene activity and the phenotype. This may make it possible to predict the effects of individual mutations on epistatic interactions without knowing the molecular identity of the mutations involved in interactions. One of the first major insights of nonlinearity was illustrated when examining dominance (Ford, 1907; Kacser & Burns, 1981; Wright, 1934). A nonlinear relationship occurs between gene activity and phenotype, such that a fractional change (i.e. the same delta) in gene activity may have different consequences depending on the form of the curve. Kacser and Burns (1981) illustrated a non-linear relationship between gene activity and phenotype and show that dominance is not a property of genes but explains a relationship of the phenotype between genotypes. More specifically as a form of interaction among alleles within a gene. Nonlinearity is an abundant feature in development, with examples occurring for ligand binding (Gonze & Abou-Jaoudé, 2013), transcriptional regulation (Frank, T. D., Cavadas, M. A. S, Nguyen, L. K. & Cheong, 2016), diffusion of morphogens (Lander & Nie, 2002), and importantly continuing to describe quantitative relationships between gene activity and phenotypic outcome. For example, Green et al. (2017) manipulated gene dosage of *Fgf8*, a regulator of mouse development, and demonstrated that variation in activity in this signaling molecule has a nonlinear relationship to phenotypic variation. Similarly, Barkoulas et al. (2013) showed that the system for cell fate specification in the *C. elegans* vulva could tolerate a 4-fold variation in the genetic dose of an upstream signaling model, *LIN-*

3/EGF, without a phenotypic change in cell fate pattern. Interestingly, this work also exposed an epistatic relationship between *EGF* and *Notch* when combining dosage perturbations in the two pathways; overexpression of *EGF* switched the function of *Notch* from lateral induction to induced lateral cell inhibition.

Changes in gene expression can alter the effects of mutations and importantly how mutations interact whenever the relationship between gene expression and phenotype is nonlinear. Given that sigmoidal relationships are commonly observed between gene expression and phenotype, switches in interactions between mutations should be expected when the expression level of a gene changes. Li et al. (2019) introduced random mutations into the DNA binding domain of the phage lambda repressor and examined the ability of each genotype to repress expression of a fluorescent protein. When observing how mutations combine at different expression levels, they saw that a change in mutant expression transformed the magnitude of genetic interaction and the direction of the interaction. For example, a genetic interaction can be suppressive at one expression level but can enhance at another expression level. While this work focusses on the phage lambda repressor, these conclusions are likely to apply to many genes. This work also suggests that changes in gene expression alone will facilitate changes in genetic interactions.

Nonlinear relationships between changes in free energy and the activity of individual proteins and complexes can arise due to the thermodynamics of protein folding (Tokuriki & Tawfik, 2009) and molecular interactions (Diss et al., 2018). Similarly, regulatory systems have steep sigmoidal dose-response functions because of cooperativity

molecular titration and feedback (Gjuvsland, Hayes, Omholt, & Carlborg, 2007) , (Gjuvsland, Plahte, & Omholt, 2007). The kinetic coupling of enzymes can also generate non-linear relationships between gene expression and phenotype (Kacser & Burns, 1981). While previous work has provided insight into the shapes of genotype–phenotype relationships and the mechanisms that cause them, it is unclear how these shapes and mechanisms extend to genetic interactions.

Epistasis is a ubiquitous component of genetic architecture, but it remains unknown to what extent these interactions are necessary to make accurate predictions. Evidence has shown that many QTLs' effects might be masked by interactions with other loci which can make mapping difficult. For example, Carlborg et al. (2004) examined the genetic basis of chicken body size and only one QTL seemed to have a weak effect. However, when looking at epistatic interactions they were able to identify five more genomic regions associated with significant growth effects. Similarly, Stylianou et al. (2006) examined QTLs for obese mice and found epistatic interactions that showed interacting networks of multiple genes play a significant role in body weight. Illustrating not only the importance of epistasis in the prediction of complex traits, but that epistasis can reveal networks of interacting QTL. Interestingly, Forsberg et al.(2017) showed that not only are genetic interactions common, but that they are key part of genetic architectures of multiple complex traits in a yeast population. They were able to show how interactions effect model estimations and how understanding this relationship improves trait predictions.

Epistatic interactions have also shown to be important consideration when investigating drug resistance. A noteworthy example of this is shown when looking at influenza's main treatment (Domingo et al., 2019). Oseltamivir is an antiviral that blocks the active site of the neuraminidase enzyme necessary for viral replication. In clinical trials, researchers detected a mutation, H274Y, that generated resistance to this drug. However, this mutation led to attenuated viruses and it was concluded that this mutation was not clinically relevant. However, eight years after this drug was introduced, antiviral-resistant strains appeared with the mutation H274Y. This mutation was no longer deleterious (to the virus) in newly evolved strains as the virus acquired additional mutations that suppressed the deleterious effects of H274Y(Moscona, 2009). A frightening example of the consequences epistatic interactions can have in human health and reinforces the importance of investigating how mutations in pathogens interact.

While epistatic interactions can have detrimental implications, there have been efforts to use these interactions to our advantage. Synthetic lethality is an extreme negative genetic interaction where the inactivation of two genes individually has little effect on viability, but the combination of both genes leads to cell death (Ashworth et al., 2011). This has been of interest of cancer drug companies as it allows for targeted therapies that kill cancer cells that lack a specific tumor suppressor gene but spare normal cells. For example, a BRCA1 mutant cell and a pharmacological inhibition of another leads to death, while normal cells (which lack the BRAC1 mutation) are not affected by the effect of the drug (Nijman & Friend, 2013).

1.5 Genetic Background Effects

It has been shown that the genetic context of a mutation can have substantial effects on a phenotype, a phenomenon known as genetic background effects (Chandler et al., 2017). The interaction of mutant alleles with naturally occurring variants throughout the genome, creates substantial variation in phenotypic expressivity and penetrance. Genetic background effects occur across a range of taxa and mutant classes, proving to be a pervasive feature of the genetics of all living systems. Dowell et al. (2010) performed a systematic deletion of 5100 genes in two distinct strains of *Saccharomyces cerevisiae* and identified essential genes for viability. When scoring colonies as dead or alive, they observed that 894 genes were essential for viability in both S288c and Σ1278b. While 44 genes were essential only in Σ1278b, and 13 genes were essential in S288c, thus identifying "conditional essentials". Such results suggest that inferences from one strain may not be generalizable to other strains as mutant phenotypes can change drastically by segregating allelic variation among wild type genetic backgrounds. Toivonen et al. (2007) examined longevity in *Drosophila*. When using an *Indy* mutation previously linked to longevity as a control, they discovered that the mutation did not increase longevity when the wild type genetic background is altered. Again, illustrating how our genetic inferences can change drastically when accounting for genetic background effects. In this instance it led to a misleading appearance of a single gene effect. Illustrating that genetic interactions of genes under study with other variants in the genome can have a larger effect than the

effects of the mutations under study. Comparisons across species, conditions, time and cell types have repeatedly found that genetic interactions are plastic, changing in different cells and conditions (Li et al. 2019).

It also has become apparent that genetic background effects extend to genetic interactions. Remold and Lenski (2004) examined the effects of 18 random insertion mutations in *Escherichia coli* in two environments and five genetic backgrounds. Half of the mutations had epistatic interactions that varied among genetic backgrounds in an environment-dependent manner. Similarly, two beneficial mutations examined in two strains of *Escherichia coli* were found to have background dependent interactions. Notably, interactions between the focal mutations and background specific modifiers were common, but also the interactions between the two focal mutations varied in a background dependent manner (Wang et al. 2013). Background effects were also shown to extend beyond single mutations when Dworkin et al. (2009) revealed a background-dependent epistatic interaction between two mutations in *Drosophila melanogaster* influencing wing size. These studies reinforce that the phenotypic effect of a mutation in a given background can depend on an individual's genotype at a potentially large number of loci that interact in complex ways. Therefore, not only are pairwise interactions important for determining phenotypic variation but so are higher order level interactions.

In addition, what appear to be gene-gene interactions in a specific experiment can become gene-gene-environment-genetic background interactions when additional experiments are performed. For example, environmental influences of epistasis have also been observed in phage (You & Yin, 2002), bacteria (Remold & Lenski, 2004b) and yeast

(Musso et al., 2008). An excellent example of this is shown in a yeast study that examined interactions between polymorphisms influencing sporulation efficiency in crosses that generated 32 yeast strains and saw a direct change across 8 environmental conditions (Gerke et al 2010). These strains differed by four nucleotide changes in three transcription sites, illustrating that a small number of nucleotides can create complex, quantitative variation in phenotype.

A central goal in genetics is the identification of variants that influence susceptibility to disease. Most statistical modeling approaches currently used, including polygenic risk scores, consider just the additive contribution of allelic effects for simplicity. For instance, the common-disease-common variant hypothesis predicts that disease-causing variants will have a small additive or multiplicative effect on the trait or disease phenotype (Blanco-Gómez et al., 2016). However, association studies have often failed to account for observed heritability of diseases and traits, a problem known as missing heritability (Zuk, Hechter, Sunyaev, & Lander, 2012). An example of this can be illustrated when looking at the risk associated loci for Crohn's disease. GWAS has identified 71 associated loci, yet under the assumption that disease arises from an additive genetic architecture, these loci account for 21.5% of the estimated heritability of the disease (Zuk et al., 2012). To account for this missing heritability, explanations have been proposed: (1) There are larger numbers of variants of smaller effect that are yet to be found. (2) Rare variants of large effect are yet to be detected. (3) Shared environment among relatives has yet to be accounted for in these association studies. (4) Genetic interactions (epistasis) has not been embraced in models (Algahtani, Aldarmahi, Al-

Rabia, & Yar, 2013).

It is easy to find variation in the human genome as it can differ at millions of sites (Abecasis et al., 2011). Thousands of variants affect the copy number of large, multi-kilobase segments (Handsaker, Korn, Nemesh, & Mccarroll, 2011). There are also about a hundred gene disrupting variants, ranging from large deletions to single nucleotide polymorphisms (MacArthur et al. 2012). Additionally, we have thousands of variants that affect expression of nearby genes and sets of regulatory variants acting in different tissues (Nica et al., 2011). Lastly, thousands of protein coding genes possess missense variants that may influence their function in complex ways (Abecasis et al., 2011). These examples show that it is easy to find variation in our genomes. However, it makes it difficult to truly identify what variants matter in terms of contributing to complex traits. We know that these variants interact in complex ways with each other and with focal mutations, and as such it is vital to establish how often higher-order interactions account for phenotypic variation between individuals. Epistasis detectable in an individual could differ significantly from the population level measurements. This has the power to complicate the detection of epistasis in human association studies.

While previous work has exposed some insight into the way context-dependence affects allelic expressivity, many unknowns remain. Critically, how context-dependence affects genetic interactions and if the influence of genetic background can be predicted for genetic interactions. Chandler et al. (2017) explored how genetic background effects impact phenotypic expressivity of allelic series for two genes in the *Drosophila* wing network, *scalloped* and *vestigial*. Intriguingly, they observed that alleles with moderate

effects had the greatest background dependence, while alleles with weak or strong effects had considerably less background dependence. An essential outcome from this work is that the magnitude of the individual allelic effect influences the allele's sensitivity to genetic background, such that the impact of genetic background may be predictable. The results from this work suggest that alleles with moderate effects are most sensitive to the impact of other variants across genetic backgrounds. Whereas alleles with strong effects are less affected by modifiers in the genetic background as strong allelic effects leave little room for variability. Similarly, alleles with weak effects are less affected by other variants in the background as they only slightly perturb the network and are well above the required gene dosage threshold. While this work does an excellent job illustrating the predictably of individual alleles, it is unclear how this predictability extends to epistatic interactions.

1.6 Measuring Epistasis

It has been proven difficult to detect epistasis in quantitative genetic studies as gene effects may only be detected in an experimental framework that accommodates epistasis, otherwise those interactions could be confounded with the main (additive) effects. For example, an alleles' biological effect might be too small to detect with any statistical power and sample size, but it might be a critical epistatic modulating allelic effects at a second gene. If a mutation functions through a complex mechanism that involves multiple genes, the effect might be missed if the gene is examined in isolation without allowing for its potential interactions with other unknown factors. Due to the

challenges of detecting epistasis there has been motivation to develop new analytical approaches that help detect these interactions (Boucher & Jenna, 2013; Mafhukar, Elemento, & Pandey, 2015; Uppu, Krishna, & Gopalan, 2018). In some cases, the motivation is to increase the power to detect effects (Kraft, Yen, Stram, Morrison, & Gauderman, 2007), in other cases the motivation is to detect statistical interactions that are informative about the biological and biochemical pathways involved in complex traits (Moore, 2003).

While epistasis has proven to be an important part of the genetic architecture of complex traits, the link between statistical estimates of epistasis to molecular interactions remains largely unknown. In the statistical sense epistasis is the deviation from additivity between the effects of two mutations but what does this mean in terms of biological function? Epistatic effects estimated in a standard linear model (regression framework) are statistically well defined, can be estimated with standard techniques and the properties of these estimates are well understood. However, it is not always clear how epistasis components connect to biological mechanisms. We need to identify types and patterns of epistasis that are biologically relevant, but it is not always clear what those patterns mean.

Data transformations are necessary in data analysis as the appropriate scale of effect aids in biological interpretations. The choice of scale can become important when measuring epistasis as mutations that are additive for a phenotype measured on one scale may not be additive when a different transformed scale is used (Frankel & Schork, 1996). For example, a wildtype individual may produce an average phenotypic value of 1.0, a heterozygote produces a phenotypic value of 2.0, and the homozygote produces a value of

4.0. This appears to be a non-additive relationship as the difference between the heterozygote and the homozygote is greater than the difference between the wildtype and heterozygote. However, when transformed on a log scale the phenotypic values are 0, 0.30 and 0.60. This relationship would then appear to be additive. This is an example on how the scale effect could lead to an inference that epistasis is present when it may not be. If a transformation can eliminate a statistical interaction, we have no reason to think that it reflects a mechanistic reality (Wagner, 2015). Two scales that will be used in this thesis are square root and logarithm of the measured trait (wing area). Square root is a measurement scale and easy to interpret as it has units of length. In addition, a square root transformation to wing area measurements compresses high values and low values become more spread out. Mutants can have a range of mutant effects ranging from weak to severe phenotypic effects. This transformation increases the relative difference between observations of large values (weak to moderate mutants) while increasing these relative differences for small values (severe mutants). While log transforming data compresses high and spreads low values by expressing the values as orders of magnitude. It is important to consider whether we know enough biologically to know the scale effects that are relevant to our questions. This is crucial to make statistical and functional interactions mechanistically meaningful. It is clear that scale choice is important, but it is not always clear on what is best to use. It is also important to note that it may not be possible to compare properties of genetic architectures across species and populations measuring epistasis unless they are on a common scale.

1.7 Outstanding Research questions

Understanding how loci interact is vital to understanding how variation at the genomic level is linked to phenotypic variation. However, before such an understanding can be reached there are several outstanding questions regarding epistasis that remain. Firstly, can differences between the magnitude and the sign of epistatic effects be explained solely through the distinctive effects of particular combinations of mutations, or can such differences be explained by the quantitative nonlinearity between gene activity and the phenotype. Consequently, the magnitude of the individual mutants may make it possible to predict the effects of individual mutations on epistatic interactions without knowing the molecular identity of the mutations involved in interactions. Specifically, can the relationship between gene activity (via magnitude of mutational effects) and phenotype explain which mutant combinations will have positive or negative, or strong vs weak epistatic interactions. Examining this relationship will not only allow predictions for which mutations will show interactions and how, but also may give insight into a model for how alleles interact.

In addition, it is important to identify how genetic interactions vary as a function of genetic background. Therefore, the context dependent nature of genetic interactions needs to be explored as this will allow for identification of any patterns or relationships between genetic background and genetic interactions.

The majority of studies that have examined epistasis use high throughput approaches that observe interactions between gene deletions mutants and common

deletion backgrounds. Indeed, these approaches can provide important outcomes and give some understanding on how complex gene networks build robustness (Hartman, Garvik, & Hartwell, 2016), but results are often largely qualitative (Segrè, DeLuna, Church, & Kishony, 2005), and the distribution of epistatic effects observed might not reflect what would be observed with alleles differing in magnitude, in particular for allelic series within a gene. Therefore, is it crucial to examine epistatic interactions with alleles of differing severity, as there is no reason to assume that all forms of epistasis will be revealed by null mutations.

1.8 Project Overview

For the first part of my project, I generated a large series of crosses and genetic interactions were estimated as a function of the magnitude of individual allelic effects and genetic background using the *Drosophila melanogaster* wing as a model system. This system has proven to be a good model when examining epistasis as previous work has demonstrated that genes involved in the wing development network show substantial amounts of epistatic interactions (Gilchrist & Partridge, 2001; Roch, Baonza, Martin-Blanco, & Garcia-Bellido, 1998; Sturtevant, Roark, & Bier, 1993). Weak, moderate, and severe mutations in the *scalloped* gene have been used in combination with mutations in *beadex (bx)*, *vestigial (vg)*, and *bifid/Omb (bi),* as these genes interact with the *scalloped* protein or with genes known to be regulated by the *scalloped* protein (SD). In addition, the gene pathway for wing development has been well characterized (Connahs, Rhen, & Simmons, 2016) as shown in (Figure 1.3)**.** *Drosophila* wings can be easily dissected and

changes in wing size can be readily quantitatified. Genes chosen in the pathway offer an allelic series, meaning that known mutations exist for each gene with a range of phenotypic severity. This allows for the relationship between gene activity and phenotype to be examined for these genetic interactions. These mutant combinations were examined in two wild type genetic backgrounds, Samarkand (SAM) and Oregon- R (ORE). These are two common lab wild-type strains that have previously illustrated genetic background effects for single alleles and genetic interactions (Chandler et al., 2017; Chandler, Chari, Tack, & Dworkin, 2014; Dworkin et al., 2009). Therefore, they were rational choice to explore these relationships further.

The second part of my project is an extension of Chari and Dworkin (2013) that examined modifiers of sd^{E3} in Samarkand and Oregon-R. The results from this work illustrated that ~74% of all identified modifiers of sd^{E3} are background dependent. These results suggested that Samarkand and Oregon-R vary in sensitivity to mutational perturbations, as well as having strain specific responses to modifiers. The majority of background effects changed the magnitude of modifier effects, however there were examples where the deletion modified the phenotypic expressivity of sd^{E3} in opposite directions. For example, a deletion suppressed the sd^{E3} phenotype in Samarkand, but the same deletion enhanced the sd^{E3} phenotype in Oregon-R. Using a subset of these previously identified modifiers (co-isogenic deletions) used in Chari and Dworkin (2013), we examined how background dependence changes and how the magnitude of modifier effects changed when using *scalloped* alleles differing in magnitude of phenotypic effects. For example, does the background dependence of modifiers decrease when using

a weaker *scalloped* allele? Do we see larger magnitude of modifier effects for moderate *scalloped* alleles? To address these questions, we examined the combination of various *scalloped* alleles with molecularly defined deletions in two genetic backgrounds, Samarkand and Oregon-R.

The Drosophila Wing Network

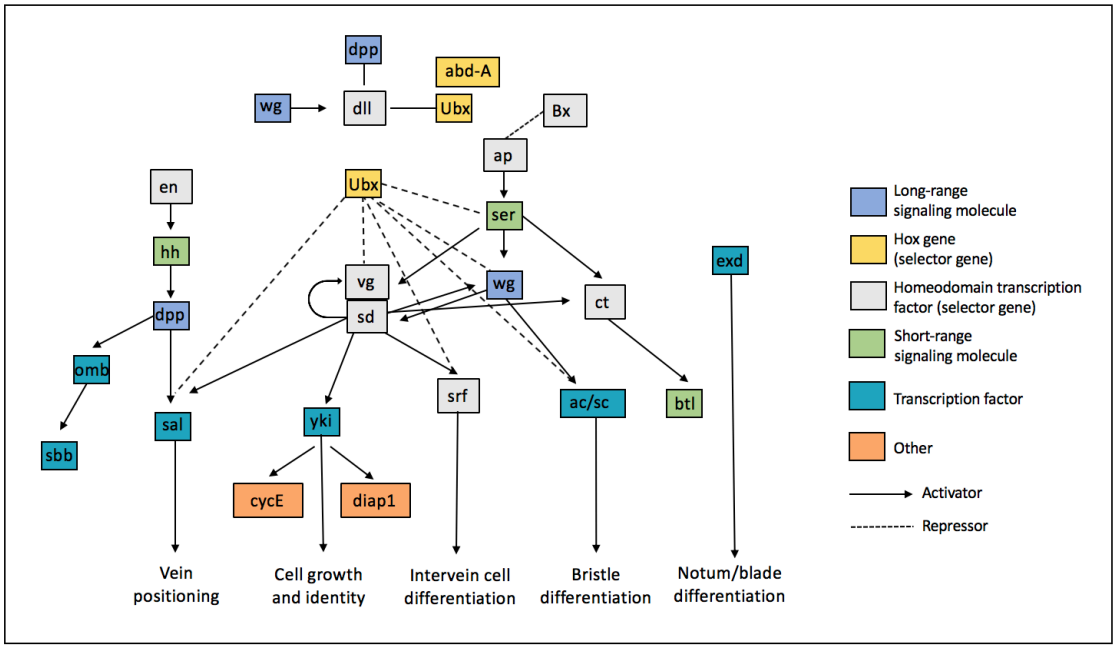

Figure 1.3: A simplified view of the genetic pathway for *Drosophila* wing development. Figure by Caitlyn Daley adapted from "Transcriptome analysis of the painted lady butterfly, Vanessa cardui during wing color pattern development" by Coonahs, Rhen, & Simmons, 2016,. *BMC Genomics*, *17*(1), 1–16.

1.9 Key Genes

The development of the *Drosophila* wing is governed by the action of two long range signaling proteins encoded by *decapentaplegic* (*dpp*) and *wingless* (*wg*) (Nellen, Burke, Struhl, & Basler, 1996; Zecca, Basler, & Struhl, 1996). These genes are expressed at the borders of the anterior/posterior (A/P) and the dorsal/ventral (D/V) compartments and promote cell proliferation and pattern of the wing (Resino, Salama-cohen, & Garcı, 2002). *Scalloped* (*sd*) and *vestigial* (*vg*) are also main players in this gene network as the expression of these is crucial for wing development. *sd* encodes a transcription factor that encodes a TEA protein with a DNA binding domain and its activity regulates the cis-regulatory elements of genes that promote wing growth and morphogenesis (Lunde et al., 2003). Sd has two coactivators, Vg and Yorkie (yki) (Guss et al., 2014). The VG-Sd complex is necessary for wing development (Simmonds et al., 1998), while the latter Yki-Sd complex is crucial for wing growth and proliferation (Bandura & Edgar, 2008). Importantly the Sd-Vg heterodimer regulate transcription of both *sd* and *vg*. Specifically, Sd is needed for early *vg* expression, while Vg is needed to maintain *sd* expression (Bray, 1999). *sd* and *vg* are expressed at low levels during the second larval instar in the wing imaginal disc but as development continues into third instar the expression of both increases and they become well defined in the progenitor cells of the wing margin via induction by Wg (Paumard-Rigal, Zider, Vaudin, & Silber, 1998; Simmonds et al., 1998). In late third instar wing discs *sd* and *vg* expression continues to increase and extend to the primordia of the wing pouch and hinge regions (Simmonds et al., 1998). Sd and Vg then direct wing development as a dimer activating the transcription of several target genes.

For example, this complex drives cell cycle progression by inducing expression of the *dE2F1* transcription factor, which regulates genes involved in DNA replication and cell-cycle progression (Delanoue, Legent, Godefroy, & Flagiello, 2004).

Sd also regulates cell growth and proliferation with its complex with Yki in the hippo signalling pathway. Yki is downstream of the hippo signalling pathway, which controls cell proliferation and cell apoptosis (Goulev, Fauny, Gonzalez-marti, Flagiello, & Silber, 2008). In the absence of hippo signalling, Yki binds with sd in the nucleus where it induces cell proliferation and inhibits apoptosis by regulating the activity of genes downstream. In the presence of hippo signalling, Yki is transported into the cytoplasm and is inactivated as a result (Goulev et al., 2008) .

Beadex (Bx) has shown to regulate Apterous (Ap) levels (Milan, Diaz-benjumea, & Cohen, 1998). The LIM-homeodomain protein Ap is a selector gene for the dorsal compartment wing imaginal disc (Cohen, Mcguffin, Pfeifle, Segal, & Cohen, 1992). An additional LIM-homeodomain protein, Chip, is a cofactor for Ap (Morcillo, Rosen, Baylies, & Dorsett, 1997). When Bx is overexpressed it binds Chip, interfering in the complex between Ap and Chip. Therefore, Bx and Ap look to function in an antagonistic feedback loop to regulate *ap* expression. The binding of Chip to Ap is necessary for *ap* expression and the formation of the D/V boundary as they form a functional complex (Cohen et al., 1992). Gain of function mutations in *bx* reduce *ap* expression, while loss of function mutations increases *ap* expression. Therefore, Mutant phenotypes for *bx* overexpression mutants are due to Ap loss of function (Sorrosal, Bejarano, & Luque, 2008). Loss of function of Ap is detrimental as the binding of Chip to Ap is crucial for Ap

stability (Weihe, Milán, & Cohen, 2001). While selector genes are often though of as a switch, the Chip and bx interaction illustrates that this process is complex and that Ap levels are modulated during wing development (Weihe et al., 2001).

Along the A/P the precise expression of *dpp* and its receptors is required for the transcriptional regulation of specific target genes (Entchev, Schwabedissen, and Gonzalez-Gaitan, 2000). *Bifid* (*bi/omb*) is a target gene of Dpp that encodes a T-box transcription factor modulating cell proliferation, viability and cell migration (Shen, Dorner, Bahlo, & Pflugfelder, 2005). The expression of *thickveins*(*tkv)* is reduced in *dpp* producing cells along the A/P boundary by the transcription factor *master of thickness* (*mtv*) (Rogriguz, Felix, & Diaz-Benjumea, 2001). *tkv* and *mtv* are upregulated in *omb* mutants and it appears that Omb is required for Mtv to repress *tkv*. Lack of *omb* leads to cell death in its expression domain which leads to misactivation of the notch pathway and overproliferation of lateral wings (Rogriguz et al., 2001). In addition, Omb is required for the expression of dpp targets spalt *(sal*) and *vg* (Tabata, 2001). While more work needs to be conducted in determining the role that Omb has in wing development, it seems probable that Omb helps in maintaining the A/P boundary and that target genes much exist in this process.

2.0 Hypothesis and Predictions

My primary hypothesis is that there is a relationship between the type and magnitude of genetic interaction and individual magnitude of effect (severity) of alleles. Additive genetic interactions will occur most frequently between weak alleles. This is

anticipated as previous research and models have shown that alleles of weak effect tend to act in an additive manner (Mackay 2014). Epistatic interactions will occur most frequently between alleles of moderate and strong severity. Alleles of strong effect will disrupt the system so greatly that they will completely mask the effect of a second allele, similar to complete dominance. While epistatic interactions are predicted to occur when alleles of moderate effect are involved, specific predictions about the type or magnitude cannot be made. Figure 1.4 illustrates how negative epistasis may arise between two moderate alleles. Two mutations may decrease tissue growth individually, and a double mutant with these mutations have an additive effect on gene expression, but reduction for tissue growth is more than expected from the additive phenotypic effects of the individual mutants.

It is also predicted that the degree of background dependence for genetic interactions will be predicable by the magnitude of individual allelic effects involved in the interaction. Genetic interactions involving alleles of weak effect will be more robust and have less context dependence than alleles of moderate effect. In addition, there will be interesting and important genetic background effects when alleles of moderate effect are combined in a double mutant as slight changes in gene activity will have a stronger impact on the resulting magnitude and type of genetic interaction due to the predicted nonlinearity between gene activity and phenotypic outcome (illustrated in Figure 1.5) Two mutations may decrease tissue growth individually to varying degrees in two different genetic backgrounds due to differences in gene expression. Therefore, the gene expression of the double mutant with these mutations is also different between the two

backgrounds and as a result the phenotypic outcome is different. Lastly, genetic interactions involving alleles of strong magnitude will not show strong background dependence, as the gene activity for these alleles is so low that slight changes in gene activity will not affect phenotypic outcome.

Moderate Alleles Predicted to Have Negative Epistatic Interactions

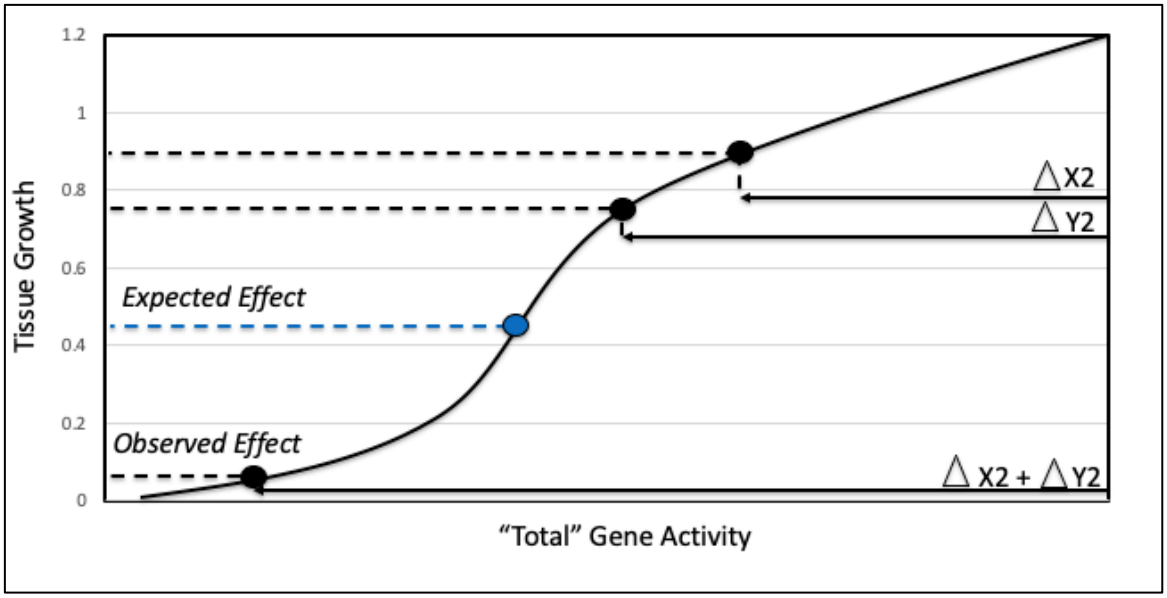

Figure 1.4: Negative epistasis generated from moderate alleles. The effect of mutation X2 and the effect of mutation Y2 may have an additive effect on gene expression but the phenotype (tissue growth) is more than the additive effects of the mutants.

Genetic Background Effects Predicated to Be Stronger with Moderate Alleles

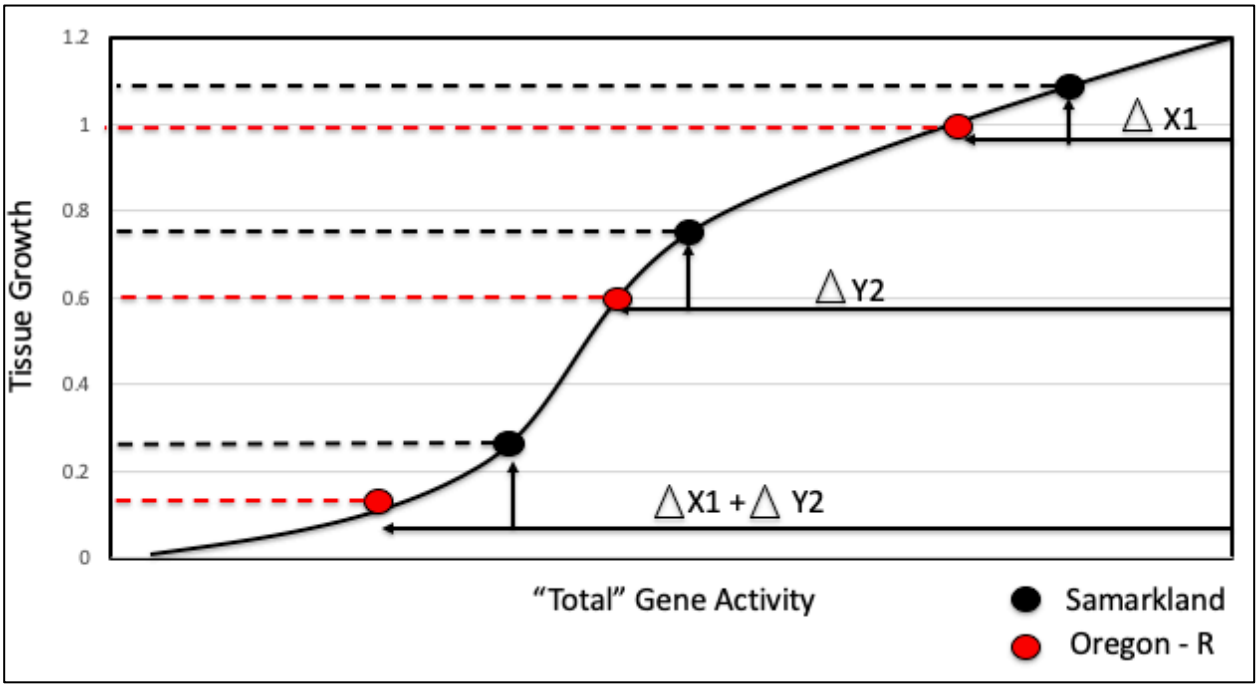

Figure 1.5: Genetic background effects for epistatic interactions with moderate alleles. This figure illustrates changes in the effects of variants X1 and Y2 due to variants in the genetic background. The resulting total gene activity changes, which in turn affects the phenotypic outcome and the magnitude of the genetic interaction.

2. Methods

Experimental Methods

Table 2.1:Summary of *scalloped* mutant alleles.

Allele	Allele Strength	Allele Class	Mutagen	DNA Lesion	Description of Allele	Reference
29.1	Weak	Hypomorph	P-element insertion	Insertion in the first intron after the translation start site, close to 5`-splice site	Homozygotes show minor scalloping at the posterior wing margin.	(Shyamala & Chopra, 1999)
1	Weak	Hypomorph	X-ray	Polytene chromosomes normal.	Homozygotes have weak scalloping and gaps in bristles at wing margin.	(Campbell, Duttaroy, Katzent, & Chovnick, 1991; Paumard-Rigal et al., 1998)
ETX4	Moderate	Hypomorph	P-element insertion	Insertion ~ 400bp upstream of the translation start site	Homozygotes show nicking of the anterior and lateral margins of the wing blade.	(Inamdar, Vijayraghavan, & Veronica, 1993)
E3	Moderate	Hypomorph	P-element insertion	Insertion of element in an intron, approximately 5kb downstream of the transcription start site.	Homozygotes have severely *scalloped* wings.	Vijayraghavan, & Veronica, 1993)
58d	Strong	Hypomorph	Gamma Ray	Gamma ray	Homozygotes have strong reduction in wing tissue.	(Campbell et al., 1991; Williams, Bell, & Carroll, 1991)

Table 2.2:Summary of *vestigial* mutant alleles.

Allele	Allele Strength	Allele Class	Mutagen	DNA Lesion	Description of Allele	Reference
21-3	Moderate - Strong	Hypomorph	P-element insertion	Insertion has a deletion of bases 1862-2015 with a 2bp AT insertion at the deletion site. The inserted element also has a single A to T transversion at position 32.	Homozygotes have strong reduction in wing tissue.	(Anderson, Davis, & Hodgetts, 2006; Hodgetts & Keefe, 2001)
1	Strong	Hypomorph	Spontaneous	Insertion of an 8kb 412 in intron 3 and an insertion of 6kb of unknown DNA at the 3' end of intron 2.	Homozygotes have strong reduction in wing tissue.	(Silber, Menn, Chevillard, Zider, & Paumard, 1993)
83b27	Strong	Hypomorph	Gamma Ray	Deletion of a major part of intron 2.	Homozygotes have extremely strong reduction in wing tissue.	(Silber et al., 1993)

Table 2.3:Summary of *bifid/Omb* mutant alleles.

Allele	Allele Strength	Allele Class	Mutagen	DNA Lesion	Description of Allele	Reference
1	Weak	Hypomorph	Spontaneous	An insertion in the first intron	Homozygotes have proximal fusion of all longitudinal veins and variable defects at the tip of the wing.	(Grimm & Pflugfelder, 1996; Shen et al., 2005)
GAL4	Weak	Hypomorph	P-element insertion	Enhancer trap insertion	Homozygotes have scalloping of the wings and vein defects.	(Lecuit et al., 1996)
md653	Moderate	Hypomorph	P-element insertion	Enhancer trap insertion	Homozygotes have scalloping of the wings and vein defects.	(Enerly, Larsson, & Lambertsson, 2002)

Table 2.4: Summary of *beadex* mutant alleles.

Allele	Allele Strength	Allele Class	Mutagen	DNA Lesion	Description of Allele	Reference
ms1096	Weak		P-element insertion	Enhancer trap insertion	Homozygous females have wing venation defects.	(Milan et al., 1998)
1	Weak	Hyper morph	Spontaneous	Roo element insertion is within the 3' untranslated region of Bx.	Homozygotes have loss of posterior wing margin. Heterozygotes have weaker loss of posterior wing margin.	(Tsai, Bainton, Blau, & Heberlein, 2004)
2	Weak - Moderate	Hyper morph	Spontaneous	Insertion of gypsy element approximatel y 8kb into the 3' UTR.	Homozygotes have loss of posterior wing margin. Heterozygotes have weaker loss of posterior wing margin.	(Shoresh et al., 1998)
3	Strong	Hyper morph	Spontaneous	Insertion of roo element approximatel y 9kb into the 3' UTR.	Homozygotes have loss of posterior wing margin. Heterozygotes have weaker loss of posterior wing margin.	(Rabinow, Chian, & Birchler, 1993; Shoresh et al., 1998)

Introgression of Mutations into Each Genetic Background

Mutations were introgressed into Samarkand and Oregon-R through backcrossing. This entails crossing a donor individual (with the mutation) to a recipient for ~ 10 generations while selecting for the mutant allele. This allows for rapid recombination and consequently removes the majority of the genome of the donor and replaces it with the recipient's genetic background. Stocks were given to me at generation 3 in this process and consequently had to be backcrossed for 7 more generations. Samarkand and Oregon-R strains both are marked with white eyes (w^-) and mutations with eye markers ($sd^{29.1}$, sd^{E3}, bi^{md653}, $bi^{omb-GAL4}$, bx^{ms1096}) and alleles with dominant effects (bx^1, bx^2, bx^3,) were selected for after each cross and heterozygous females were repeatedly crossed to recipient population. Remaining alleles (sd^1, sd^{ETX4}, sd^{58d}, bi^1, vg^1, vg^{21-3}, vg^{83b27}) only have phenotypic effects that are visible in hemizygous males and homozygous females. As such, backcrossing these alleles into each genetic background required selection of males and heterozygous females every other generation. In *Drosophila* recombination only occurs in females, therefore, recombination only occurred every other generation. A balancer mediated replacement of the complete second and third chromosome was performed to account for this limitation.

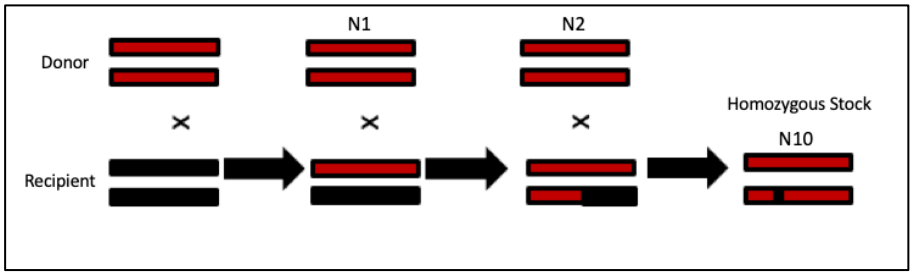

Figure 2.1: Backcrossing that takes place for allele introgression from one genetic background to another. Donor stocks with allele were backcrossed for a total of 10 generations, replacing most of the genome via recombination.

Generating Recombinant Double Mutants

Scalloped, *bifid* and *beadex* are all located on the X chromosome. Therefore, to obtain desired double mutants I generated recombinant X chromosomes. Homozygous females for one allele were crossed to a male carrying the second allele of interest. Heterozygous females from this cross were then crossed to a male with an Fm7 balancer on the X chromosome. Progeny from this cross were screened for the necessary genotype. At times the presence of both alleles was more obvious than others. For example, if ~4% (the expected recombinant rate) of individuals had a novel phenotype that was much more severe than either individual allele we could deduce that this was the double mutant phenotype. At other times, the presence of two alleles was much less obvious. In this case complementation tests were set up to verify the presence of both alleles.

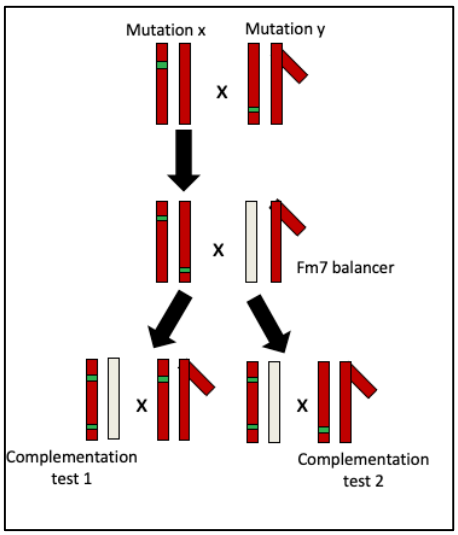

Figure 2.2: Crossing scheme to generate recombinants. A female with mutation x is crossed to a male with mutation y. The female progeny from this cross were then crossed to a male with a balancer and recombinants were then screened and verified using complementation tests. Green rectangles represent the mutant alleles. Balancer chromosomes are represented in grey.

Generating *scalloped* and *vestigial* Double Mutants

scalloped is on the X chromosome and *vestigial* is on the second chromosome. In order to make *scalloped* and *vestigial* double mutants, multiple crosses using balancers and a dominant marker was necessary. Fm7 is a first chromosome balancer that is marked with an eye shape change mutant (*Bar*, *B*). Curly-of-Oster (CyO) is a second chromosome balancer marked with curly wings (*Cy*). *Sternopleural* (*Sp*) is a dominant second chromosome marker with increased sternopleural bristle number. By selecting for and against balancers and markers at various crosses we could verify the presence of both *scalloped* and *vestigial.*

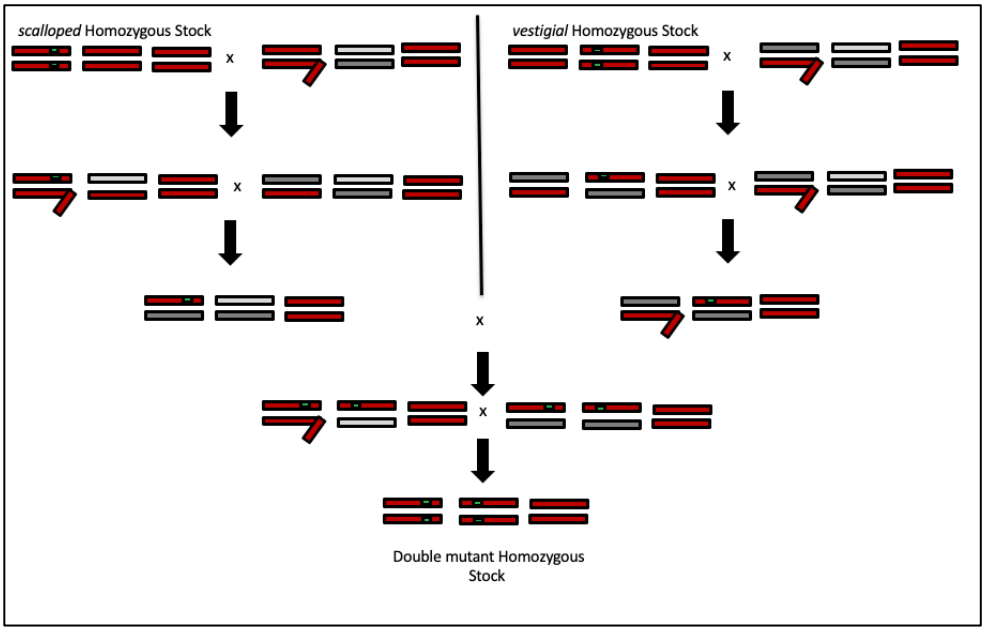

Figure 2.3: Crossing scheme for *scalloped* and *vestigial* mutants. The light grey chromosomes represent chromosomes with a dominant marker. The darker grey chromosomes represent balancer chromosomes. The green rectangles represent the mutant alleles.

Crossing Scheme to Generate All Possible Genotypic Combinations for Each

In order to examine the epistatic effects for a given allelic pair, I had to construct all nine two-locus genotypes. Table 2.5 illustrates how each of these genotypes were created in Samarkand and Oregon-R for 50 allelic pairs. Repeat genotypes, such as those specific to $sd^1$and bx^1were not repeated for each allelic pair, but a higher number of individuals were dissected to ensure an accurate comparison. 654 unique genotypes (in each background) were generated over the course of seven experimental blocks. Across all blocks, each genotype is represented in at least two biological replicates (distinct vials

across blocks) with at least 5 individual samples per replicate.

Table 2.5: Experimental Crosses to Generate 9 Genotypic Combinations

Female Parent	**Male Parent**	**F1 Female Genotype**	**Notes**	**Rep 1**	**Rep 2**
+/+	+/+	+/+	Specific for WT	Block 1	Block 2
sd^1/sd^1	sd^1/Y	sd^1/sd^1	Specific for sd^1	Block 1	Block 2
sd^1/sd^1	sd^+/Y	$sd^1/+$		Block 1	Block 2
bx^1/bx^1	bx^1/Y	bx^1/bx^1	Specific for bx^1	Block 1	Block 2
bx^1/bx^1	bx^+/Y	$bx^1/+$		Block 1	Block 2
$sd^1, bx^1/sd^1, bx^1$	sd^1, bx^1/Y	$sd^1, bx^1/sd^1, bx^1$	Specific for bx^1,sd^1	Block 1	Block 2
$sd^1, bx^1/sd^1, bx^1$	sd^1/Y	$sd^1, bx^1/sd^1$		Block 1	Block 2
$sd^1, bx^1/sd^1, bx^1$	bx^1/Y	$sd^1, bx^1/bx^1$		Block 1	Block 2
$sd^1, bx^1/sd^1, bx^1$	bx^+/Y	$sd^1, bx^1/+$		Block 1	Block 2

Evaluating Epistatic Interactions with Known Modifiers of *Scalloped* Function

The Exelixis Deletion lines have molecularly defined deletions spanning 90% of the autosomes, with an average deletion of 400kb to 140kb (Parks et al., 2004). A subset of 41 deletions were used that span the genome. These deletions were previously used in Chari & Dworkin (2013) and chosen because they span the range of modifier phenotypes across both severity and background dependence observed in the genome wide dominant screen for sd^{E3}. Male deletion-bearing individuals were crossed to homozygous females with *scalloped* alleles (sd^+, $sd^{29.1}$, sd^1, sd^{ETX4}, sd^{E3}, sd^{58d}) from Samarkand and Oregon-R over the course of four blocks. Male progeny from this cross were hemizygous

for the *scalloped* allele but heterozygous at all other loci. Each genotype is represented in at least two replicate vials with at least 5 individual samples per vial.

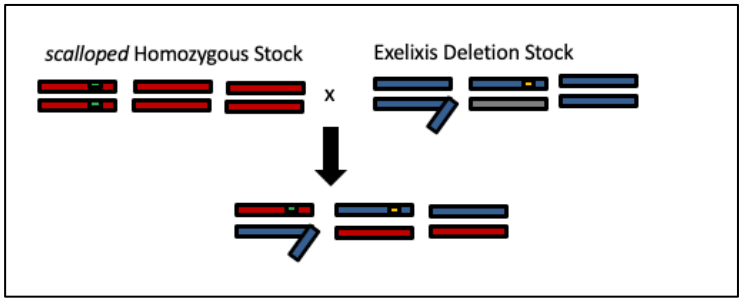

Figure 2.4: Crossing scheme for modifiers. Male deletion-bearing individuals were crossed to homozygous females with *scalloped* alleles. Male offspring that were hemizygous for the *scalloped* and heterozygous at all other loci were compared between Samarkand and Oregon-R. Green rectangles represent the *scalloped* allele and the yellow rectangles represents the deletion. A Balancer chromosome is represented in grey. Red represents the Samarkand background and blue represents the Exelixis isogenic background.

General Methods:

Fly Rearing and Collections

All crosses were reared at 24°C in a Percival incubator on a 12:12 hour day: night cycle. Progeny were collected from crosses via standard CO_2 procedures. Collection continued for 20 days after the cross was set (as some crosses will be developmentally delayed). Flies were stored by genotype in 70% ethanol. All flies were reared on a standard cornmeal media (recipe https://github.com/DworkinLab/Protocols/blob/master/Recipes.md)

Wing Dissections, Imaging and Measurement

The right wing of each fly was dissected using standard lab procedures. Wings were then mounted onto microscope in 70% glycerol and 30% PBS solution. Wings were

imaged with a Olympus BX43 microscope using a 4X objective (40X magnification). Images were taken with cellSens Standard software at a resolution of 4080 x 3072 pixels (0.0005375 mm/px) using an Olympus Dp80 camera. A custom ImageJ macro was used to measure wing area.

Statistical Methods:

The Natural and Orthogonal InterActions (NOIA) model

The Natural and Orthogonal InterActions (NOIA) model provides a mathematical tool to estimate genetic effects as allele substitutions on one specific genotype (Alvarez-Castro & Carlborg, 2007). While this method allows any genotype to be the reference, the reference point for this work is the wildtype genotype which can be used to estimate a Genotype-Phenotype (GP) map for wing size. The NOIA model uses a similar notation to the maps used for one locus and two alleles, where $\boldsymbol{G = S \bullet e}$ (Zeng, Wang, & Zou, 2005)

$$\begin{pmatrix} \boldsymbol{sd^{+}sd^{+}} \\ \boldsymbol{sd^{1}sd^{+}} \\ \boldsymbol{sd^{1}sd^{1}} \end{pmatrix} = \begin{pmatrix} \mathbf{1} & \mathbf{0} & \mathbf{0} \\ \mathbf{1} & \mathbf{1} & \mathbf{1} \\ \mathbf{1} & \mathbf{2} & \mathbf{0} \end{pmatrix} \cdot \begin{pmatrix} \boldsymbol{R} \\ \boldsymbol{a} \\ \boldsymbol{d} \end{pmatrix}$$

As shown above for an example with a single bi-allelic locus (*sd*^{1} vs *sd*$^{+}$), **G** is the vector of genotypic values (the phenotypes for all 3 genotypes). **S** is the genetic effect design matrix. The first column of this matrix demonstrates that the phenotypes are measured as deviations from the reference point, in this case wildtype. The second column is the contribution of additive effects added to the wildtype for each *scalloped*^{1} allele, and the third column the dominance deviation for heterozygotes. **e** is the vector of estimated

genetic effects (reference - **R**, additive effects- **a** and dominance- **d**), accounting for the reference (wild type) in the model and additive and dominance effects.

Using the NOIA package this equation is extended for two alleles at two loci. In this case **G** is the vector of genotypic values for the 9 genotypes for each allelic pair. The design matrix expands to include the additive and dominance effects for the second locus, as well as the interactions between additive and dominance effects across both loci. Consequently, for the 2-loci model with epistatic interactions, the vector **e** expands to include additive-by-additive, dominance-by-additive, additive-by-dominance, and dominance-by-dominance interaction effects. An example of this is shown below with the allelic pair sd^1bx^1.

$$\begin{pmatrix} \boldsymbol{sd^+sd^+bx^+bx^+} \\ \boldsymbol{sd^1sd^+bx^+bx^+} \\ \boldsymbol{sd^1sd^1bx^+bx^+} \\ \boldsymbol{sd^+sd^+bx^1bx^+} \\ \boldsymbol{sd^+sd^+bx^1bx^1} \\ \boldsymbol{sd^1sd^+bx^1bx^+} \\ \boldsymbol{sd^1sd^1bx^1bx^+} \\ \boldsymbol{sd^1sd^+bx^1bx^1} \\ \boldsymbol{sd^1sd^1bx^1bx^1} \end{pmatrix} = \begin{pmatrix} \mathbf{1} & \mathbf{0} & \mathbf{0} & \mathbf{0} & \mathbf{0} & \mathbf{0} & \mathbf{0} & \mathbf{0} & \mathbf{0} \\ \mathbf{1} & \mathbf{1} & \mathbf{0} & \mathbf{1} & \mathbf{0} & \mathbf{0} & \mathbf{0} & \mathbf{0} & \mathbf{0} \\ \mathbf{1} & \mathbf{2} & \mathbf{0} & \mathbf{0} & \mathbf{0} & \mathbf{0} & \mathbf{0} & \mathbf{0} & \mathbf{0} \\ \mathbf{1} & \mathbf{0} & \mathbf{1} & \mathbf{0} & \mathbf{1} & \mathbf{0} & \mathbf{0} & \mathbf{0} & \mathbf{0} \\ \mathbf{1} & \mathbf{0} & \mathbf{2} & \mathbf{0} & \mathbf{0} & \mathbf{0} & \mathbf{0} & \mathbf{0} & \mathbf{0} \\ \mathbf{1} & \mathbf{1} & \mathbf{1} & \mathbf{1} & \mathbf{1} & \mathbf{1} & \mathbf{1} & \mathbf{1} & \mathbf{1} \\ \mathbf{1} & \mathbf{2} & \mathbf{1} & \mathbf{0} & \mathbf{1} & \mathbf{2} & \mathbf{0} & \mathbf{0} & \mathbf{0} \\ \mathbf{1} & \mathbf{1} & \mathbf{2} & \mathbf{1} & \mathbf{0} & \mathbf{2} & \mathbf{2} & \mathbf{1} & \mathbf{0} \\ \mathbf{1} & \mathbf{2} & \mathbf{2} & \mathbf{0} & \mathbf{0} & \mathbf{4} & \mathbf{0} & \mathbf{0} & \mathbf{0} \end{pmatrix} \cdot \begin{pmatrix} \boldsymbol{R} \\ \boldsymbol{a_{sd}} \\ \boldsymbol{a_{bx}} \\ \boldsymbol{d_{sd}} \\ \boldsymbol{d_{bx}} \\ \boldsymbol{aa} \\ \boldsymbol{da} \\ \boldsymbol{ad} \\ \boldsymbol{dd} \end{pmatrix}$$

The second column of this matrix demonstrates that one additive effect is added to the wildtype for each *scalloped* allele, and the third column illustrates one additive effect is added for each *beadex* allele. The fourth and fifth columns illustrate the dominance effect that is added when the individual is a heterozygote. Columns 6-9 represent epistatic interactions. This model was fit for each allelic pair in each background. Models were fit using the linearRegression() function in the NOIA package (v0.97.1)(Le Rouzic,

Gjuvsland, & Ariste, 2015) . We confirmed the results from the NOIA package using the standard lm() (v4.0.2), linear modelling function in R using custom design (**S**) matrices, with identical estimates to NOIA.

Linear Models

Using the NOIA linear regression we estimated the genetic effects summarized in the vector **e**, from each "set" of 9 genotypes as shown above. Using these estimates (**e**) we analyzed the influence of the genetic background and average mutant effect (eg, from a_{sd^1} and a_{bx^1}) to each of the epistatic effects ($aa_{(sd^1\ bx^1)}$, $dd_{(sd^1\ bx^1)}$, $ad_{(sd^1\ bx^1)}$, $da_{(sd^1\ bx^1)}$). To assess these relationships, a linear mixed model was fit with the epistasis value as described above as the response variable. The genetic background (Samarkand or Oregon-R) was a fixed effects and average allelic effect (eg, average of a_{sd^1} and a_{bx^1}) was a continuous predictor. The allelic pair, *scalloped* allele, and the second allele (from gene 2) were fit as random effects, allowing for random intercepts. We included these terms as each epistatic estimate contains some related information (e.g same wild type data was used to estimate epistatic terms for all *sd* alleles). Therefore, the measurements are not statistically independent, and this random effect is necessary to account this relationship. The allelic pairs are created from various combinations of *scalloped*, *bifid*, *beadex* and *vestigial* alleles. Therefore, the same allele is present in multiple measurements. Consequently, measurements may be correlated, and it would appear that we have more independent replicates than we really have if this was not accounted for as a random effect. While it was important for us to assess how genetic background and average mutant effect influence epistatic effects individually, we also needed to examine the

interaction for these effects. For example, do we see different relationships between average mutant effect and epistasis in each background (i.e. separate slopes for each background). To assess this, a linear mixed model was fit with epistasis as the response variable. The genetic background and average allelic effect, and the interaction between them were fit as predictors. The *scalloped* allele, and the second allele (from gene 2) were fit as random effects, allowing for random intercepts. In this model the random effect for Allelic pair is removed as this is accounted for explicitly in the interaction term. Models were fit using the lmer() function in the lme4 R library (v1.1.23) (Bates, Maechler, Bolker, & Walker, 2015).

To assess block effects for this experiment, two linear models were fit. For the first one block effects were estimated across all genotypes. For this model, the wing area was the response variable. The genetic background and genotype, and the interaction between them were fit as fixed effects. Block was fit as a random effect, allowing for random intercepts. For the second model block effects were estimated for each genotype. For this model wing area was the response variable. The genetic background and genotype, and the interaction between them were fit as fixed effects. Block was fit as random effect, allowing genotype and background specific variation for each block. Models were fit using the lmer() function.

For the modifier screen, in order to assess the phenotypic variability for each *scalloped* allele among all deletion lines two linear models were used. For the first model, wing area is the response variable. The genetic background, *scalloped* allele, and the interaction between them were fit as fixed effects. Deletion was fit as random effect,

allowing allele and background specific variation for each block. A diagonal, heterogeneous variance-covariance matrices was fit for the random effect. This allowed us to analyze the variability for each *scalloped* allele in each background among all deletions, but with effects assumed to be independent across alleles of *sd*. For the second model, wing area is the response variable. The genetic background, *scalloped* allele, and the interaction between them were fit as fixed effects. Deletion was fit as random effect, allowing allele specific variation for each block. This allowed us to analyze the variability for each *scalloped* allele among all deletions without accounting for differences in genetic background. Models were fit using the glmmTMB() (v1.0.2.1) function from the glmmTMB library (Brooks et al., 2017). All other analyses were performed in R using functions in base R (v4.0.2)

Summary of Epistasis Terminology and Calculations

A central aim for this project is to determine if the magnitude and direction of epistatic interactions can be predicted from the individual allelic effects. For example, is epistasis larger in magnitude for alleles of moderate effect? In order to examine this, we had to observe the magnitude of epistasis by using the absolute values of the epistatic components. In this case, the sign or direction of individual epistatic components is not relevant. We simply wanted to observe how the overall magnitude of effects changes for different genetic backgrounds and allelic combinations. We also wanted to examine how the direction of epistasis changes for different gene and allele combinations and genetic

backgrounds. For example, are Oregon-R epistasis values more likely to be negative? In this case, it was important for us to examine the sign of epistatic components. Epistasis estimates can be negative or positive, indicating the direction of the effect. When these values are used it will be referred to as signed epistasis, referring to the fact that it can be either positive or negative. However, the "signed epistasis" I discuss should not be confused with "sign epistasis" as described in the introduction.

Magnitude Epistasis: The phenotype associated with a double mutant deviates from the mutants' additive effects, but not in a way that will change the sign (or direction) of either allele's individual effect.

Positive epistasis: double mutant has a less severe (or more fit) phenotype than expected from the additive effects of the mutants individually.

Negative epistasis: a double mutant's observed phenotype is more severe (or less fit) than what is expected.

Sign Epistasis: the sign (i.e. from deleterious to beneficial) of an individual alleles phenotypic effect changes in the presence another mutation. An example of this is when a mutation is beneficial individually, but it can act deleterious when in the presence of another mutation.

Average Magnitude Epistasis: The absolute average of all 4 epistasis components.

$$Average\ magnitude\ epistasis\ = \frac{abs(aa) + abs(ad) + abs(da) + abs(dd)}{4}$$

Average Signed Epistasis: The average of all 4 epistasis components.

$$Average\ signed\ epistasis\ = \frac{(aa + ad + da + dd)}{4}$$

Average Mutant Effect: The average mutant effect is the average of the two additive allelic effects for *scalloped* and Gene2 (the second gene used in combination with *scalloped*).

$$Average\ mutant\ effect\ = \frac{(a_{sd}\ +\ a_{Gene2})}{2}$$

3. Results

Genetic Background Effects for Homozygotes

Mean wing size was estimated for *scalloped*, *beadex*, *bifid*, and *vestigial* homozygous mutants in Samarkand and Oregon-R (shown in figure 3.1). The genetic background has a significant effect on wing area (P-value = 9.0e-11) but importantly there is also an interaction effect between the genetic background and allelic effect (P-value = < 2.2e-16). Indicating that the genetic background influences alleles to varying degrees, allowing some alleles to be more background dependent than others as expected

based on previous work (Chandler et al. 2017). While we see various alleles with substantial size differences between Samarkand and Oregon-R, we see the greatest variation for alleles of moderate effect. For example, for *scalloped* we see the largest variation in wing size between genetic backgrounds in sd^{ETX4} and sd^{E3}. While Samarkand has larger wings for these moderate alleles, Oregon-R has slightly larger wings for weaker alleles ($sd^{29.1}$ and sd^{1}). In *beadex*, we see the greatest difference in mean wing size between Samarkand and Oregon-R for bx^{2}. For this moderate allele, Oregon-R is larger than Samarkand. There is less variation between backgrounds for the *vestigial* alleles overall, but we see the greatest variation between vg^{21-3} as Samarkand wings are significantly larger. While we see differences in the expressivity of these alleles in the two genetic backgrounds, the ordering of allelic effects stays generally consistent between the genetic backgrounds.

Genetic Background Effects For *scalloped*, *beadex*, *bifid*, and *vestigial* Homozygotes

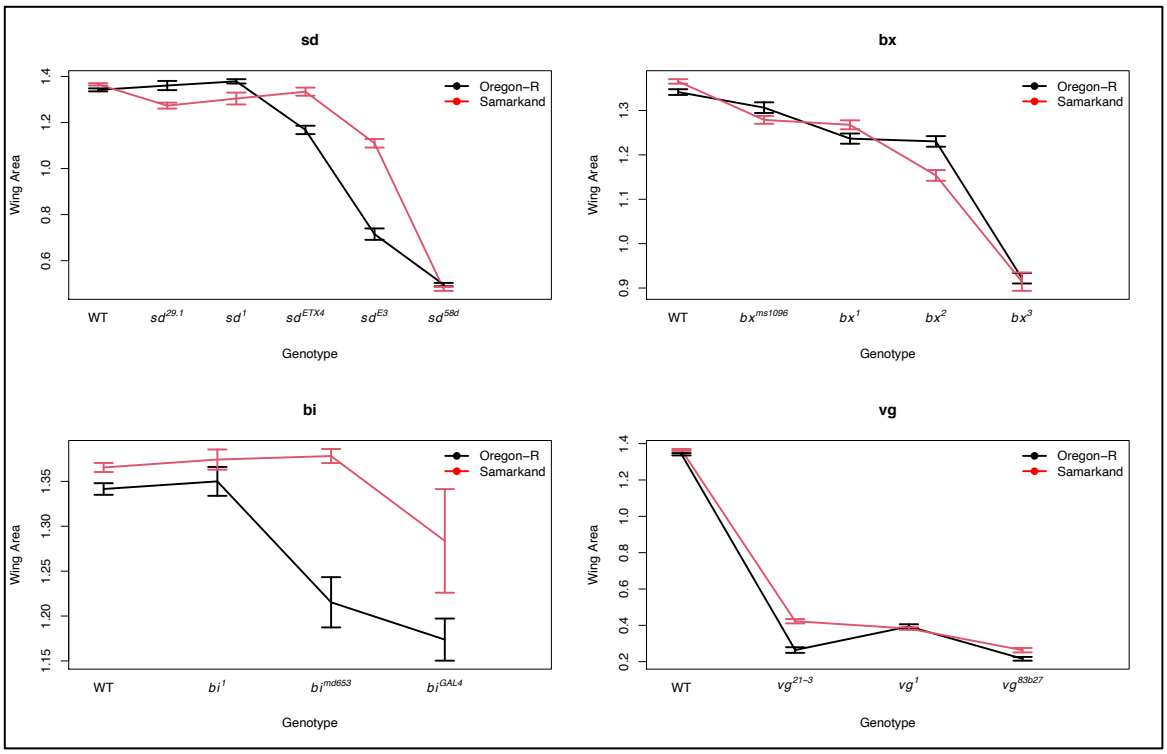

Figure 3.1: The influence of genetic background on the expressivity of allelic series in *scalloped*, *beadex*, *bifid* and *vestigial* genes. The mean phenotypic effect is shown for each homozygote in Samarkand and Oregon-R. The greatest variation between Samarkand and Oregon-R is for alleles of moderate effect. Error bars reflect 95% confidence intervals. N = 476.

Visualizing Epistatic Interactions Using Reaction Norms

A graphical representation of epistatic effects is shown by plotting the mean wing size for the nine possible genotypes for each allelic pair in both the Samarkand and Oregon-R wild type genetic backgrounds as shown in Figure 3.2. A purely additive effect takes place when the additive and dominance effects are the same at each locus, despite the genotype at the other locus. This would result in parallel lines in the reaction norm plot. A partial example of this is shown in the panel for $bx^{ms1096}sd^{58d}$. While there are still epistatic effects for this allelic pair, the magnitude of epistatic effects is very small with this allele pair. The relationship between the alleles is not linear due to a large dominance effect of sd^{58d} but after taking this effect into account these alleles behave in a mostly additive manner. An epistatic interaction takes place when the effect of one locus depends on the genotype at the other locus. Meaning that there is a change in the direction or slope of the lines in the reaction norm plot. Examples of this are shown in the 3 other panels. For example, in the $bx^{1}sd^{58d}$ panel we see that bx^{+}/bx^{+} and bx^{1}/bx^{+} behave similarly with increasing copies of sd^{58d} but we see slope and direction changes in bx^{1}/bx^{1} when a copy of sd^{58d} is added. While it is hard to visually "dissect" the 4 epistatic components from this plot, it clearly shows that there are epistatic interactions taking place.

We also see differences in the ways the alleles behave in the two genetic backgrounds. For example, for the genotype $bx^{1}, sd^{58d}/bx^{1}$ we see differences in the average wing area between Samarkand and Oregon-R. Indicating that the phenotypic effect of bx^{1}/bx^{1} manifests differently in the two backgrounds when a copy of sd^{58d} is

added. Interestingly, the direction of the same epistatic effect for these backgrounds switches for $bx^3, sd^{58d}/bx^3$ compared to $bx^1, sd^{58d}/bx^1$. These plots indicate that epistasis is taking place, and that epistatic effects may change depending on the alleles involved in the interaction and in different backgrounds. However, these plots make it difficult to make direct comparisons between allele strength and genetic backgrounds with resulting epistatic interactions.

Genotypic Effects for *beadex* and sd^{58d}

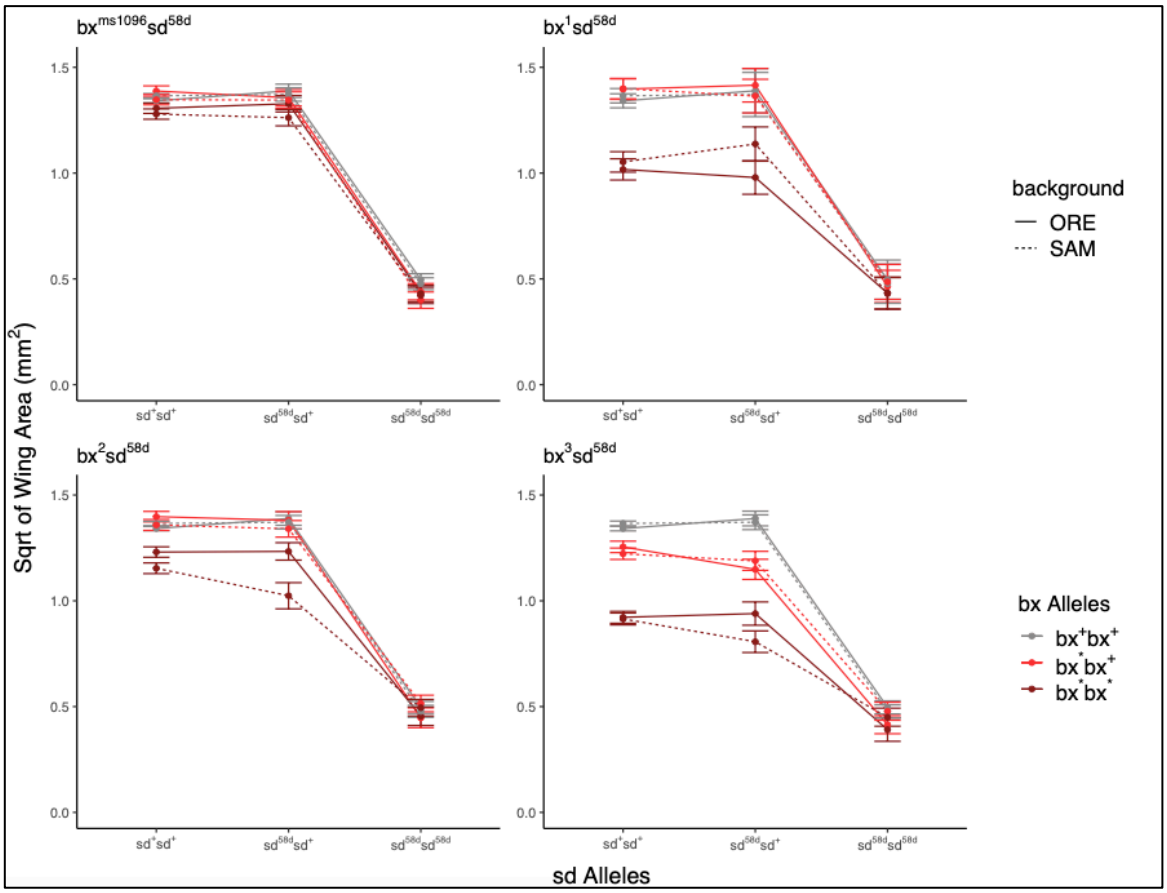

Figure 3.2: Graphical representations of genotypic effects at two biallelic loci as a reaction norm. The magnitude and direction of epistatic effects change depending on the alleles involved in the interaction and in different backgrounds. Error bars reflect 95% confidence intervals. N = 2,426. 35 individuals scored/genotype.

Examining Epistasis as A Function of Average Mutant Effect and Genetic Background

The central goal for this project is to examine genetic interactions as function of the magnitude of the individual allelic effects and genetic background. To observe this relationship, mutants were created by combining *scalloped* alleles along an allelic series with alleles in *beadex*, *bifid*, and *vestigial* in both the Samarkand and Oregon-R genetic background. The four epistatic outputs consist of additive-by-additive, dominance-by-additive, additive-by-dominance, and dominance-by-dominance. The average of all 4 of these effects was calculated in order to give us an average epistasis value. This value can be negative or positive, indicating if this effect is "better" or "worse" than expected. In this case, the sign of epistasis indicates if the wings are smaller or larger compare to the additive effects of the individual alleles. When these values are used it will be referred to as signed epistasis, referring to the fact that it can be either positive or negative. However, the "signed epistasis" I discuss should not be confused with "sign epistasis" referring to the change of direction of allelic substitutions based on the genotype at a second locus. The epistasis values can also be looked at as an absolute value which illustrates how the magnitude of all epistatic effects contribute to phenotypic change. When these values are used it will be referred to as magnitude epistasis. The average mutant effect is simply the average of the two additive allelic effects (a_{sd} and a_{geneX}).

Models were used to estimate the mean magnitude and signed epistasis among all allelic pairs for each epistatic component and each gene combination in both genetic backgrounds. An ANOVA analysis was then performed to examine how much variation occurs for epistasis estimates between Samarkand and Oregon-R. A summary of these

results is in Table 3.1, which is then described in detail below. A second model was used to estimate the effect of the average mutant effect on the mean magnitude and signed epistasis among all allelic pairs for each epistatic component and each gene combination in both genetic backgrounds. An ANOVA analysis was performed to examine the significance of the average mutant effect on epistasis. A summary of these results is in Table 3.2. This second model also allowed us to estimate interaction effects between average mutant effect and the genetic background on epistasis. An ANOVA analysis was performed to examine the significance of these interaction effects. A summary of these results is in Table 3.3.

Table 3.1: Summary of significant genetic background effects for magnitude and signed epistasis among all allelic pairs for different gene combination and types of epistasis. A "**Yes**" indicates a significant effect from the genetic background on epistasis (P-value < 0.05) while a "No" indicates no significant effect (P-value > 0.05). P-Value estimated from ANOVA.

Gene 2	Magnitude: Difference in Backgrounds	Signed: Difference in Backgrounds	Type of Epistasis
bx	No	**Yes**	Average
bi	No	**Yes**	
vg	**Yes**	No	
Total	No	**Yes**	
bx	No	**Yes**	Additive-by-additive
bi	No	No	
vg	No	No	
Total	No	No	
bx	**Yes**	**Yes**	Additive-by-dominance
bi	No	**Yes**	
vg	No	No	
Total	No	**Yes**	
bx	No	**Yes**	Dominance-by-additive
bi	No	**Yes**	
vg	No	No	
Total	No	**Yes**	
bx	No	**Yes**	Dominance-by-dominance
bi	No	No	
vg	No	No	
Total	No	No	

Table 3.2: Summary of significant mutant effects for magnitude and signed epistasis among all allelic pairs for different gene combination and types of epistasis. A "**Yes**" indicates a significant effect from the average mutant effect on epistasis (P-value < 0.05) while a "No" indicates no significant effect (P-value > 0.05). P-Value estimated from ANOVA.

Gene 2	Magnitude: Mutant Effect	Signed: Mutant Effect	Type of Epistasis
bx	**Yes**	No	Average
bi	No	No	
vg	**Yes**	No	
Total	**Yes**	No	
bx	No	**Yes**	Additive-by-additive
bi	**Yes**	**Yes**	
vg	**Yes**	**Yes**	
Total	**Yes**	**Yes**	
bx	No	No	Additive-by-dominance
bi	No	**Yes**	
vg	No	No	
Total	**Yes**	**Yes**	
bx	**Yes**	**Yes**	Dominance-by-additive
bi	No	No	
vg	**Yes**	**Yes**	
Total	**Yes**	**Yes**	
bx	No	No	Dominance-by-dominance
bi	No	**Yes**	
vg	Yes	**Yes**	
Total	Yes	**Yes**	

Table 3.3: Summary of significant interaction effects between the genetic background and average mutant effect for magnitude and signed epistasis among all allelic pairs for different gene combination and types of epistasis. A "Yes" indicates a significant effect from the interaction from average mutant effect and genetic background on epistasis (P-value < 0.05) while a "No" indicates no significant effect (P-value > 0.05). P-Value estimated from ANOVA.

Gene 2	Magnitude: Mutant Effect	Signed: Mutant Effect	Type of Epistasis
bx	No	No	Average
bi	**Yes**	No	
vg	No	No	
Total	No	**Yes**	
bx	No	No	Additive-by-additive
bi	No	No	
vg	No	No	
Total	No	No	
bx	No	No	Additive-by-dominance
bi	**Yes**	No	
vg	No	No	
Total	No	No	
bx	No	No	Dominance-by-additive
bi	**Yes**	**Yes**	
vg	No	No	
Total	**Yes**	**Yes**	
bx	No	No	Dominance-by-dominance
bi	No	No	
vg	No	No	
Total	No	No	

Average Epistasis

Estimates of average epistasis was calculated for each allelic pair in Samarkand and Oregon-R allowing for direct comparisons between the two backgrounds. Epistasis values were estimated from square root transformed wing areas for epistasis plots, but the importance of scale is examined later in this section "How Much Does Scale Matter" (short answer, not a lot). When examining signed epistasis, we see much more variation between the genetic backgrounds compared to magnitude epistasis. For example, *beadex* and *scalloped* mutants, *bifid* and *scalloped* mutants, and all mutants combined show significant differences for signed epistasis estimates between Samarkand and Oregon-R (Figure 3.4).

Oregon-R is more likely to be a negative value, meaning for these genotypes wing size are more likely to be smaller than expected based on the additive contributions of individual mutants. While Samarkand is more likely to be (slightly) positive, indicating that these wings are bigger than expected based on the additive effects of individual mutants. When looking at the magnitude of average epistasis, there is only a significant difference between the backgrounds for *vestigial* and *scalloped* mutants (Figure 3.7).

The average mutant effect were also estimated to get further insight on how this influences genetic interactions. For the signed estimate of epistasis there appears to be no significant relationship between the average mutant effect and the resulting epistasis (Table 3.5). However, there is a significant effect from the interaction of the background

and the average mutant effect for all mutant combinations. In Samarkand, the average epistasis is more likely to be a positive value at a weaker average mutant effect but become increasingly more negative as the average mutant effect increases. While in Oregon-R the average epistasis is more likely to be negative at a weaker average mutant effect and remain negative with a gentle slope as the average mutant effect increases (Figure 3.5). For magnitude epistasis the contribution of the average mutant is significant for *beadex* and *scalloped* mutants, *vestigial* and *scalloped* mutants, and all mutants combined (Figure 3.8). As the average mutant effect increases in severity, so does the average epistasis. There is also a significant effect from the interaction of the background and the average mutant effect for *bifid* and *scalloped* mutants (Figure 3.8). Interestingly, in Samarkand the average epistasis decreases as average mutant effect increases, whereas in Oregon-R as average epistasis increases with average mutant effect, demonstrating a form of classic "sign" epistasis where mutational effects change direction depending on background.

In summary, we see that both the genetic background and the magnitude of average mutant effect do influence epistasis. We see more variation between genetic backgrounds when including the direction of these interactions than the magnitude of these effects alone. Though, we see a relationship between the average allelic effect and epistasis more often when looking at the magnitude of epistasis, rather than the average of signed components. It is important to note that for Figures 3.3 and 3.6 each point on this plot represents the epistasis estimated derived from each set of 9 genotypes. The title of

these plots indicates the second gene that *scalloped* is combined with. Additionally, a plot was made for all the genes combined (for the full range of phenotypic effects).

Average Signed Epistasis of Samarkand and Oregon-R Allelic Pairs

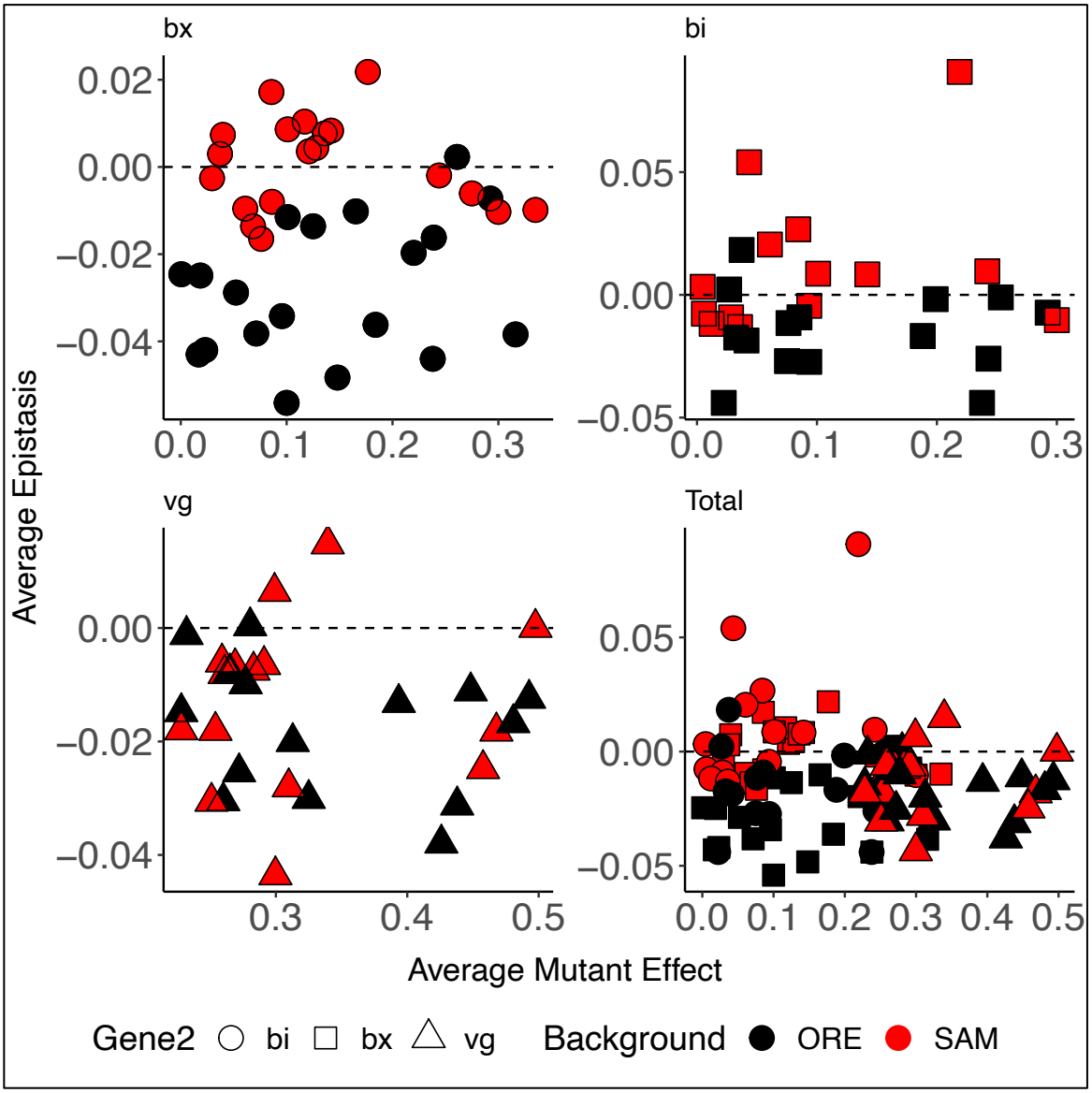

Figure 3.3: Model estimates of signed epistasis for each allelic pair in Samarkand and Oregon-R for the different gene combinations. N = 5,905.

Table 3.4: Statistical model estimates of the average signed epistasis for Samarkand and Oregon-R among all allelic pairs for each gene combination. The P-value representing the difference in genetic backgrounds was estimated from ANOVA analysis.

Type of Epistasis	Gene	Background	Average Mean Epistasis	Standard Error	P-Value
avg	bx	ORE	-0.0281	0.0034	**1.5E-12**
avg	bx	SAM	0.0007	0.0034	
avg	bi	ORE	-0.0156	0.0084	**4.5E-04**
avg	bi	SAM	0.0119	0.0084	
avg	vg	ORE	-0.0206	0.0064	2.98E-01
avg	vg	SAM	-0.0164	0.0064	
avg	Total	ORE	-0.0206	0.0040	**4.7E-09**
avg	Total	SAM	-0.0005	0.0040	

Table 3.5: Statistical model estimates of the effect of the average mutant effect on the average signed epistasis among all allelic pairs for each gene combination. P-value and estimated from ANOVA analysis.

Type of Epistasis	Gene	Effect of Average Mutant Effect	Standard Error	P-Value
avg	bx	0.0458	0.0332	0.53
avg	bi	-0.0465	0.0773	0.85
avg	vg	-0.0187	0.0402	0.74
avg	Total	-0.0062	0.0233	0.11

Table 3.6: Statistical model estimates of the effect of the interaction between genetic background and the average mutant effect on average signed epistasis among all allelic pairs for each gene combination. P-value estimated from ANOVA analysis.

Type of Epistasis	Dataset	Effect of Background: Average Mutant	Standard Error	P-Value
avg	bx	0.0434	0.0725	0.15
avg	bi	0.0755	0.0845	0.37
avg	vg	0.0172	0.0478	0.72
avg	Total	-0.0590	0.02578	**0.022**

Impact of Genetic Background on Average Signed Epistasis

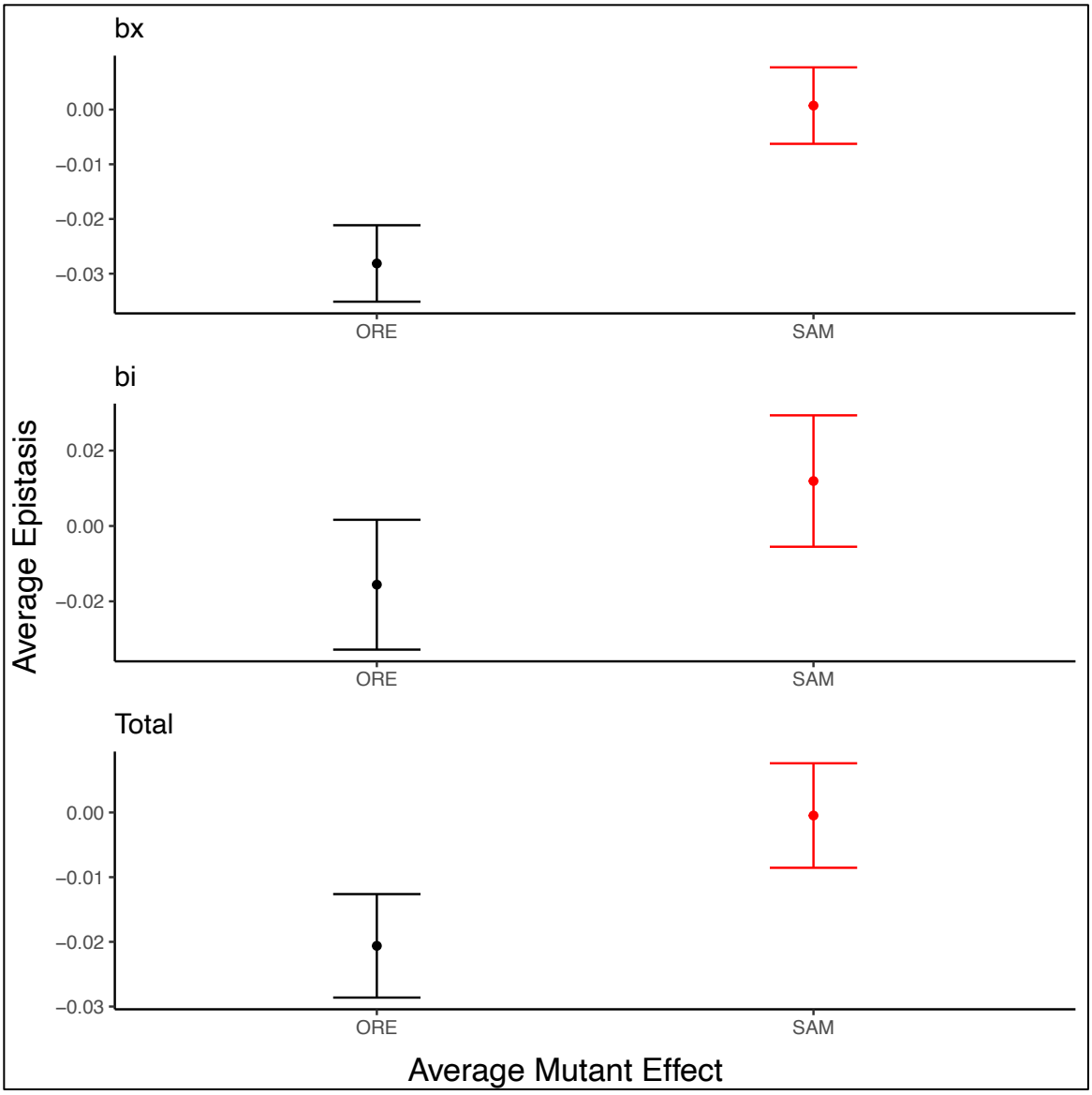

Figure 3.4: Model estimates of the average signed epistasis in Samarkand and Oregon-R for *beadex* and *scalloped* mutants (P-value =1.47E-12), *bifid* and *scalloped* mutants (P-value = 4.51E-04), and all mutants (P-value = 4.72E-09). Error bars reflect 95% confidence intervals. (Table 3.4) N = 5,905.

Impact of The Interaction between Average Mutant Effect and Genetic Background on Average Signed Epistasis

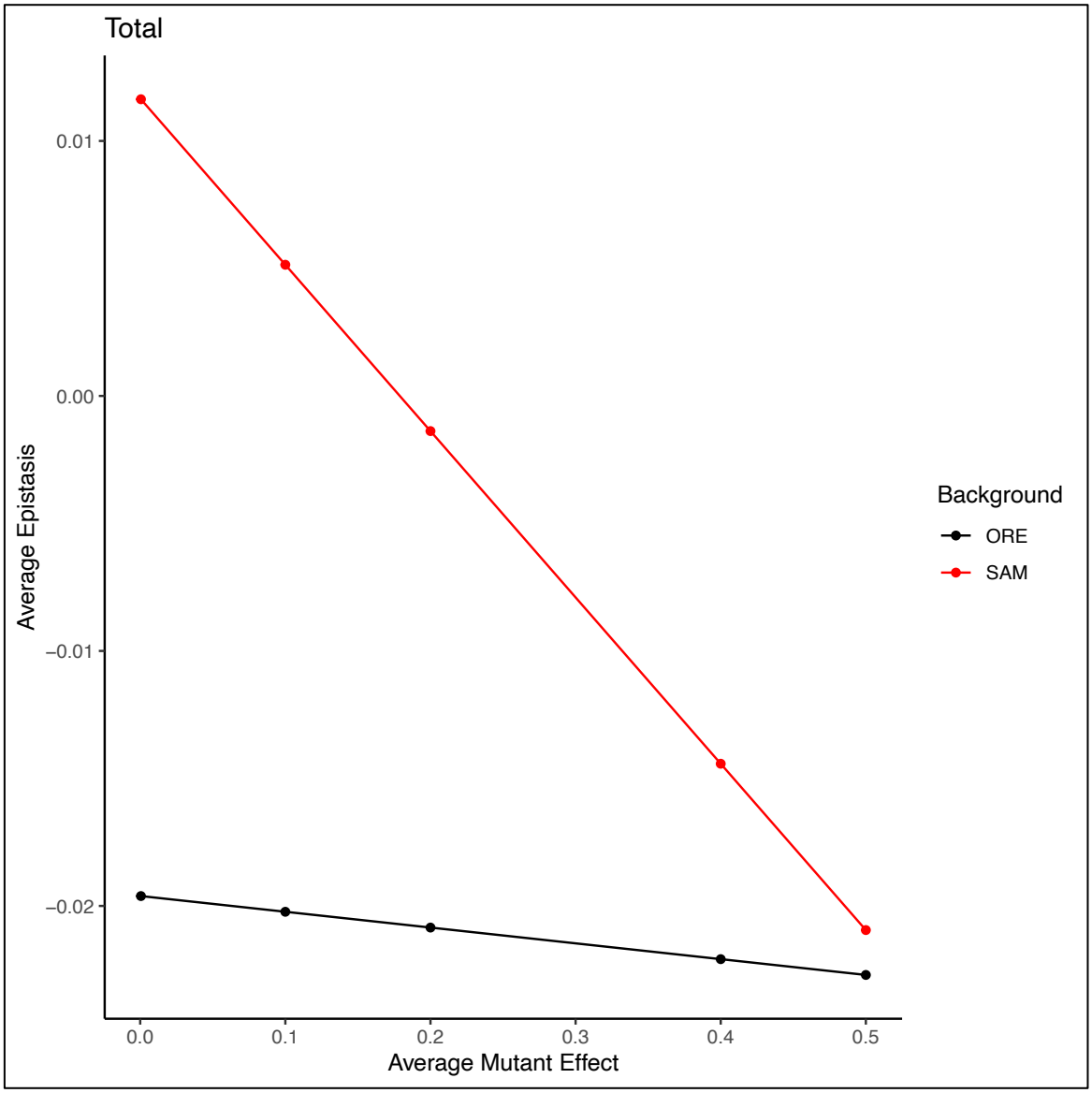

Figure 3.5: Model estimated values of the effect of the interaction between genetic background and the average mutant effect on average signed epistasis for all mutants (P-value = 0.0220). (Table 3.6) N = 5,905.

Average Magnitude Epistasis of Samarkand and Oregon-R Allelic Pairs

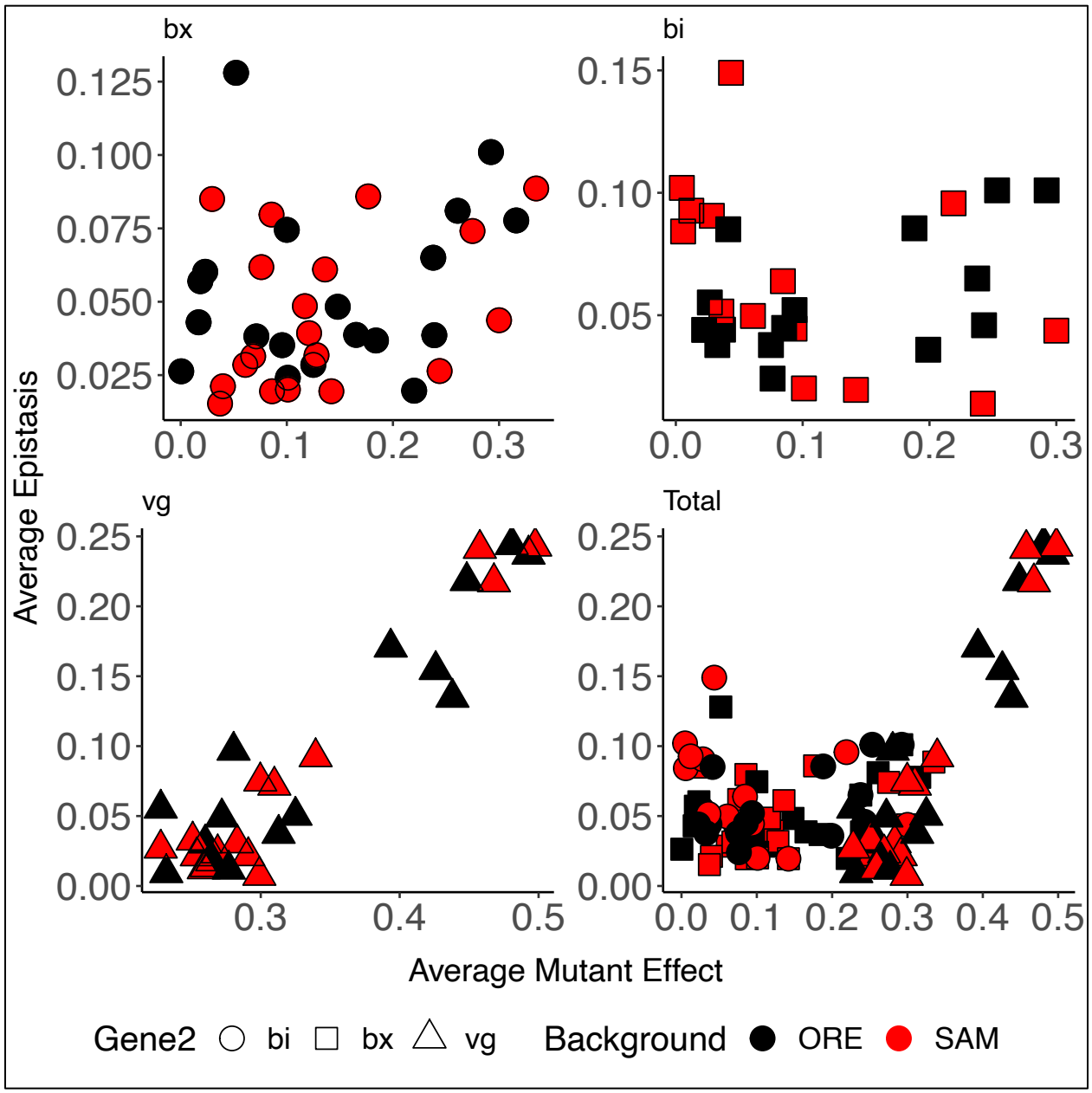

Figure 3.6: Model estimates of magnitude epistasis for each allelic pair in Samarkand and Oregon-R for the different gene combinations. N = 5,905.

Table 3.7:Statistical model estimates of the average magnitude epistasis for Samarkand and Oregon-R among all allelic pairs for each gene combination. The P-value representing the difference in genetic backgrounds was estimated from ANOVA analysis.

Type of Epistasis	Gene	Background	Average Mean Epistasis	Standard Error	P-Value
avg	bx	ORE	0.060	0.0130	2.39E-01
avg	bx	SAM	0.053	0.0130	
avg	bi	ORE	0.057	0.0084	5.14E-01
avg	bi	SAM	0.065	0.0087	
avg	vg	ORE	0.096	0.0226	**4.00E-02**
avg	vg	SAM	0.081	0.0226	
avg	Total	ORE	0.066	0.0095	2.77E-01
avg	Total	SAM	0.060	0.0096	

Table 3.8: Statistical model estimates of the effect of the average mutant effect on the magnitude epistasis among all allelic pairs for each gene combination. P-value estimated from ANOVA analysis.

Type of Epistasis	Gene	Effect of Average Mutant Effect	Standard Error	P-Value
avg	bx	0.0766	0.0514	**0.0152**
avg	bi	0.1377	0.0794	0.7565
avg	vg	0.4535	0.1135	**1.64E-05**
avg	Total	0.2414	0.0541	**7.58E-06**

Table 3.9: Statistical model estimates of the effect of the interaction between genetic background and the average mutant effect on the magnitude epistasis among all allelic pairs for each gene combination. P-value estimated from ANOVA analysis.

Type of Epistasis	Dataset	Effect of Background: Average Mutant	Standard Error	P-Value
avg	bx	0.0434	0.0725	0.5491
avg	bi	-0.3320	0.1159	**0.0041**
avg	vg	0.0820	0.0797	0.3037
avg	Total	-0.0999	0.0688	0.1469

Impact of Genetic Background on Average Magnitude Epistasis

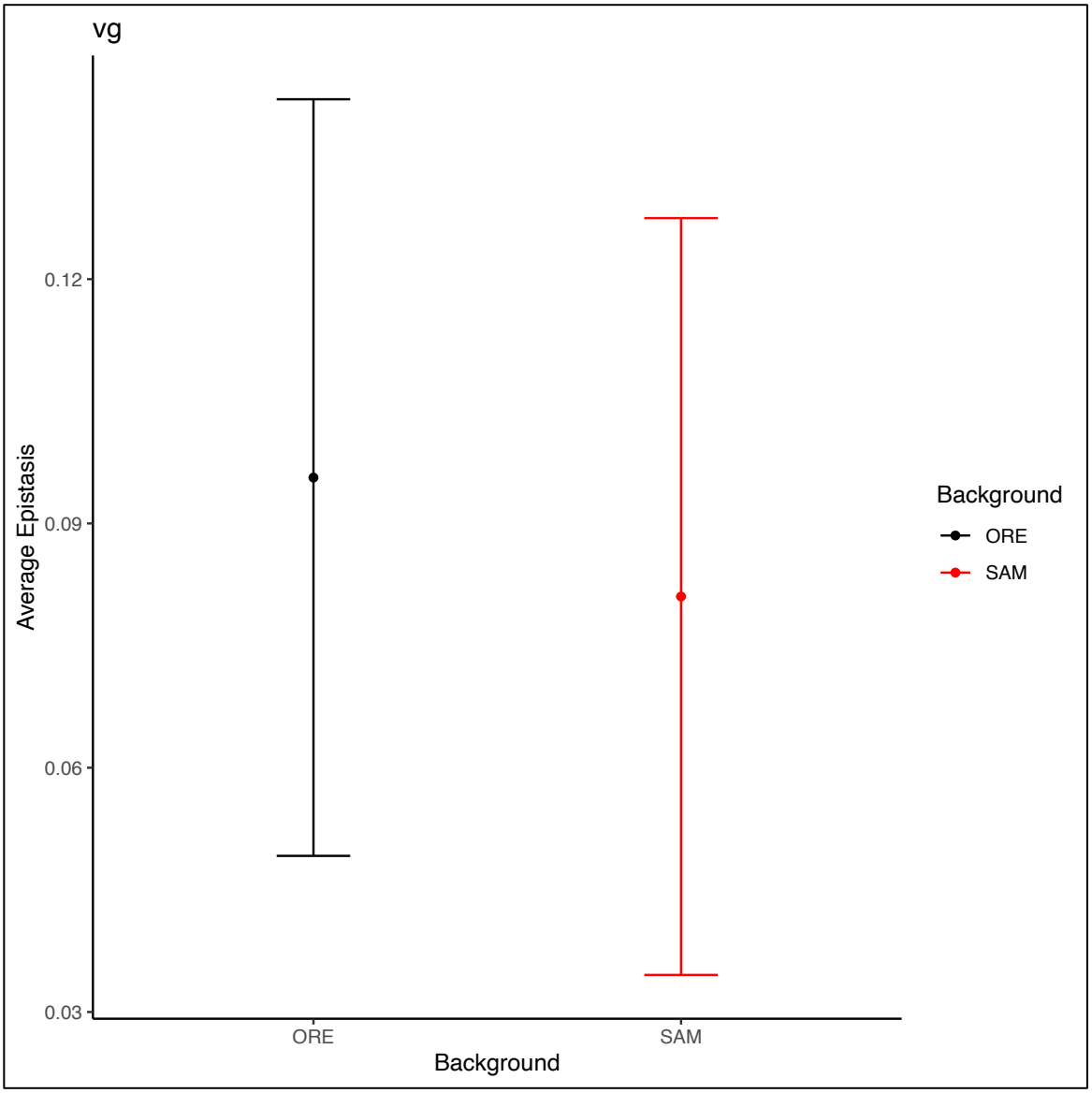

Figure 3.7: Model estimates of average magnitude epistasis for *vestigial* and *scalloped* mutants in Samarkand and Oregon-R (P-value = 4.00E-02). Error bars reflect 95% confidence intervals. (Table 3.7) N = 1,406.

Impact of Average Mutant Effect on Average Magnitude Epistasis

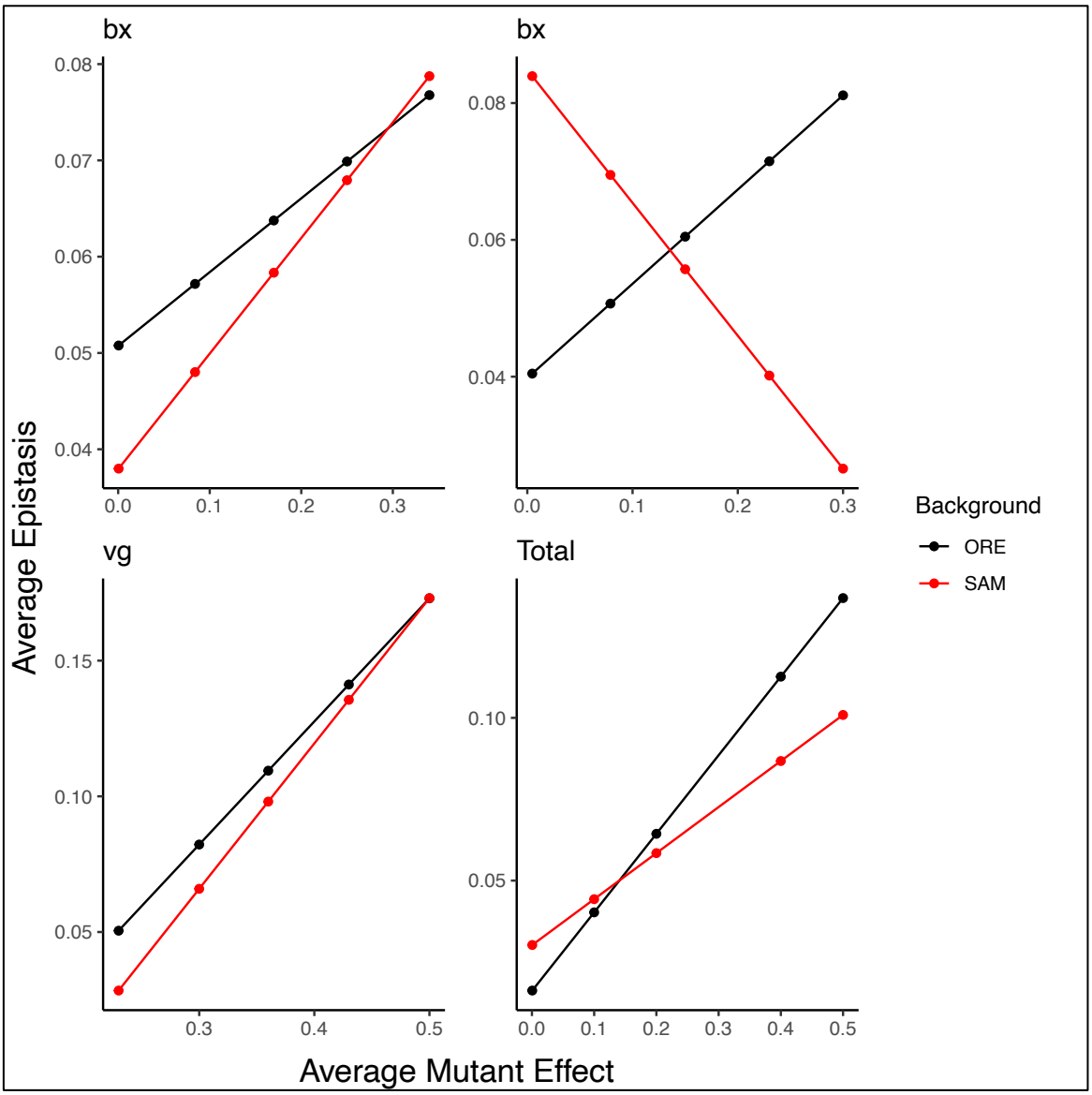

Figure 3.8: Statistical model estimated values of the effect of average mutant effect on magnitude epistasis for *beadex* and *scalloped* mutants (P-value = 0.0152), vestigial and *scalloped* mutants (P-value =1.64E-05) and all mutants (P-value =7.58E-06). There is also a significant effect for the interaction between genetic background and the average mutant effect on the magnitude epistasis for *bifid* and *scalloped* mutants (P- value =0.0041).(Table 3.8 and Table 3.9) N = 5,905.

Additive–by–Additive Epistasis

When examining epistasis as a function of average allelic effect and genetic background, it is important to examine these relationships with both the average epistasis as well as individual epistatic components as relationships may differ greatly depending on the component of epistasis. When examining the signed additive–by–additive epistasis among all allelic pairs we see a significant difference between the backgrounds for *beadex* and *scalloped* mutants (Figure 3.10). Oregon-R is more likely to more negative than Samarkand for this type of epistasis. When observing the magnitude of additive-by-additive epistasis we see no significant difference between Samarkand and Oregon-R wild type backgrounds (Table 3.13). Overall, it appears that the genetic background does not have a major influence on resulting additive-by-additive interactions for *bifid* and *scalloped* mutants, *beadex* and *scalloped* mutants and *vestigial* and *scalloped* mutants.

For signed additive-by-additive epistasis, the average allelic effect has a significant effect on the resulting epistasis for all mutant combinations (Figure 3.11). In all cases, the additive-by-additive epistatic effect is negative at a small average allelic effect but becomes increasingly positive as the average allelic effect increases. Indicating that the magnitude of the allelic effects has a direct effect on the direction of the additive-by-additive effect. When weaker mutants are involved in the interaction the wings are more likely to be smaller than expected, and for stronger mutants the wings are more likely to be bigger. The average mutant effect has a significant effect on the magnitude of additive-by-additive epistasis for *bifid* and *scalloped* mutants, and *vestigial* and *scalloped*

mutants, and all mutant combinations (Figure 3.13). For *bifid* and *scalloped* mutants, as average mutant effect increases, the magnitude for additive-by-additive epistasis decreases. For *vestigial* and *scalloped* mutants, and all mutant combinations, as average mutant effect increases so does the epistatic effect.

Additive–by–Additive Signed Epistasis Allelic Pairs across wild type backgrounds

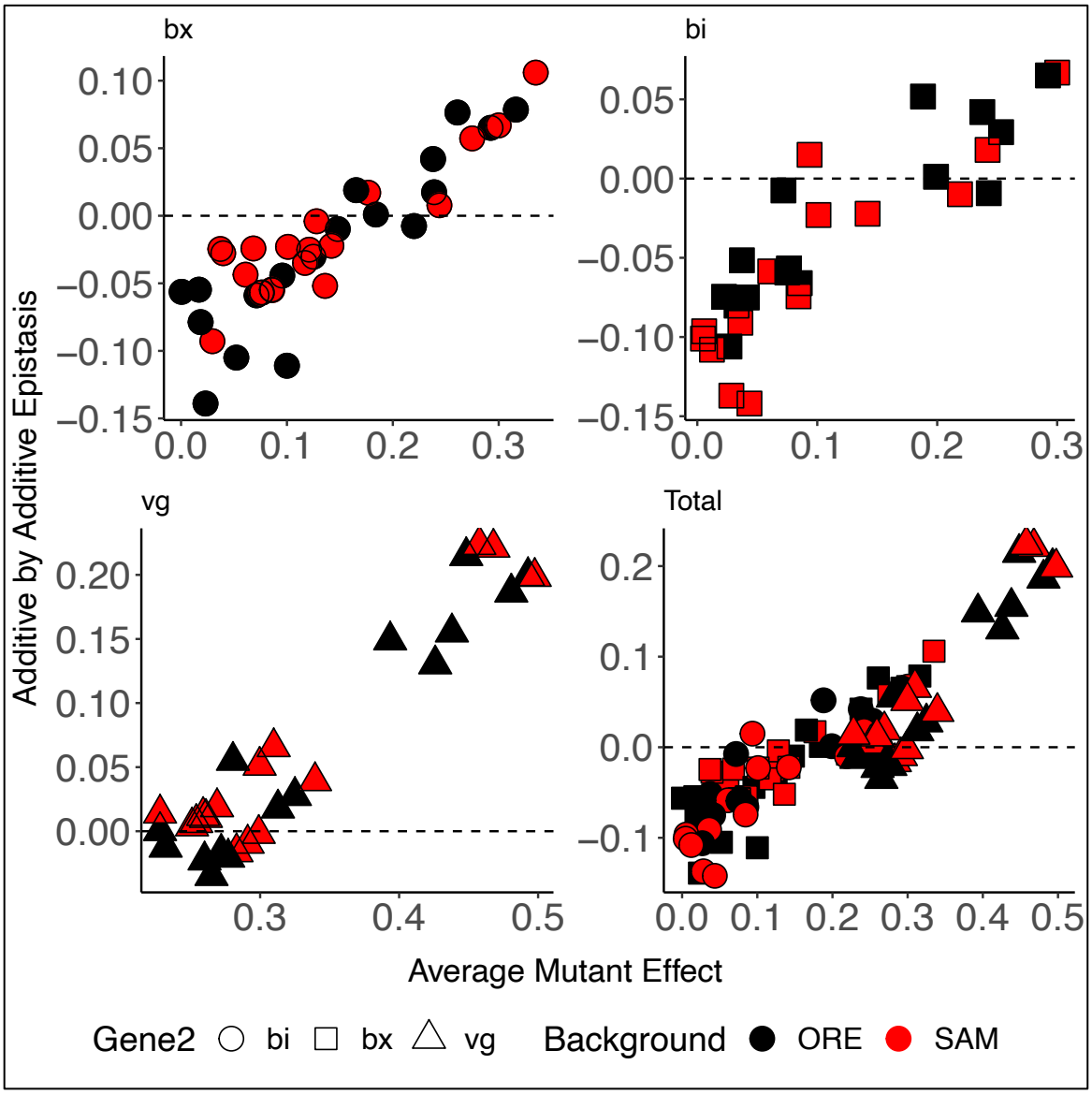

Figure 3.9: Estimates of additive–by–additive signed epistasis for each allelic pair allelic pair in Samarkand and Oregon-R for the different gene combinations. N = 5,905

Table 3.10: Statistical model estimates of the average signed epistasis for Samarkand and Oregon-R among all allelic pairs for each gene combination. The P-value representing the difference in genetic backgrounds was estimated from ANOVA analysis.

Type of Epistasis	Gene	Background	Average Mean Epistasis	Standard Error	P-Value
aa	bx	ORE	-0.0261	0.0154	**2.68E-05**
aa	bx	SAM	-0.0138	0.0154	
aa	bi	ORE	-0.0333	0.0114	9.25E-02
aa	bi	SAM	-0.0468	0.0116	
aa	vg	ORE	0.0562	0.0123	1.12E-01
aa	vg	SAM	0.0673	0.0122	
aa	Total	ORE	-0.0029	0.0076	7.01E-01
aa	Total	SAM	-0.0013	0.0076	

Table 3.11: Statistical model estimates of the effect of the average mutant effect on the signed epistasis among all allelic pairs for each gene combination. P-value estimated from ANOVA analysis.

Type of Epistasis	Gene	Effect of Average Mutant Effect	Standard Error	P-Value
aa	bx	0.679	0.0700	**< 2e-16**
aa	bi	0.531	0.0864	**1.41E-13**
aa	vg	0.984	0.0557	**<2e-16**
aa	Total	0.545	0.0451	**<2e-16**

Table 3.12: Statistical model estimates of the effect of the interaction between genetic background and the average mutant effect on the signed epistasis among all allelic pairs for each gene combination. P-value code estimated from ANOVA analysis.

Type of Epistasis	Dataset	Effect of Background: Average Mutant	Standard Error	P-Value
aa	bx	-0.0709	0.0674	0.2932
aa	bi	0.0899	0.0896	0.3155
aa	vg	-0.0136	0.0818	0.8677
aa	Total	-4.18E-3	0.0469	0.9929

Impact of the Genetic Background on Additive- by-Additive Sign Epistasis

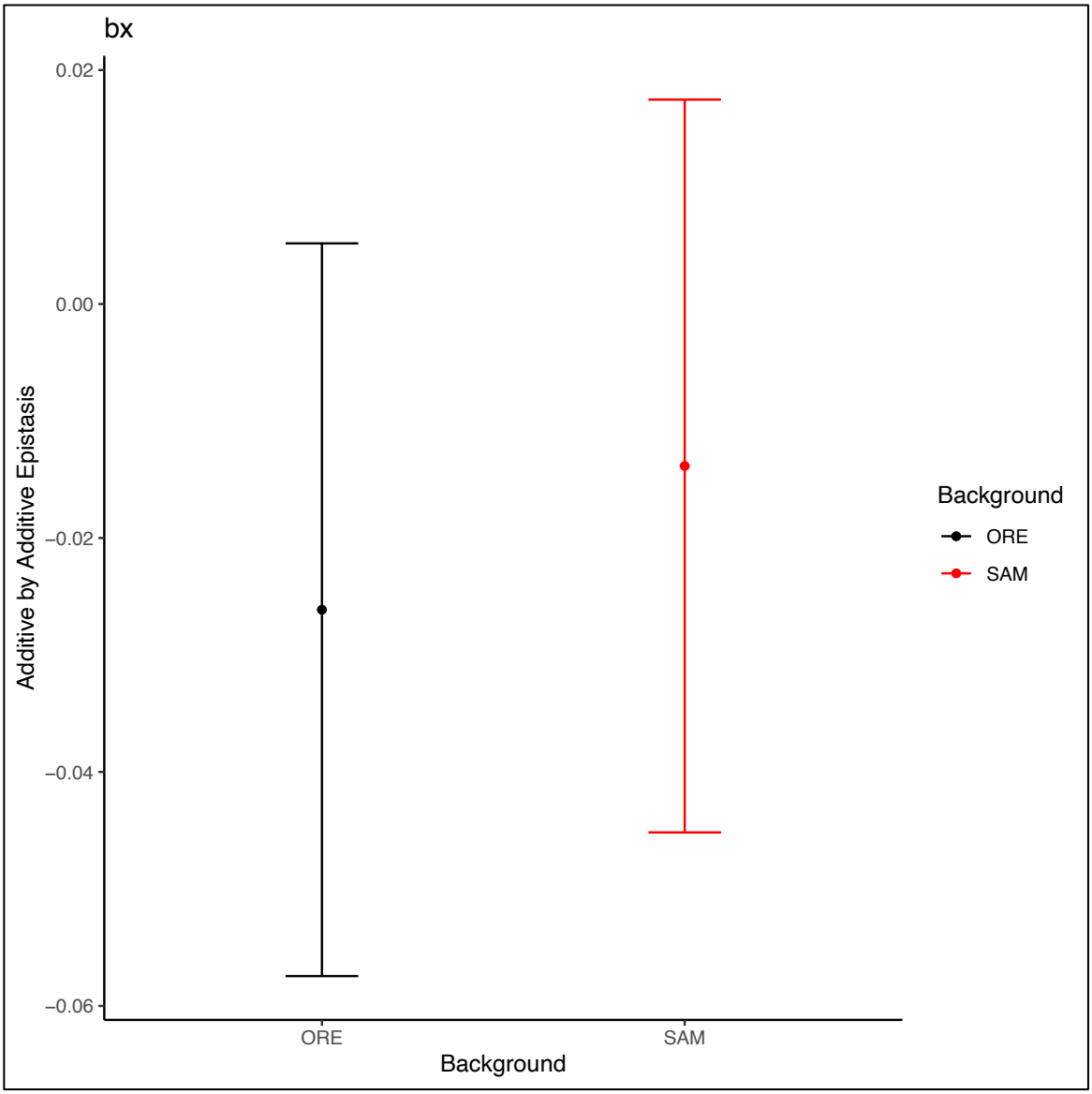

Figure 3.10: Model estimates of additive–by–additive signed epistasis for *beadex* and *scalloped* mutants in Samarkand and Oregon-R (P-value = 2.68E-05). Error bars reflect 95% confidence intervals. (Table 3.10) N = 2,460.

Impact of Average Mutant Effects on Additive-by-Additive Signed Epistasis

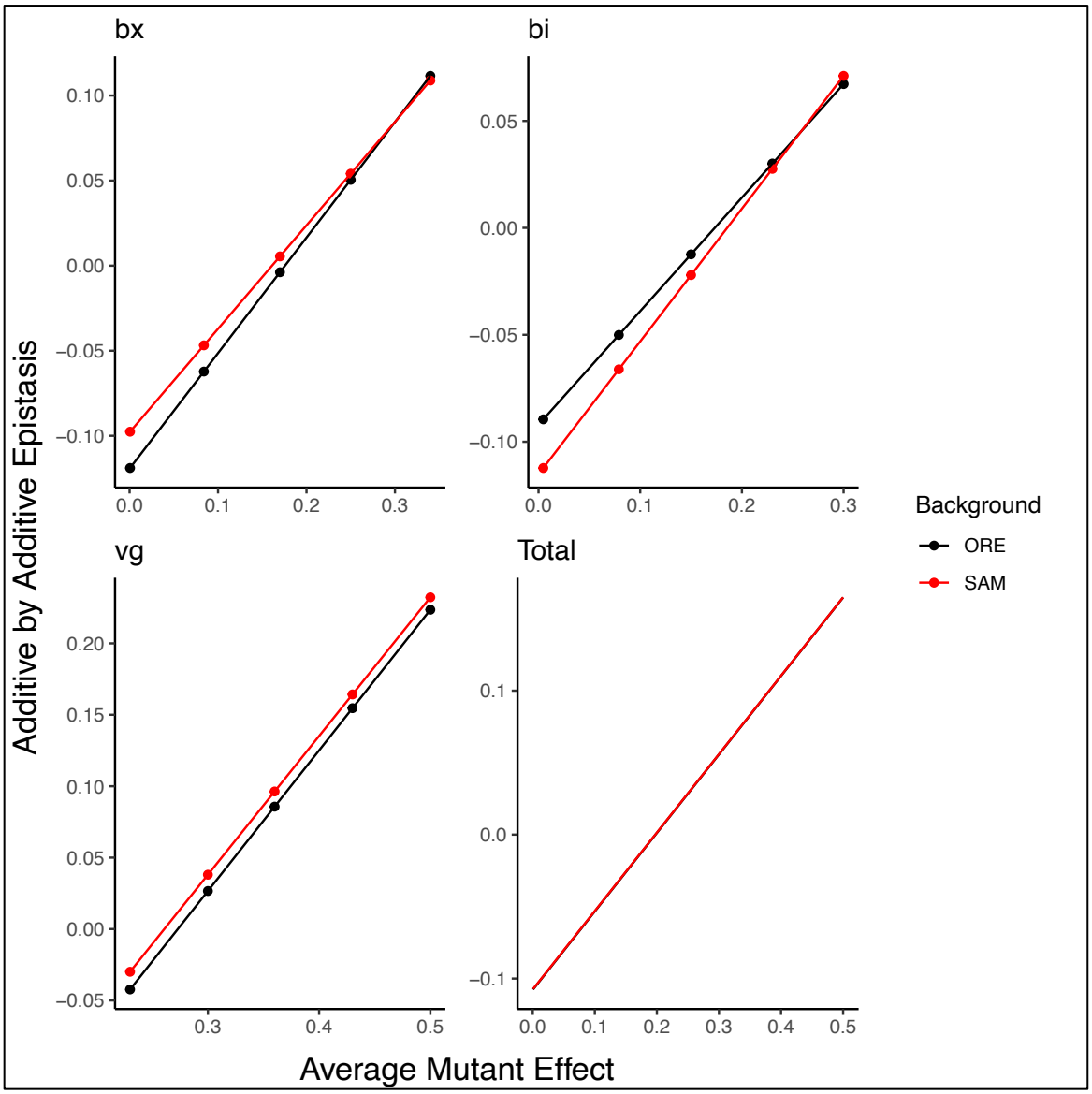

Figure 3.11:Model estimated values of the effect of average mutant effect on additive–by–additive signed epistasis for *beadex* and *scalloped* mutants (P-value = 2.20E-16), *bifid* and *scalloped* mutants (P-value= 1.41E-13), *vestigial* and *scalloped* mutants (P-value = 2.00E-16) and all mutants (P-value = 2.00E-16). (Table 3.11) N = 5,905.

Additive-by -Additive Magnitude Epistasis of Samarkand and Oregon-R Allelic Pairs

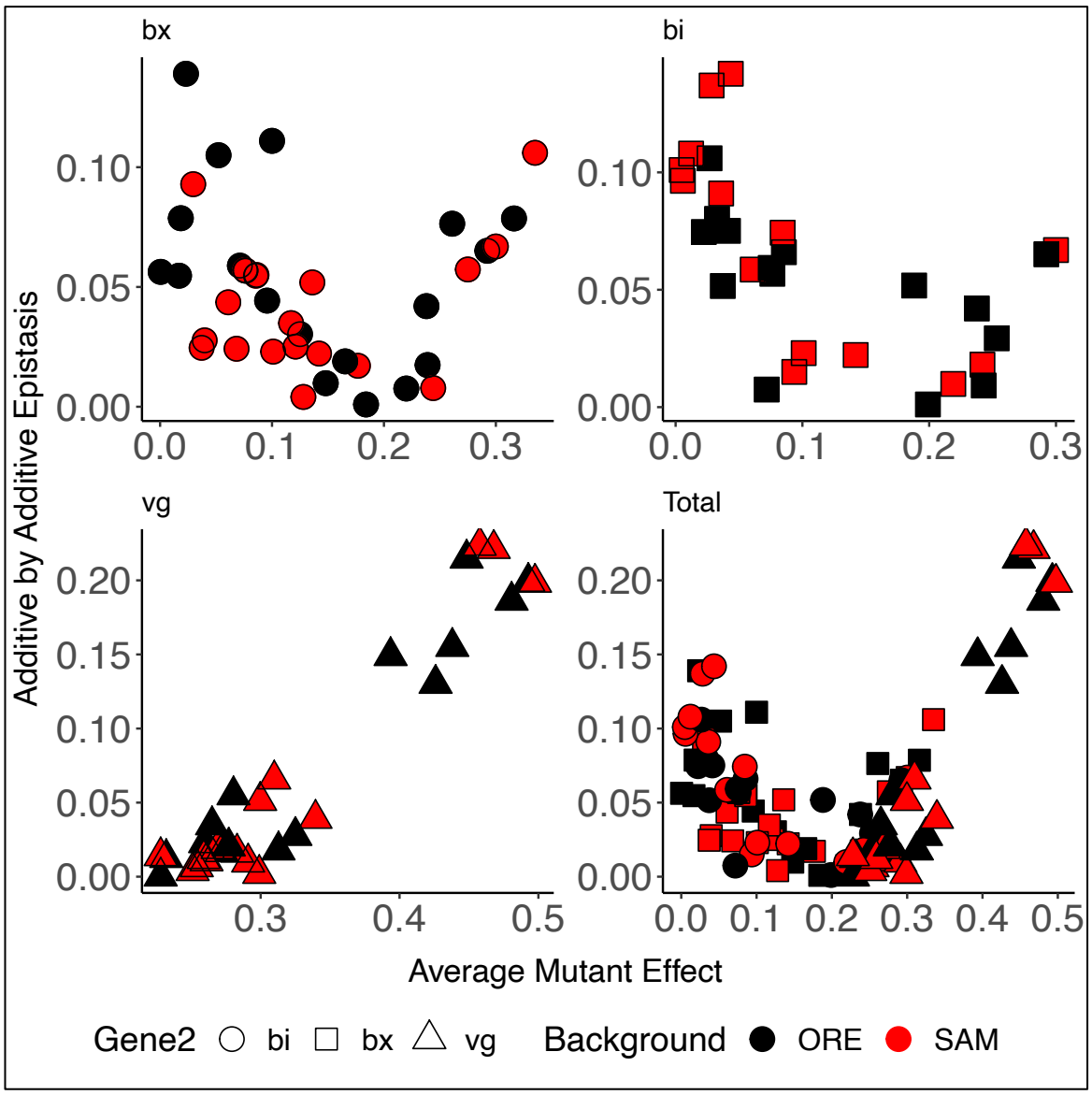

Figure 3.12: Estimates of additive–by–additive epistasis among for each allelic pair allelic pair in Samarkand and Oregon-R for the different gene combinations. N = 5,905.

Table 3.13:Statistical model estimates of the average magnitude epistasis for Samarkand and Oregon-R among all allelic pairs for each gene combination. The P-value representing the difference in genetic backgrounds was estimated from ANOVA analysis.

Type of Epistasis	Gene	Background	Average Mean Epistasis	Standard Error	P-Value
aa	bx	ORE	0.0557	0.0083	9.50E-02
aa	bx	SAM	0.0420	0.0083	
aa	bi	ORE	0.0547	0.0083	2.36E-01
aa	bi	SAM	0.0664	0.0086	
aa	vg	ORE	0.0711	0.0101	8.00E-01
aa	vg	SAM	0.0693	0.0101	
aa	Total	ORE	0.0611	0.0089	3.98E-01
aa	Total	SAM	0.0559	0.0090	

Table 3.14: Statistical model estimates of the effect of the average mutant effect on the magnitude epistasis among all allelic pairs for each gene combination. P-value estimated from ANOVA analysis.

Type of Epistasis	Gene	Effect of Average Mutant Effect	Standard Error	P-Value
aa	bx	-0.132	0.0817	0.5024
aa	bi	-0.162	0.0867	**3.03E-04**
aa	vg	0.837	0.0540	**<2e-16**
aa	Total	0.126	0.0595	**0.0258**

Table 3.15: Statistical model estimates of the effect of the interaction between genetic background and the average mutant effect on the magnitude epistasis among all allelic pairs for each gene combination. P-value estimated from ANOVA analysis.

Type of Epistasis	Dataset	Effect of Background: Average Mutant	Standard Error	P-Value
aa	bx	0.198	0.110	0.070
aa	bi	-0.144	0.127	0.25
aa	vg	0.110	0.0793	0.17
aa	Total	-0.0459	0.0781	0.56

Impact of Average Mutant Effects on Additive–by–Additive Magnitude Epistasis

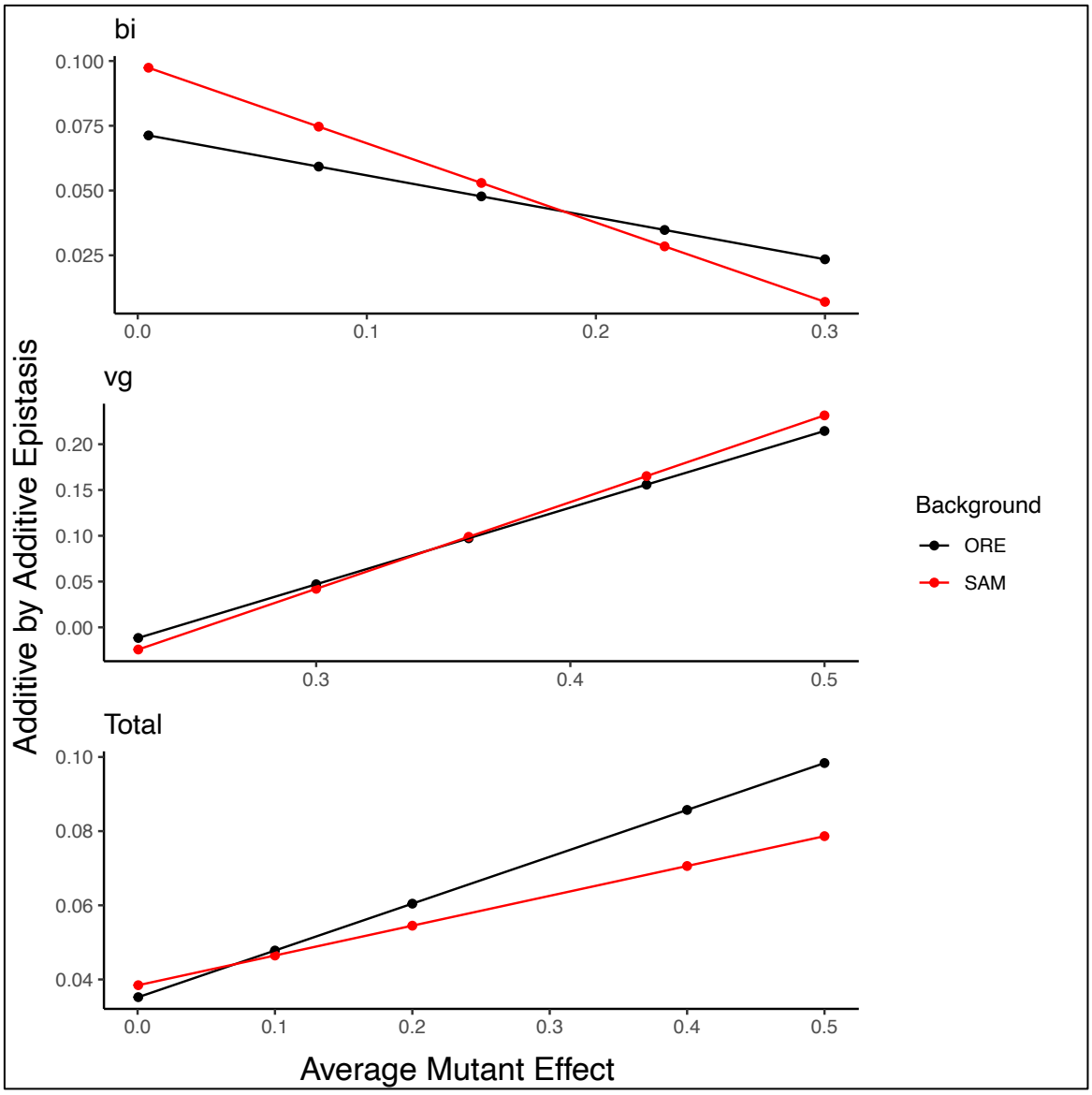

Figure 3.13: Model estimated values of the effect of average mutant effect on additive–by–additive magnitude epistasis for *beadex* and *scalloped* mutants (P-value = 3.03E-4), *bifid* and *scalloped* mutants (P-value= 2.0E-16), *vestigial* and *scalloped* mutants (P-value = 2.00E-16) and all mutants (P-value = 0.02583). (Table 3.14). N = 5,905.

Additive–by–Dominance Epistasis

For additive-by-dominance, the additive effect of Gene2 (beadex, bifid, and vestigial) is influenced by the dominance of *scalloped*. When examining the signed additive–by–dominance effects we see a significant difference between the two genetic backgrounds for *beadex* and *scalloped* mutants, *bifid* and *scalloped* mutants and all mutants combined (Figure 3.15). For these genes the additive–by–dominance effect for Oregon-R is more likely to be negative, while Samarkand is more likely to be positive. When examining the magnitude (absolute value) of additive–by–dominance effects we see less variation between the backgrounds as there is only a significant difference between the two genetic backgrounds for *beadex* and *scalloped* mutants (Figure 3.18).

The signed epistasis the average allelic effect has a significant effect for *bifid* and *scalloped* and all mutants combined (Figure 3.16). Values are more likely to be positive when the average mutant effect is weak and become more negative as the mutant effect increases. The average allelic effect is only significant when looking at all mutations together for magnitude epistasis (Figure 3.19). When the mutant effect increases so does the additive–by–dominance effect. There is also a significant interaction effect between genetic background and allelic effect for *bifid* and *scalloped* mutants (Figure 3.19). In Samarkand, as mutant effect increases, the magnitude of the additive–by–dominance effect decreases. In Oregon-R as mutant effect increases so does the magnitude of the epistatic effect.

Additive–by–Dominance Signed Epistasis of Samarkand and Oregon-R Allelic Pairs

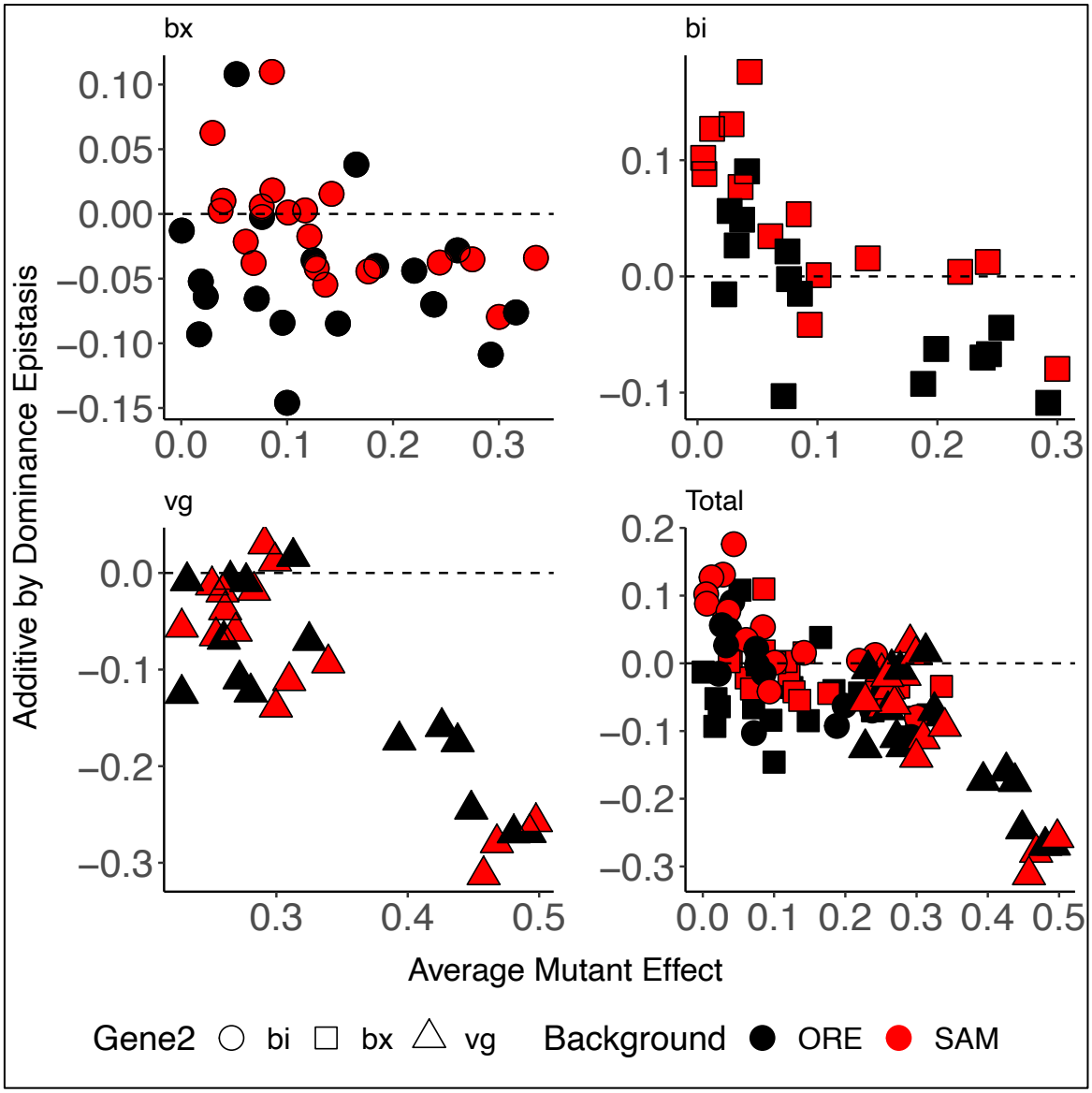

Figure 3.14: Estimates of additive–by–dominance signed epistasis for each allelic pair across Samarkand and Oregon-R wild type backgrounds for the different gene combinations. N = 5,905.

Table 3.16: Statistical model estimates of the average signed epistasis for Samarkand and Oregon-R among all allelic pairs for each gene combination. The P-value representing the difference in genetic backgrounds was estimated from ANOVA analysis.

Type of Epistasis	Gene	Background	Average Mean Epistasis	Standard Error	P-Value
ad	bx	ORE	-0.0347	0.0225	**8.49E-06**
ad	bx	SAM	0.0046	0.0225	
ad	bi	ORE	-0.0149	0.0173	**2.19E-06**
ad	bi	SAM	0.0437	0.0176	
ad	vg	ORE	-0.1178	0.0412	1.79E-01
ad	vg	SAM	-0.0974	0.0412	
ad	Total	ORE	-0.0560	0.0111	**3.61E-06**
ad	Total	SAM	-0.0195	0.0112	

Table 3.17:Statistical model estimates of the effect of the average mutant effect on the signed epistasis among all allelic pairs for each gene combination. P-value estimated from ANOVA analysis.

Type of Epistasis	Gene	Effect of Average Mutant Effect	Standard Error	P-Value
ad	bx	-0.0842	0.114	0.2912
ad	bi	-0.545	0.144	**3.97E-06**
ad	vg	-0.153	0.232	3.40E-01
ad	Total	-0.454	0.0724	**< 2.2e-16**

Table 3.18: Statistical model estimates of the effect of the interaction between genetic background and the average mutant effect on the signed epistasis among all allelic pairs for each gene combination. P-value estimated from ANOVA analysis.

Type of Epistasis	Dataset	Effect of Background: Average Mutant	Standard Error	P-Value
ad	bx	-0.0618	0.118	0.60
ad	bi	-0.125	0.142	0.37
ad	vg	-0.193	0.171	0.26
ad	Total	-0.157	0.0804	0.051

The Impact of Genetic Background on Additive–by–Dominance Signed Epistasis

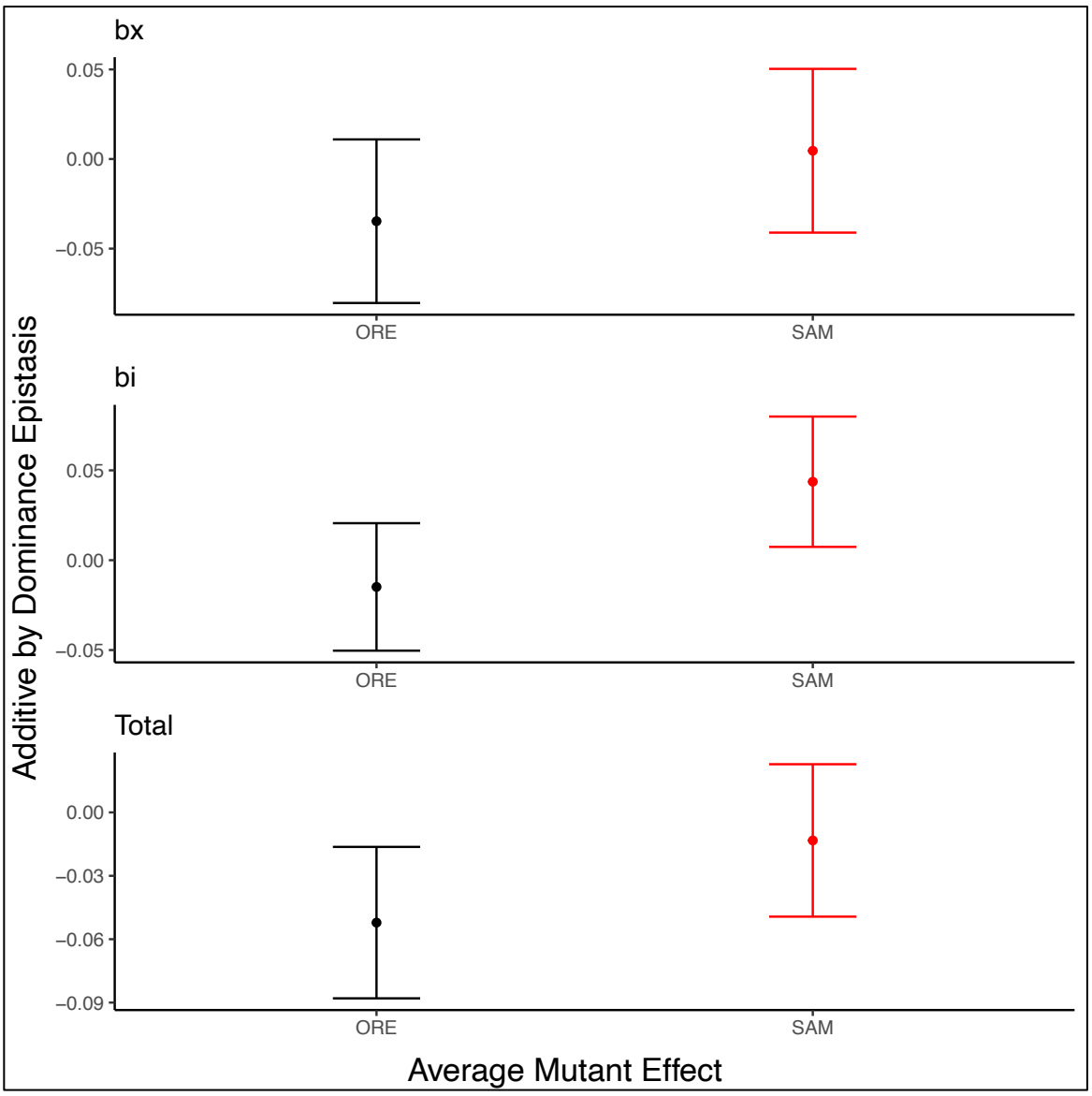

Figure 3.15: Model estimates for additive–by–dominance signed epistasis in Samarkand and Oregon-R for *beadex* and *scalloped* mutants (P-value = 8.49E-06), *bifid* and *scalloped* mutants (P-value = 2.19E-06), and all mutants (P-value =3.61E-06). Error bars reflect 95% confidence intervals. (Table 3.16) N = 5,905.

Impact of Average Mutant Effects on Additive- by-Dominance Signed Epistasis

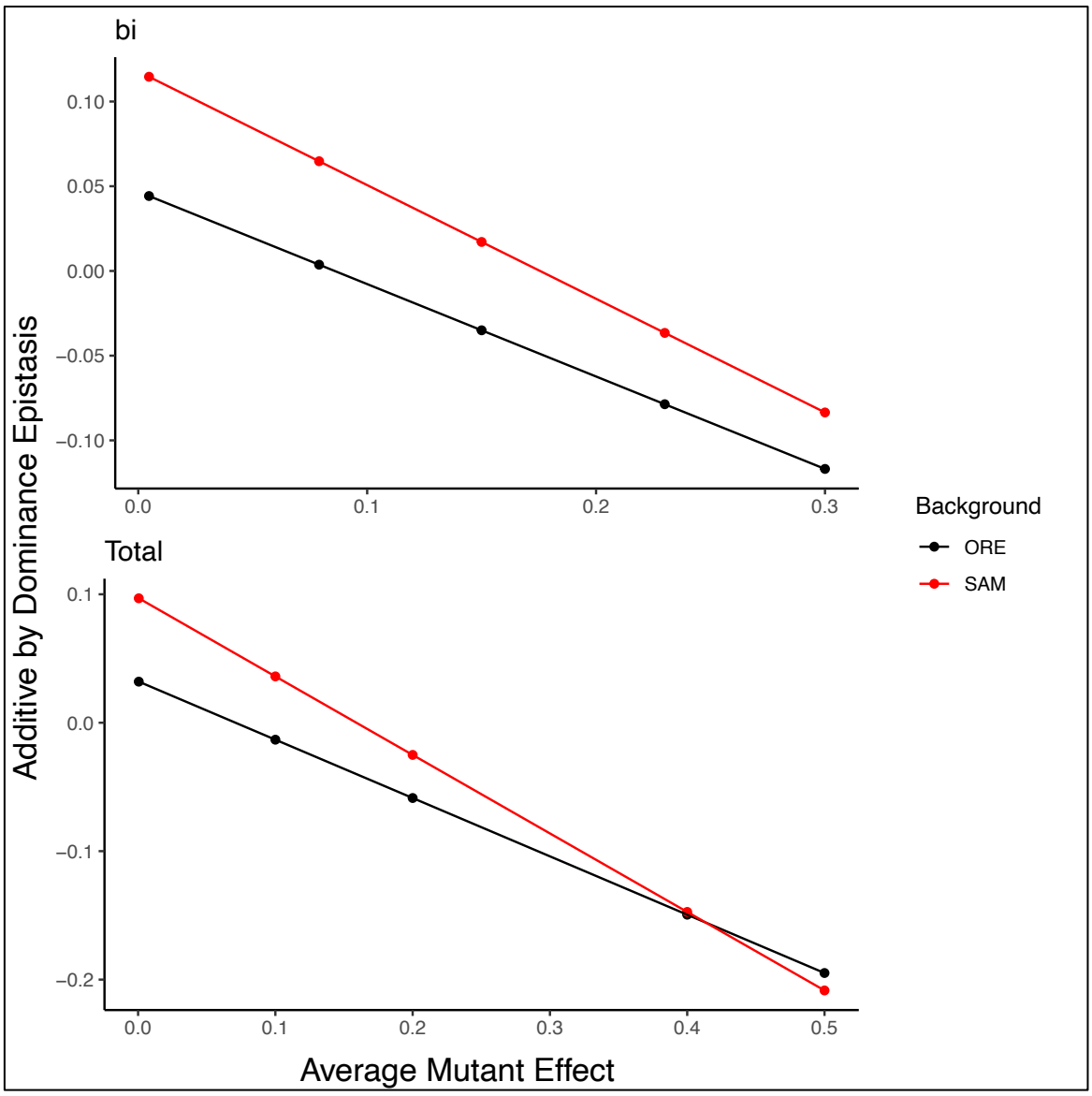

Figure 3.16: Model estimated values of the effect of average mutant effect on additive–by–dominance signed epistasis for *bifid* and *scalloped* mutants (P-value= 3.97E-06), and all mutants (P-value = 2.2E-16). (Table 3.17). N = 5,905.

Additive–by–Dominance Magnitude Epistasis of Samarkand and Oregon-R Allelic Pairs

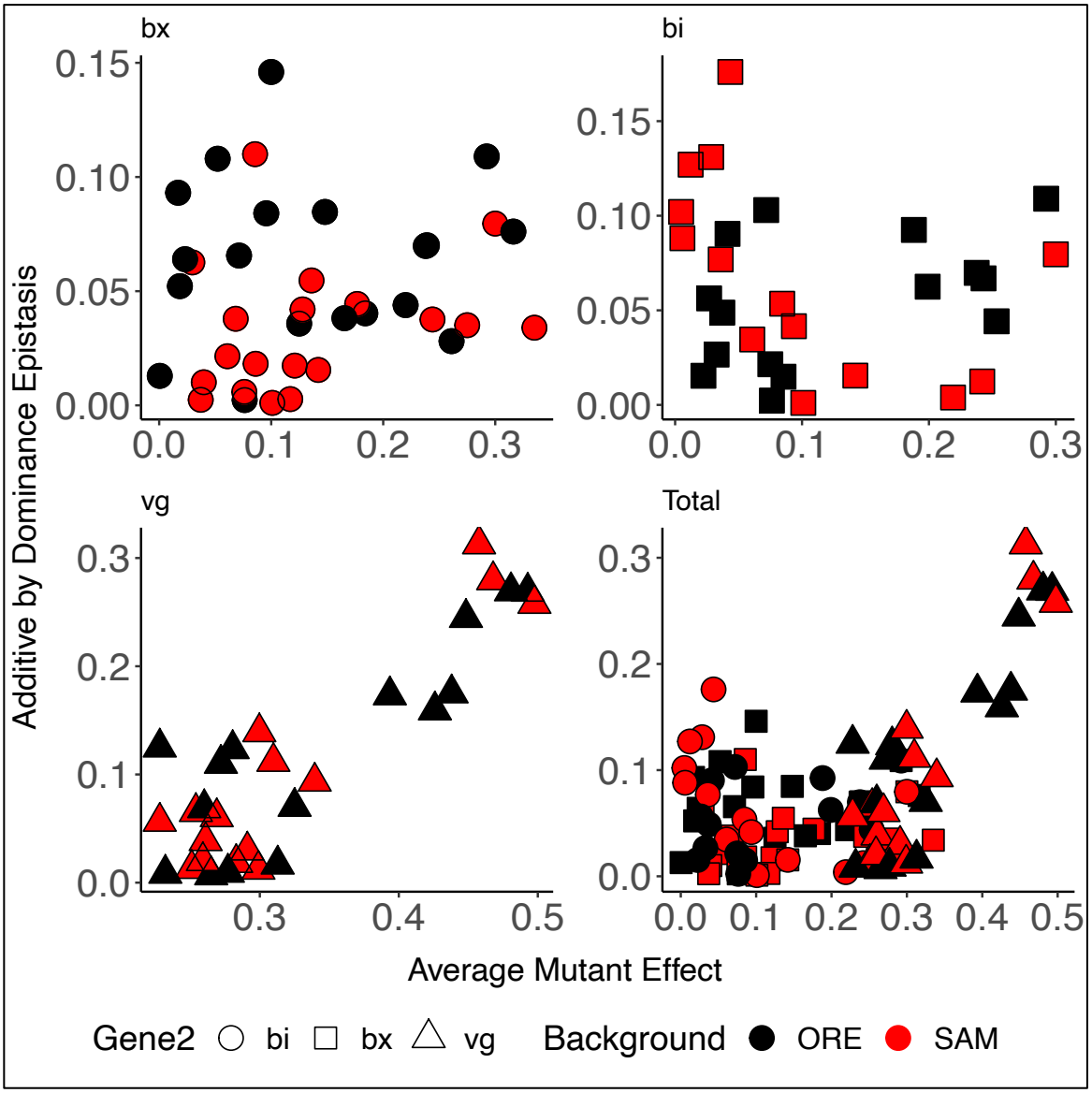

Figure 3.17: Estimates of additive- by- dominance magnitude epistasis for each all allelic pair in Samarkand and Oregon-R for the different gene combinations. N = 5,905.

Table 3.19: Statistical model estimates of the average magnitude epistasis for Samarkand and Oregon-R among all allelic pairs for each gene combination. The P-value representing the difference in genetic backgrounds was estimated from ANOVA analysis.

Type of Epistasis	Gene	Background	Average Mean Epistasis	Standard Error	P-Value
ad	bx	ORE	0.0644	0.0075	**3.49E-04**
ad	bx	SAM	0.0334	0.0075	
ad	bi	ORE	0.0557	0.0117	5.21E-01
ad	bi	SAM	0.0666	0.0121	
ad	vg	ORE	0.1187	0.0350	2.68E-01
ad	vg	SAM	0.1045	0.0350	
ad	Total	ORE	0.0782	0.0083	1.32E-01
ad	Total	SAM	0.0661	0.0084	

Table 3.20: Statistical model estimates of the effect of the average mutant effect on the magnitude epistasis among all allelic pairs for each gene combination. P-value estimated from ANOVA analysis.

Type of Epistasis	Gene	Effect of Average Mutant Effect	Standard Error	P-Value
ad	bx	0.0214	0.0771	0.4017
ad	bi	0.1581	0.1090	4.74E-01
ad	vg	0.2681	0.1950	8.56E-02
ad	Total	0.3017	0.06626	**1.39E-07**

Table 3.21: Statistical model estimates of the effect of the interaction between genetic background and the average mutant effect on the magnitude epistasis among all allelic pairs for each gene combination. P-value estimated from ANOVA analysis.

Type of Epistasis	Dataset	Effect of Background: Average Mutant	Standard Error	P-Value
ad	bx	0.0581	0.114	0.61
ad	bi	-0.462	0.160	**0.0038**
ad	vg	0.183	0.143	0.20
ad	Total	-0.0613	0.0884	0.49

The Impact of Genetic Background on Additive–by–Dominance Magnitude Epistasis

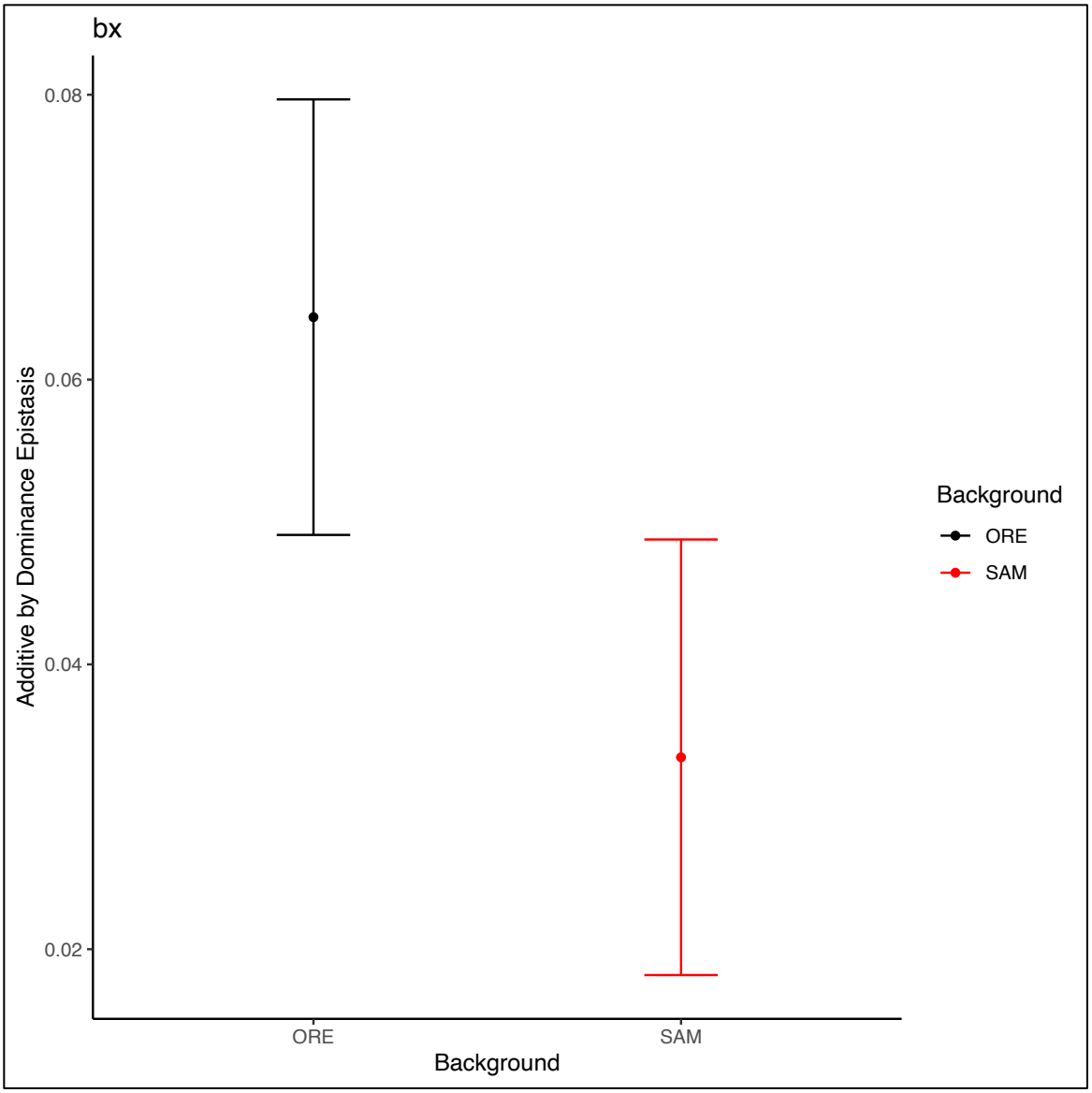

Figure 3.18: Statistical model estimates of additive-by-dominance magnitude epistasis for *beadex* and *scalloped* mutants in Samarkand and Oregon-R (P-value = 3.49E-02). Error bars reflect 95% confidence intervals. (Table 3.19). N = 2,460.

The Impact of Average Mutant Effects on Additive-by-dominance Magnitude Epistasis

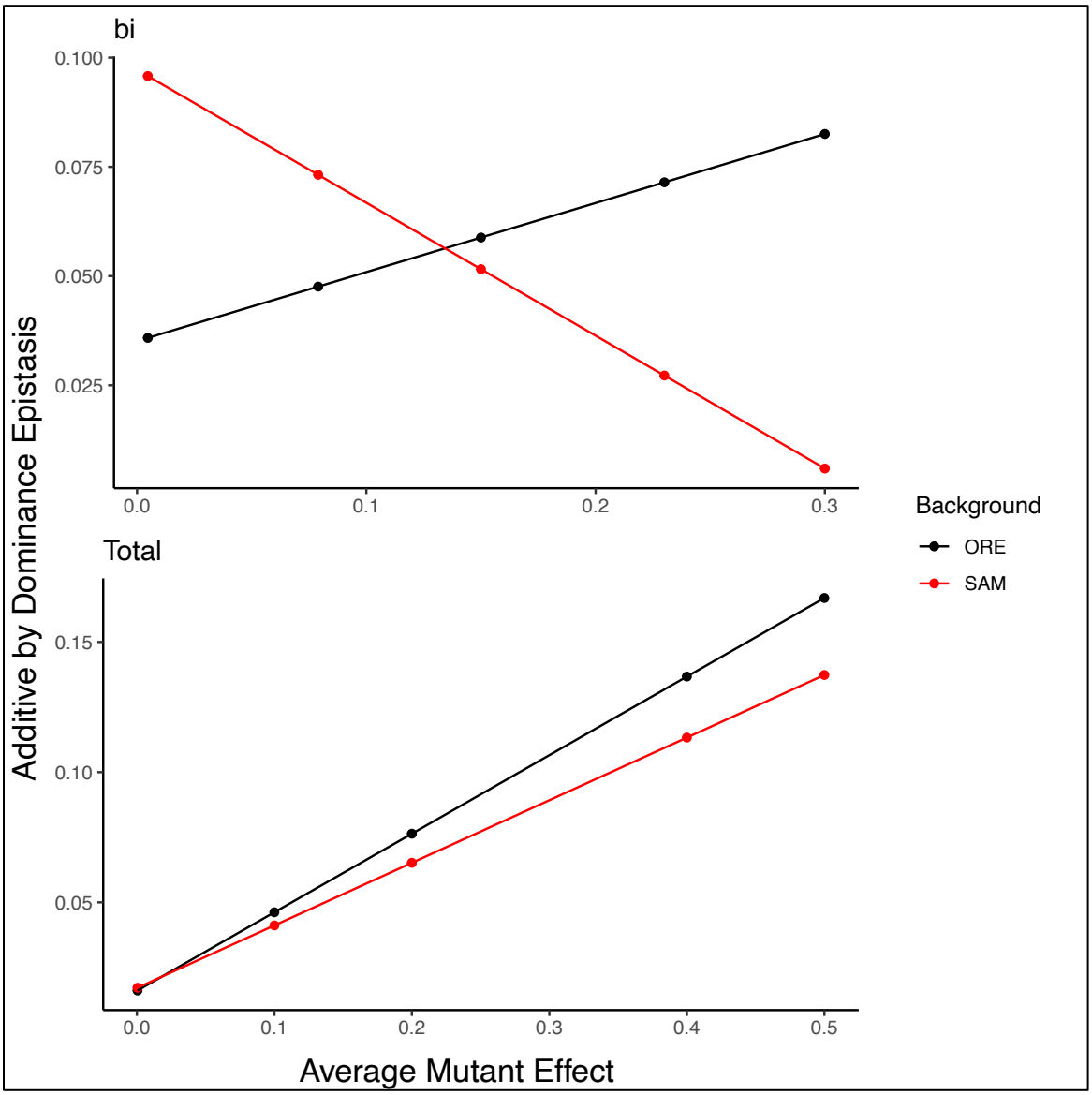

Figure 3.19: Model estimated values for the effect of average mutant effect on additive–by–dominance magnitude epistasis for all mutants (P-value = 1.39E-07) (Table 4.5). There is also a significant interaction effect between genetic background and average mutant effect for *bifid* and *scalloped* mutants (P-value= 0.0038). (Table 3.20 and Table 3.21). N = 5,905.

Dominance–by–Additive Epistatic Effects

For dominance-by-additive epistasis, the dominance of Gene2 (*beadex, bifid*, and *vestigial*) is influenced by the additive effect for *scalloped*. When examining the dominance-by-additive signed epistasis there are significant differences between Samarkand and Oregon-R for *beadex* and *scalloped* mutants, *bifid* and *scalloped* mutants, and all mutants combined (Figure 3.21). Oregon-R is likely to be more negative than Samarkand for this epistatic effect. When examining the magnitude of dominance–by–additive effects there are no significant differences between genetic backgrounds for any allelic combination (Table 3.25).

For the signed dominance-by-additive effects we see that the allelic effect is significant for *beadex* and *scalloped*, *vestigial* and *scalloped* and all mutants combined (Figure 3.22). Values are more likely to be positive when the average mutant effect is weak and become more negative as the mutant effect increases. There is also a significant interaction between mutant effect and the genetic background for *bifid* and *scalloped* mutants (Figure 3.22). In Oregon- R as the mutant effect increases, the dominance-by-additive epistasis becomes more negative. While in Samarkand as the mutant effect increases the epistatic effect becomes more positive. The average allelic effect is significant for *beadex* and *scalloped* mutants, *vestigial* and *scalloped* mutants and all mutants combined when examining magnitude epistasis (Figure 3.24). As mutant effect increases so does the magnitude of dominance-by-additive effects. Interestingly, there is a significant effect from the interaction of background and mutant effect for

magnitude epistasis (Figure 3.24). For *bifid* and *scalloped* mutants, in Samarkand as mutant effect increases, the epistatic effect decreases. While in Oregon-R as the mutant effect increases so does the epistatic effect. For all the mutants combined the magnitude of dominance-by-additive increases with average mutant effect. However, in Oregon-R this increase is faster, indicated by changes in slope.

Dominance–by–Additive Signed Epistasis of Samarkand and Oregon-R Allelic Pairs

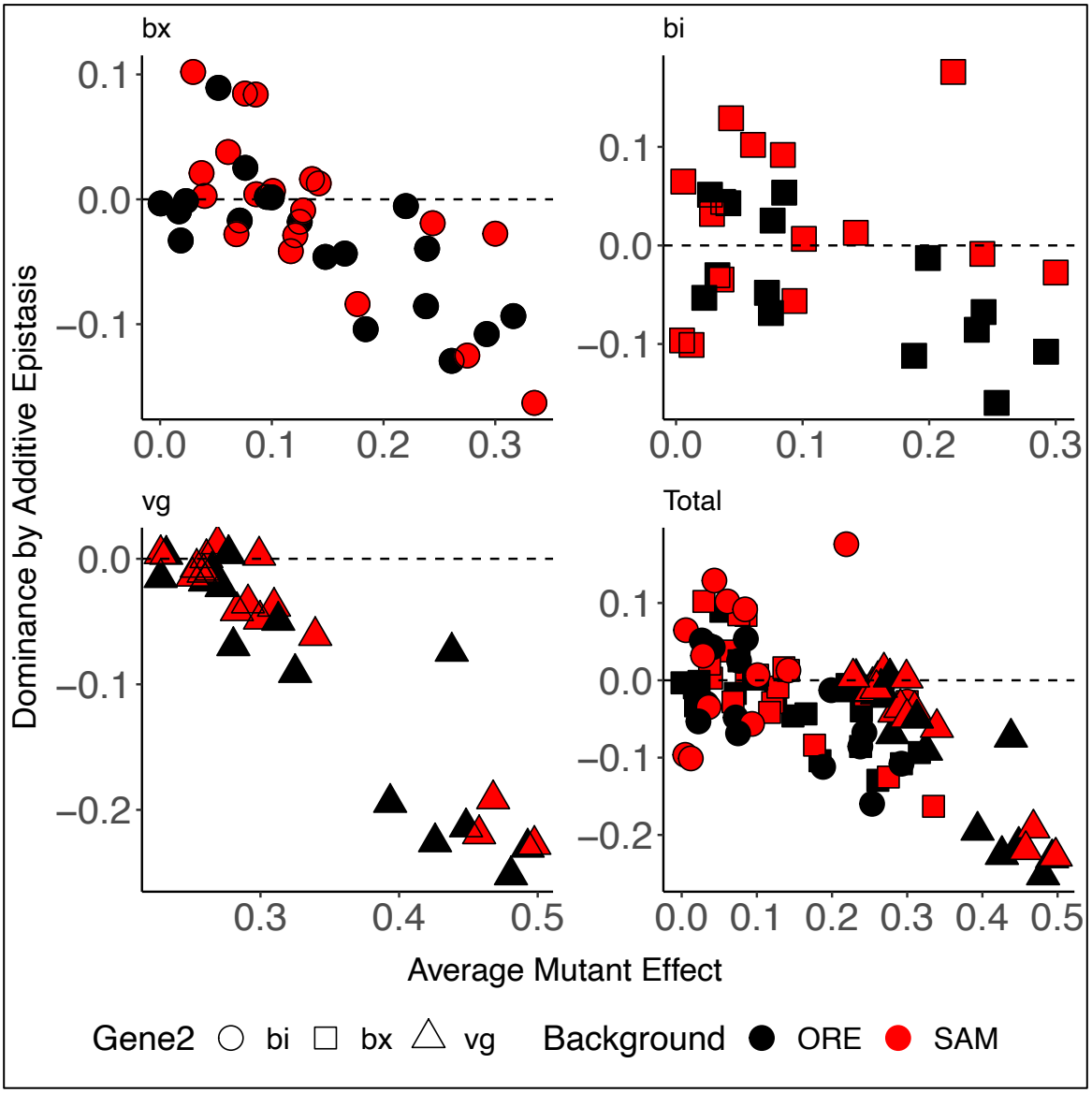

Figure 3.20: Estimates of dominance–by–additive sign epistasis for each allelic pair in Samarkand and Oregon-R for the different gene combinations. N = 5,905.

Table 3.22:Statistical model estimates of the average signed epistasis for Samarkand and Oregon-R among all allelic pairs for each gene combination. The P-value representing the difference in genetic backgrounds was estimated from ANOVA analysis.

Type of Epistasis	Gene	Background	Average Mean Epistasis	Standard Error	P-Value
da	bx	ORE	-0.0239	0.0163	**3.22E-02**
da	bx	SAM	-0.0017	0.0163	
da	bi	ORE	-0.0308	0.0228	**3.74E-02**
da	bi	SAM	0.0193	0.0232	
da	vg	ORE	-0.0882	0.0112	1.21E-01
da	vg	SAM	-0.0725	0.0112	
da	Total	ORE	-0.0472	0.0103	**2.84E-04**
da	Total	SAM	-0.0158	0.0104	

Table 3.23: Statistical model estimates of the effect of the average mutant effect on the signed epistasis among all allelic pairs for each gene combination. P-value estimated from ANOVA analysis.

Type of Epistasis	Gene	Effect of Average Mutant Effect	Standard Error	P-Value
da	bx	-0.445	0.119	**3.2E-06**
da	bi	-0.607	0.222	0.098
da	vg	-0.940	0.0926	**<2e-16**
da	Total	-0.429	0.0677	**1.06E-13**

Table 3.24: Statistical model estimates of the effect of the interaction between genetic background and the average mutant effect on the signed epistasis among all allelic pairs for each gene combination. P-value estimated from ANOVA analysis.

Type of Epistasis	Dataset	Effect of Background: Average Mutant	Standard Error	P-Value
da	bx	-0.180	0.116	0.12
da	bi	0.647	0.249	**0.0093**
da	vg	-0.0158	0.124	0.90
da	Total	0.0527	0.0870	**0.54**

Impact of Genetic Background Effects on Dominance–by–Additive Signed Epistasis

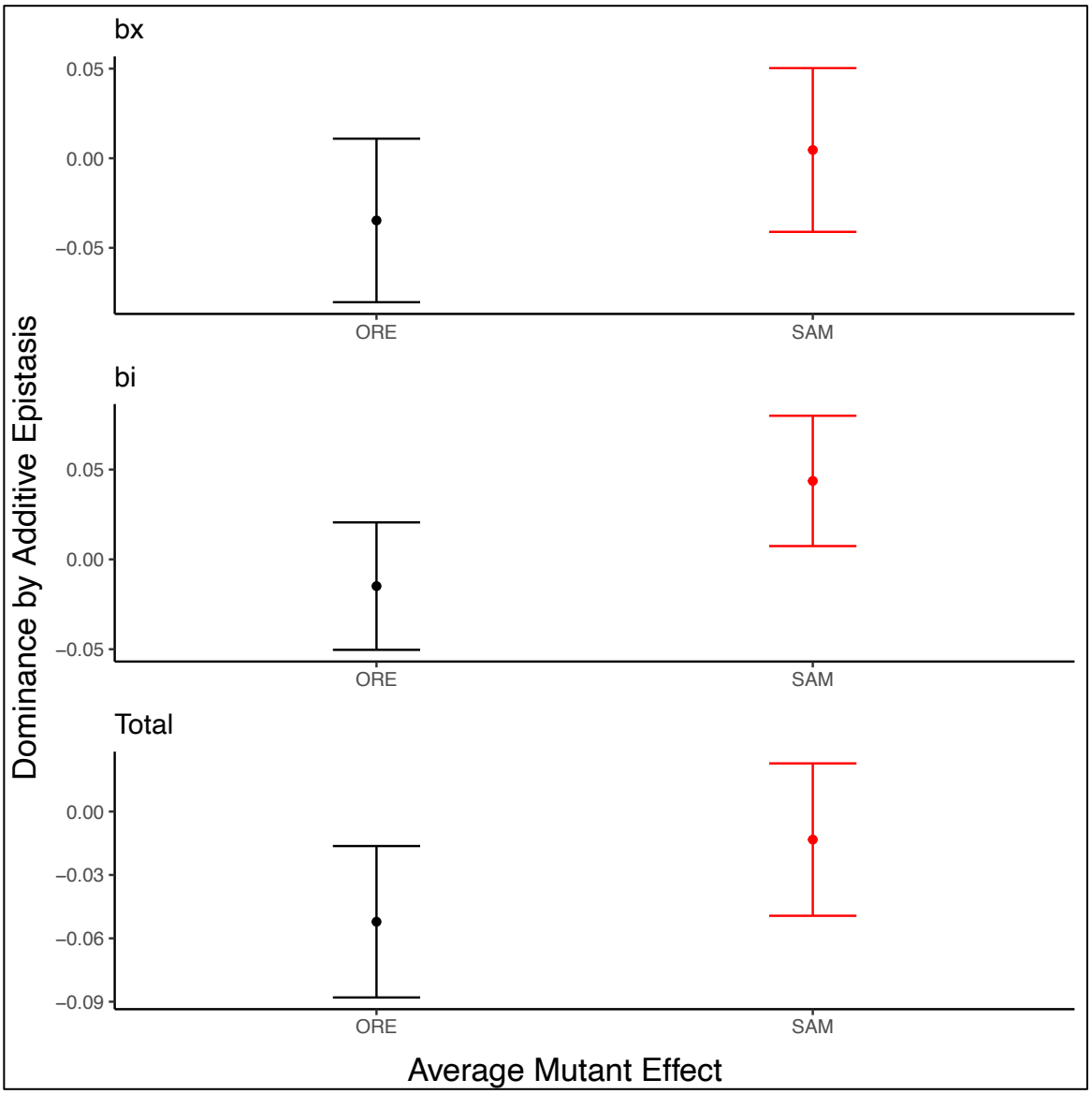

Figure 3.21: Statistical model estimates of dominance- by- additive sign epistasis in Samarkand and Oregon for *beadex* and *scalloped* mutants (P-value = 3.22E-02), *bifid* and *scalloped* mutants (P-value = 3.74E-02), and all mutants (P-value = 2.84E-04). Error bars reflect 95% confidence intervals. (Table 3.22) N = 5,905.

The impact of Average Mutant Effects on Dominance-by-additive Sign Epistasis

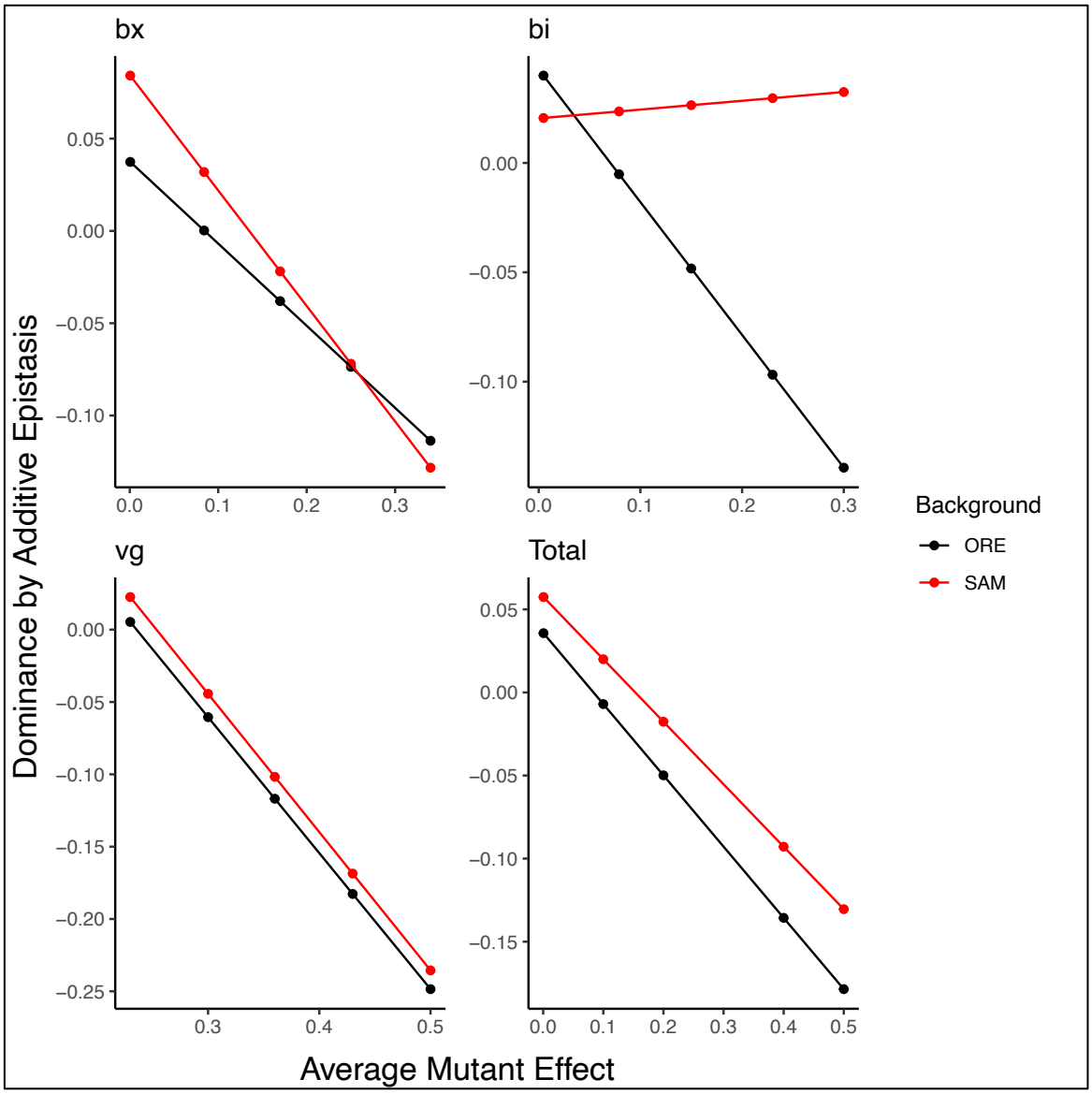

Figure 3.22: Model estimated values for the effect of average mutant effect on dominance–by–additive signed epistasis for *beadex* and *scalloped* mutants (P-value = 3.18E-06), *vestigial* and *scalloped* mutants (P-value= 2E-16), and all mutants (P-value = 1.06E-13)(Table 3.23). There is also a significant interaction effect between genetic background and average mutant effect for *bifid* and *scalloped* mutants (P-value= 0.009398). (Table 3.24). N = 5,905.

Dominance–by–Additive Magnitude Epistasis of Samarkand and Oregon-R Allelic Pairs

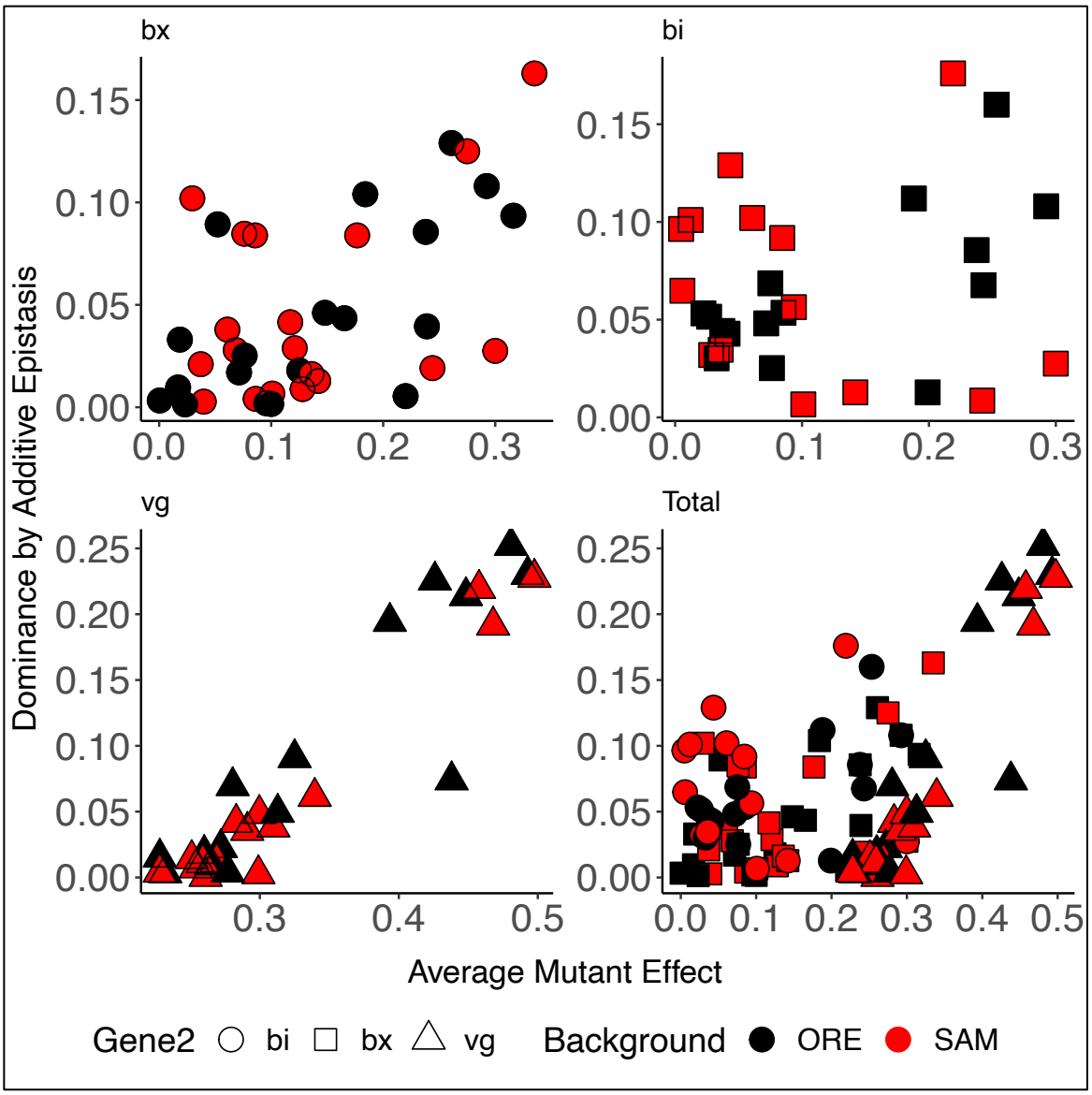

Figure 3.23: Estimates of dominance–by–additive magnitude epistasis for each allelic pair in Samarkand and Oregon-R for the different gene combinations. N = 5,905.

Table 3.25: Statistical model estimates of the average magnitude epistasis for Samarkand and Oregon-R among all allelic pairs for each gene combination. The P-value representing the difference in genetic backgrounds was estimated from ANOVA analysis.

Type of Epistasis	Gene	Background	Average Mean Epistasis	Standard Error	P-Value
ad	bx	ORE	0.0499	0.0140	7.1E-01
ad	bx	SAM	0.0534	0.0141	
ad	bi	ORE	0.0655	0.0147	6.5E-01
ad	bi	SAM	0.0726	0.0151	
ad	vg	ORE	0.0889	0.0106	1.5E-01
ad	vg	SAM	0.0746	0.0106	
ad	Total	ORE	0.0604	0.0127	4.2E-01
ad	Total	SAM	0.0538	0.0127	

Table 3.26: Statistical model estimates of the effect of the average mutant effect on the magnitude epistasis among all allelic pairs for each gene combination. P-value estimated from ANOVA analysis.

Type of Epistasis	Gene	Effect of Average Mutant Effect	Standard Error	P-Value
ad	bx	0.316	0.0862	**2.6E-05**
ad	bi	-0.607	0.222	0.098
ad	vg	0.939	0.0851	**<2e-16**
ad	Total	0.269	0.0644	**5.3E-04**

Table 3.27: Statistical model estimates of the effect of the interaction between genetic background and the average mutant effect on the magnitude epistasis among all allelic pairs for each gene combination. P-value estimated from ANOVA analysis.

Type of Epistasis	Dataset	Effect of Background: Average Mutant	Standard Error	P-Value
ad	bx	-0.0541	0.1157	0.64
ad	bi	0.647	0.2492	**0.0093**
ad	vg	0.0050	0.1227	0.97
ad	Total	-0.170	0.0726	**0.019**

The Impact of Average Mutant Effect on Dominance–by–Additive Magnitude Epistasis

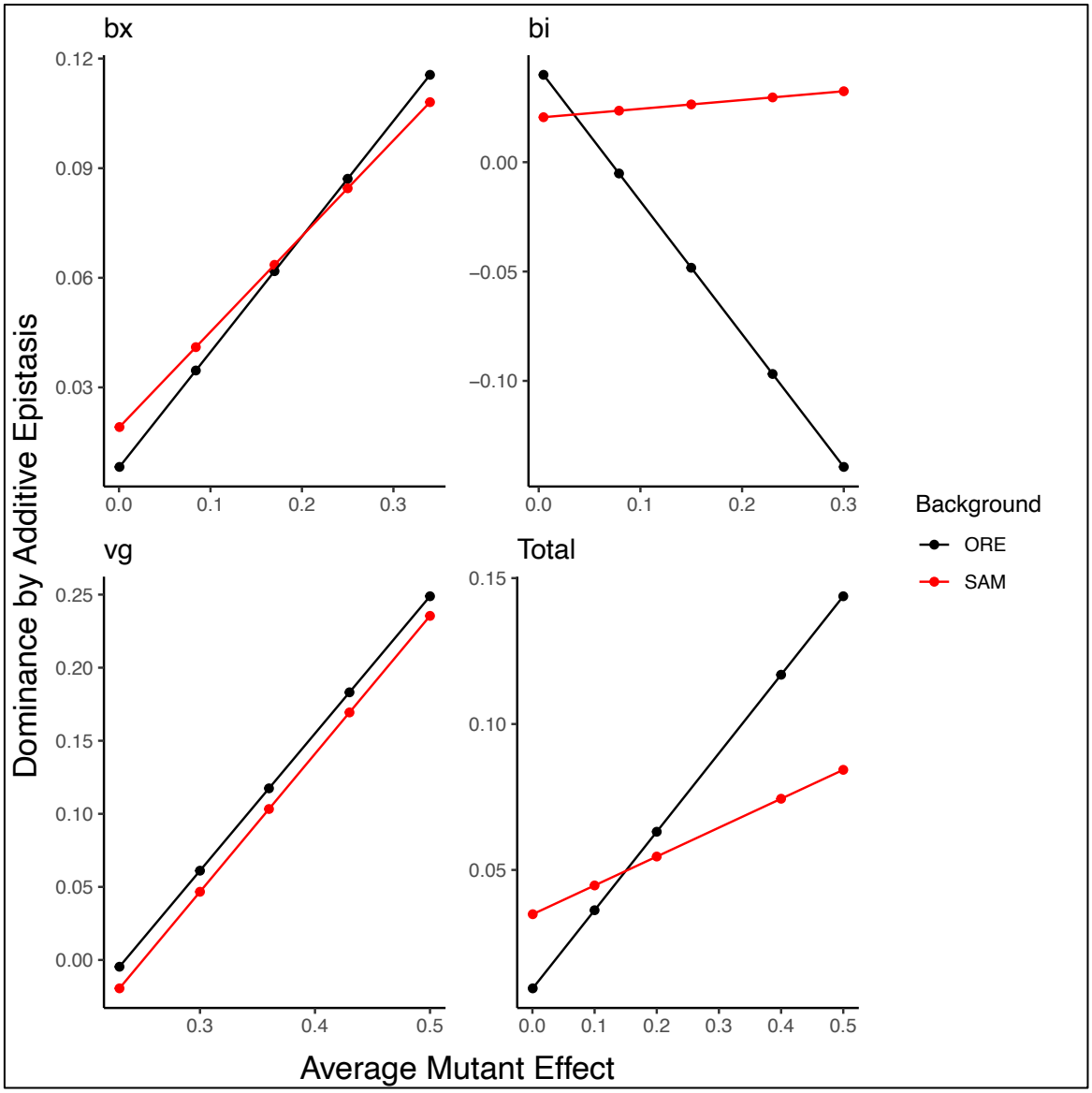

Figure 3.24: Statistical model estimates of the effect of average mutant effect on dominance–by–additive magnitude epistasis for *beadex* and *scalloped* mutants (P-value = 2.58E-05), *vestigial* and *scalloped* mutants (P-value= 2E-16), and all mutants (P-value = 5.26E-04)(Table 3.26). There is also a significant interaction effect between genetic background and average mutant effect for *bifid* and *scalloped* mutants (P-value= 0.0093), and all mutants (P-value= 0.0193). (Table 3.27). N = 5,905.

Dominance–by–Dominance Epistasis

When examining the signed dominance–by–dominance epistatic effects we see a significant difference between genetic backgrounds for *beadex* and *scalloped* mutants (Figure 3.26). Oregon-R is more likely to have a negative value, while Samarkand is more likely to be positive. However, we see no significant differences between Samarkand and Oregon-R for the magnitude of dominance–by–dominance effects (Table 3.31).

For signed epistasis, the allelic effect has a significant effect for *bifid* and *scalloped* mutants, *vestigial* and *scalloped* mutants, and all mutants combined (Figure 3.27). The dominance–by–dominance effect is more likely to be negative when the average mutant effect is small and become more positive as mutant effect increases. The average allelic effect is significant for *vestigial* and *scalloped* mutants and all mutants when examining magnitude epistasis (Figure 3.29). For both mutant combinations as the mutant effect increases so does the magnitude of the dominance–by–dominance effect.

Dominance–by–Dominance Signed Epistasis of Samarkand and Oregon-R Allelic Pairs

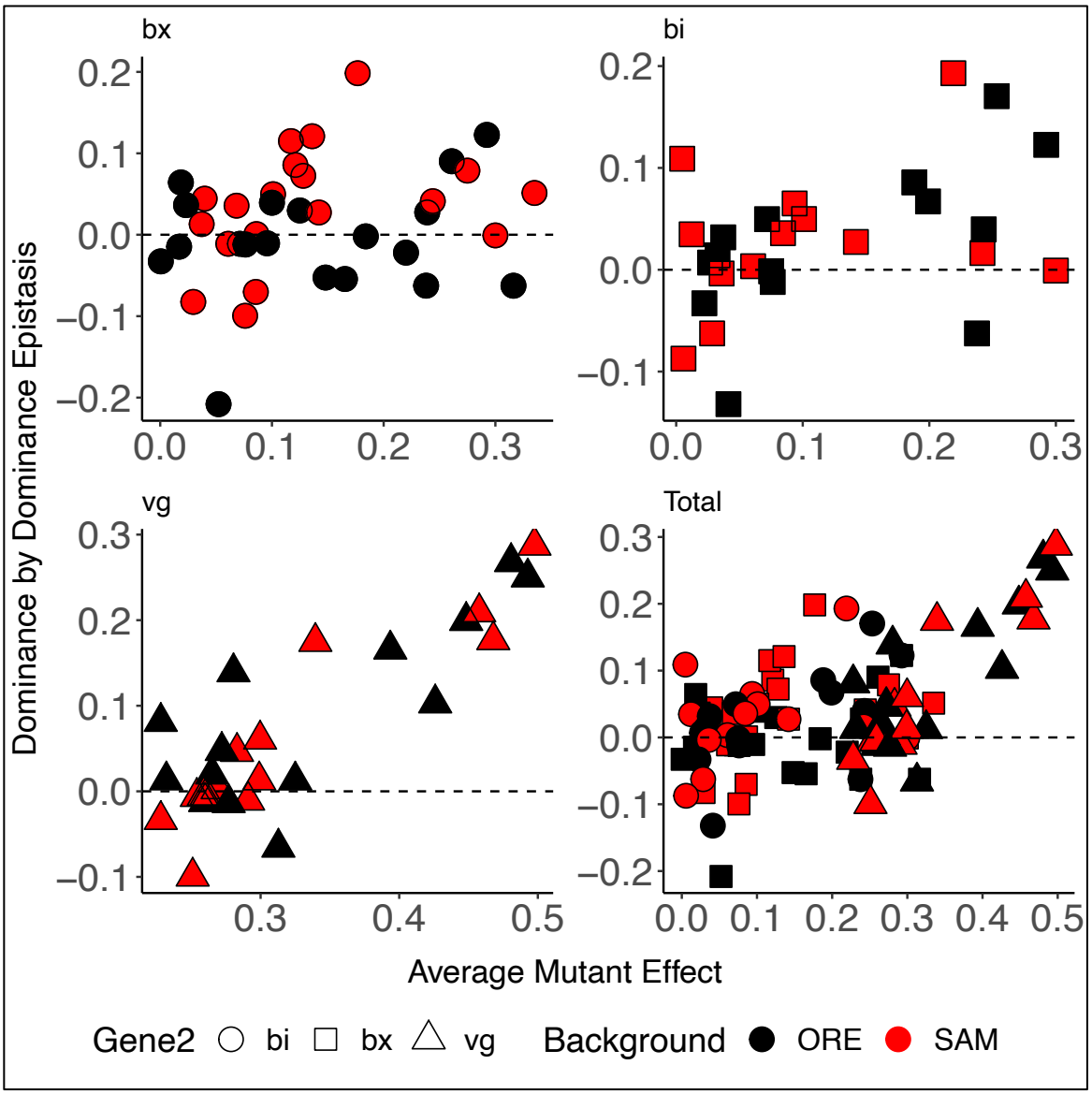

Figure 3.25:Estimates of dominance–by–dominance signed epistasis for each allelic pair in Samarkand and Oregon-R for the different gene combinations. N = 5,905.

Table 3.28: Statistical model estimates of the signed dominance–by–dominance epistasis for Samarkand and Oregon-R among all allelic pairs for each gene combination. The P-value representing the difference in genetic backgrounds was estimated from ANOVA analysis.

Type of Epistasis	Gene	Background	Average Mean Epistasis	Standard Error	P-Value
dd	bx	ORE	-0.0251	0.0287	**2.06E-02**
dd	bx	SAM	0.0177	0.0287	
dd	bi	ORE	0.0215	0.0214	5.78E-01
dd	bi	SAM	0.0353	0.0224	
dd	vg	ORE	0.0765	0.0164	6.04E-01
dd	vg	SAM	0.0657	0.0164	
dd	Total	ORE	0.0267	0.0137	2.35E-01
dd	Total	SAM	0.0417	0.0139	

Table 3.29: Statistical model estimates of the effect of the average mutant effect on the signed dominance–by–dominance epistasis among all allelic pairs for each gene combination. P-value estimated from ANOVA analysis.

Type of Epistasis	Gene	Effect of Average Mutant Effect	Standard Error	P-Value
dd	bx	0.0491	0.148	4.1E-01
dd	bi	0.448	0.182	**0.010**
dd	vg	0.890	0.162	**<2e-16**
dd	Total	0.389	0.0895	**3.8E-06**

Table 3.30: Statistical model estimates of the effect of the interaction between genetic background and the average mutant effect on the signed dominance–by–dominance epistasis among all allelic pairs for each gene combination. P-value estimated from ANOVA analysis.

Type of Epistasis	Dataset	Effect of Background: Average Mutant	Standard Error	P-Value
dd	bx	0.0993	0.214	0.64
dd	bi	-0.211	0.261	0.42
dd	vg	0.256	0.235	0.28
dd	Total	-0.123	0.113	0.28

Impact of Genetic Background on Dominance–by–Dominance Signed Epistasis

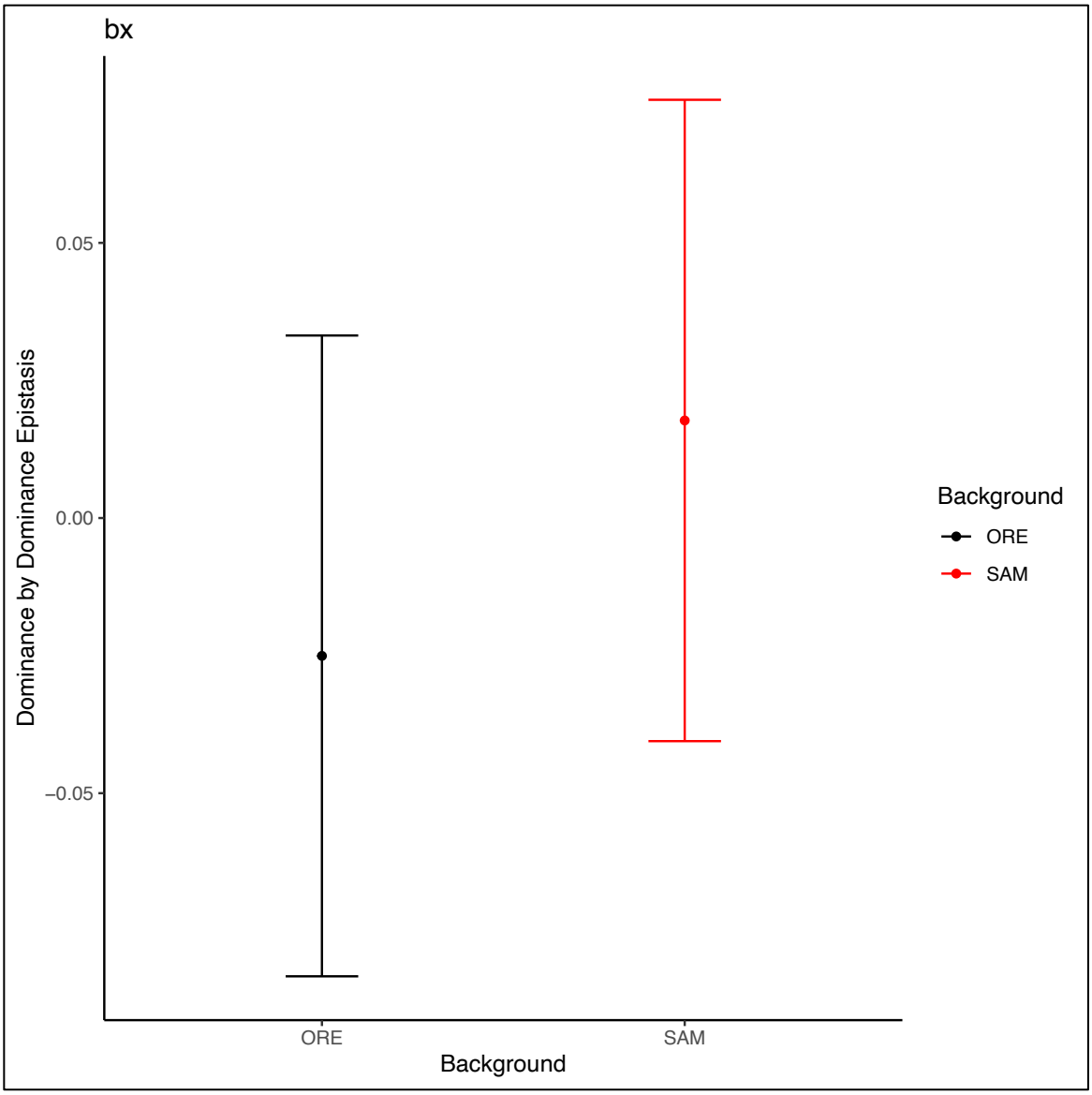

Figure 3.26: Statistical model estimates of dominance–by–dominance signed epistasis for *beadex* and *scalloped* mutants in Samarkand and Oregon-R (P-value = 2.06E-02) Error bars reflect 95% confidence intervals. (Table 3.28). N = 2,460.

Impact of Average Mutant Effect on Dominance-by-Dominance Signed Epistasis

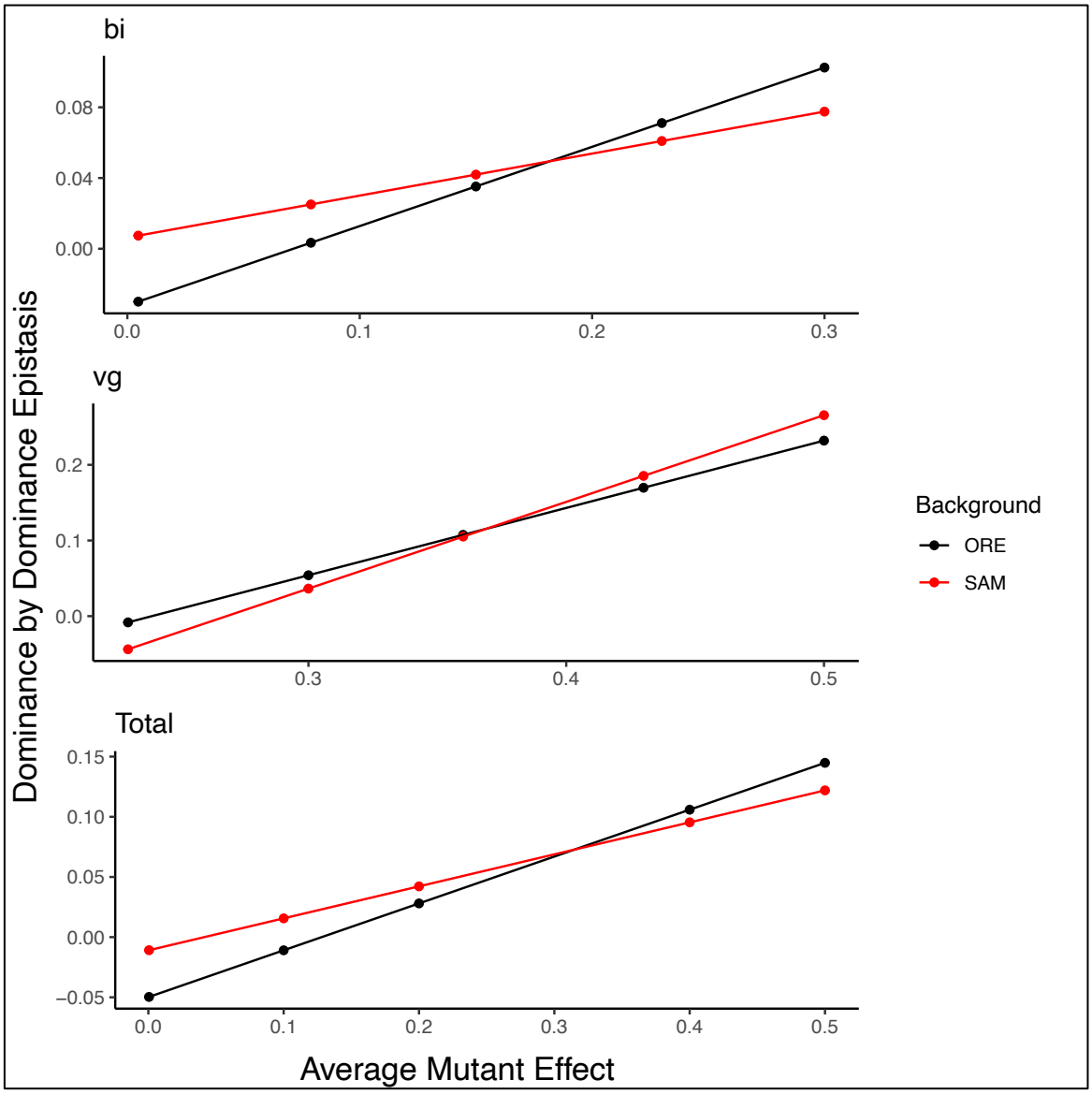

Figure 3.27: Model estimated values for the effect of average mutant effect on dominance–by–dominance signed epistasis for *bifid* and *scalloped* mutants (P-value = 0.01022), *vestigial* and *scalloped* mutants (P-value =2.00E-16) and all mutants (P-value = 3.76E-06). (Table 3.29). N = 5,905.

Dominance–by–Dominance Magnitude Epistasis of Samarkand and Oregon-R Allelic Pairs

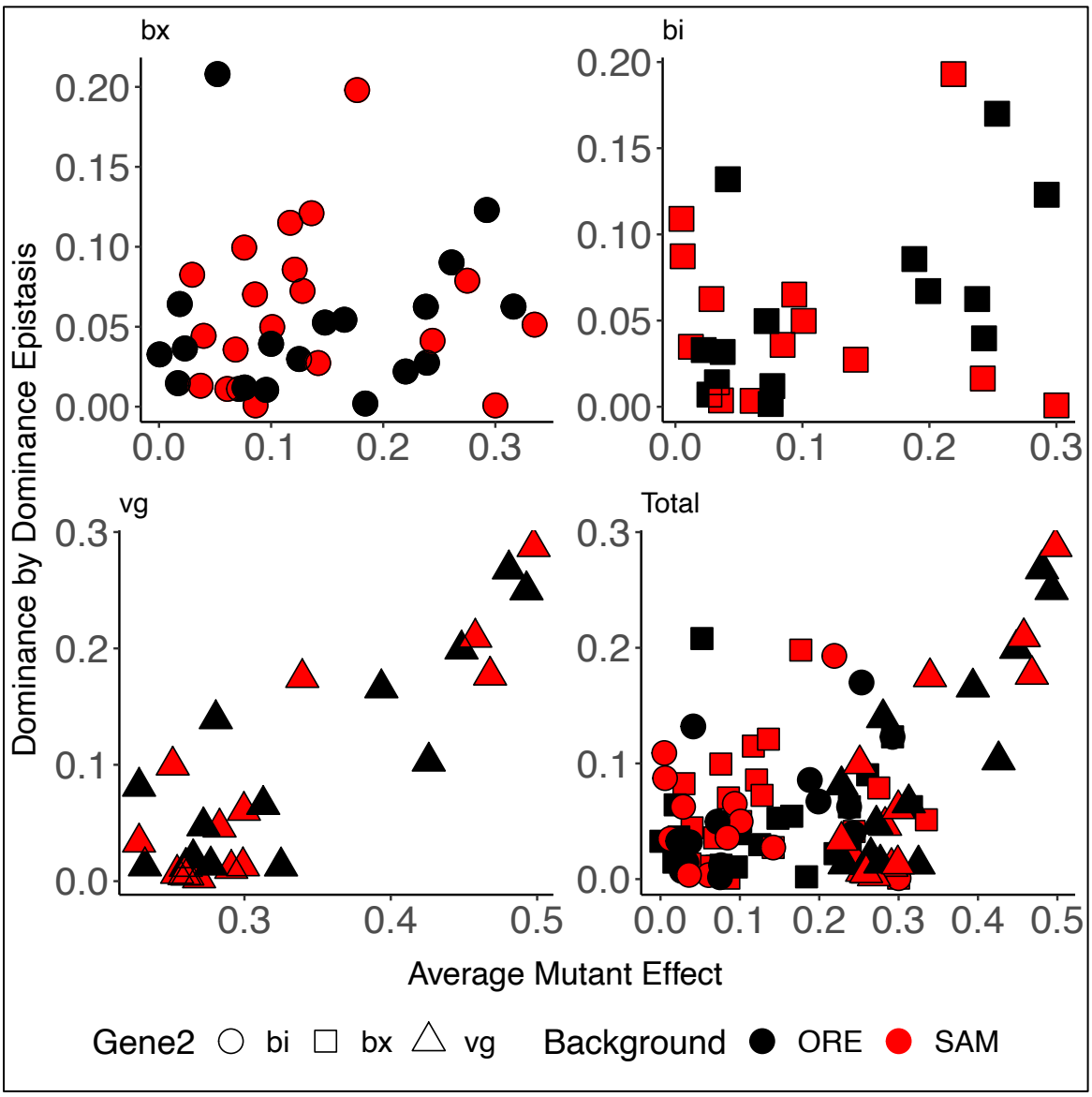

Figure 3.28: Estimates of dominance–by–dominance magnitude epistasis for each allelic pair in Samarkand and Oregon-R for the different gene combinations. N = 5,905.

Table 3.31:Statistical model estimates of the average magnitude epistasis for Samarkand and Oregon-R among all allelic pairs for each gene combination. The P-value representing the difference in genetic backgrounds was estimated from ANOVA analysis.

Type of Epistasis	Gene	Background	Average Mean Epistasis	Standard Error	P-Value
dd	bx	ORE	0.0584	0.0191	3.51E-01
dd	bx	SAM	0.0714	0.0191	
dd	bi	ORE	0.0575	0.0144	8.53E-01
dd	bi	SAM	0.0539	0.0150	
dd	vg	ORE	0.0920	0.0124	8.30E-01
dd	vg	SAM	0.0882	0.0124	
dd	Total	ORE	0.0645	0.0109	9.60E-01
dd	Total	SAM	0.0640	0.0110	

Table 3.32: Statistical model estimates of the effect of the average mutant effect on the magnitude epistasis among all allelic pairs for each gene combination. P-value estimated from ANOVA analysis.

Type of Epistasis	Gene	Effect of Average Mutant Effect	Standard Error	P-Value
dd	bx	0.0692	0.1104	5.72E-01
dd	bi	0.2900	0.1418	0.1769
dd	vg	0.8279	0.1389	**<2e-16**
dd	Total	0.2610	0.0704	**8.38E-05**

Table 3.33: Statistical model estimates of the effect of the interaction between genetic background and the average mutant effect on the magnitude epistasis among all allelic pairs for each gene combination. P-value estimated from ANOVA analysis.

Type of Epistasis	Dataset	Effect of Background: Average Mutant	Standard Error	P-Value
dd	bx	-0.0458	0.1543	0.7665
dd	bi	-0.3162	0.2016	0.1169
dd	vg	0.1085	0.2016	0.5905
dd	Total	-0.0917	0.0915	0.3164

The Impact of Average Mutant Effects on Dominance- by -Dominance Magnitude Epistasis

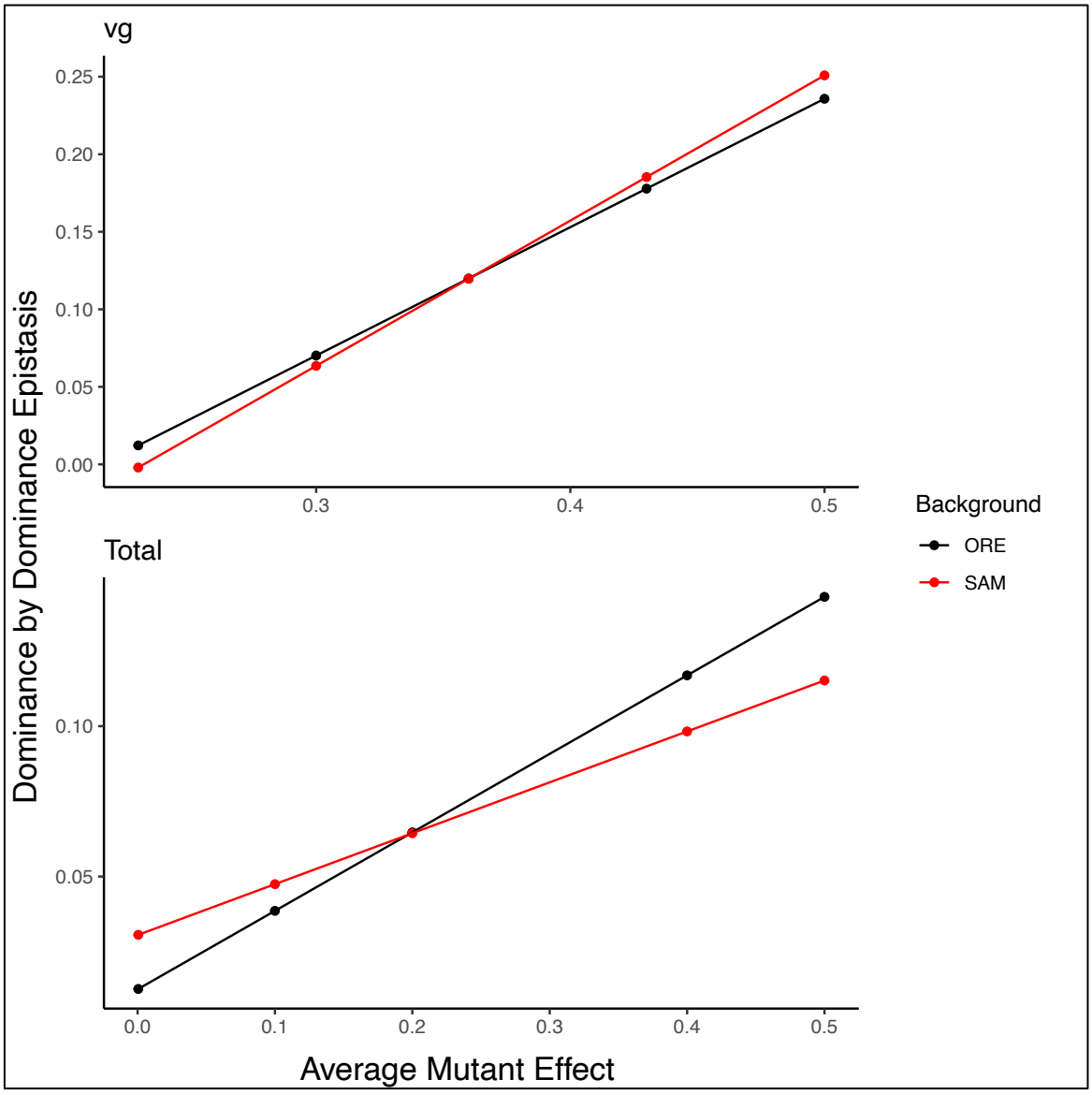

Figure 3.29: Model estimated values for the effect of average mutant effect on dominance–by–dominance magnitude epistasis for *vestigial* and *scalloped* mutants (P-value = 2.00E-16) and all mutants (P-value = 8.38E-05) (Table 3.32). N = 5,905.

Correlation of epistatic effects across wild type genetic backgrounds

One of the main goals of this study is to examine how wild type genetic background influences the strength of epistatic interactions. In the previous section I demonstrated that the genetic background can have a strong influence when estimating epistasis among all allelic pairs for different epistatic components and gene combinations. To further assess this relationship, the Pearson correlation coefficient was estimated using epistasis values estimated within each wild type genetic background. Correlation estimates indicate how similar the epistasis values are in Samarkand and Oregon-R for each allelic pair. For example, when the epistasis value is smaller for an allelic pair in Samarkand, does it also tend to be smaller for the same allelic pair in Oregon-R as well? Estimates were calculated for average magnitude and signed epistasis, and for each type of epistasis. A summary of significant correlations between Samarkand and Oregon-R wild type backgrounds for magnitude epistasis among all allelic pairs of different gene combinations and types of epistasis is shown in Table 3.34. A Summary of significant correlations for signed epistasis is shown in Table 3.35. In general, the results suggest that the estimated epistatic effects are not well correlated across wild type genetic backgrounds (i.e. epistatic effects differ across backgrounds).

For magnitude epistasis we see that the backgrounds are not well correlated overall. The only time we see a significant correlation between Samarkand and Oregon-R is for additive-by-additive epistasis for *bifid* and *scalloped* mutants (P-value= 0.025).

When examining signed epistasis, we see examples where the two backgrounds are moderately correlated. Interestingly, we do not see significant correlations between

Samarkand and Oregon-R for average epistasis, but we do see examples of correlation for other epistatic components. For example, additive-by-additive and additive-by-dominance show correlation between backgrounds for *beadex* and *scalloped* mutants, *bifid* and *scalloped* mutants and all of the mutants combined. *vestigial* and *scalloped* allelic pairs have no significant correlation between Samarkand and Oregon-R for any of the types of epistasis.

Table 3.34: Summary of correlations between Samarkand and Oregon-R wild type backgrounds for magnitude epistasis among allelic pairs among all allelic pairs for different gene combination and types of epistasis.

Gene 2	Correlation	P-Value	Type of Epistasis
bx	-0.32	0.19	Average
bi	0.12	0.69	
vg	0.24	0.38	
Total	-0.07	0.62	
bx	0.39	0.098	Additive–by–additive
bi	***0.59***	***0.025***	
vg	-0.11	0.68	
Total	0.06	0.69	
bx	0.35	0.14	Additive–by–dominance
bi	-0.14	0.64	
vg	0.10	0.723	
Total	0.22	0.13	
bx	0.43	0.066	Dominance–by–additive
bi	-0.20	0.50	
vg	0.04	0.88	
Total	0.12	0.40	
bx	0.11	0.66	Dominance–by–dominance
bi	-0.27	0.40	
vg	0.37	0.21	
Total	0.15	0.34	

Table 3.35: Summary of correlations between the Samarkand and Oregon-R wild type backgrounds for signed epistasis among allelic pairs among all allelic pairs for different gene combination and types of epistasis.

Gene 2	Correlation	P-Value	Type of Epistasis
bx	0.15	0.53	Average
bi	0.09	7.70E-01	
vg	0.29	3.0E-01	
Total	0.14	0.34	
bx	**0.73**	**0.0004**	Additive–by–additive
bi	**0.73**	**0.0031**	
vg	-0.10	0.71	
Total	**0.48**	**0.0006**	
bx	**0.73**	**0.0003**	Additive–by–dominance
bi	**0.78**	**0.0010**	
vg	0.06	0.82	
Total	**0.54**	**8.4E-05**	
bx	**0.62**	**0.0050**	Dominance–by–additive
bi	0.05	0.85	
vg	0.02	0.94	
Total	**0.32**	**0.025**	
bx	0.39	0.0963	Dominance–by–dominance
bi	0.21	0.5115	
vg	0.37	0.2078	
Total	**0.38**	**0.01**	

Correlation of Samarkand and Oregon-R Average Epistasis Among Allelic Pairs

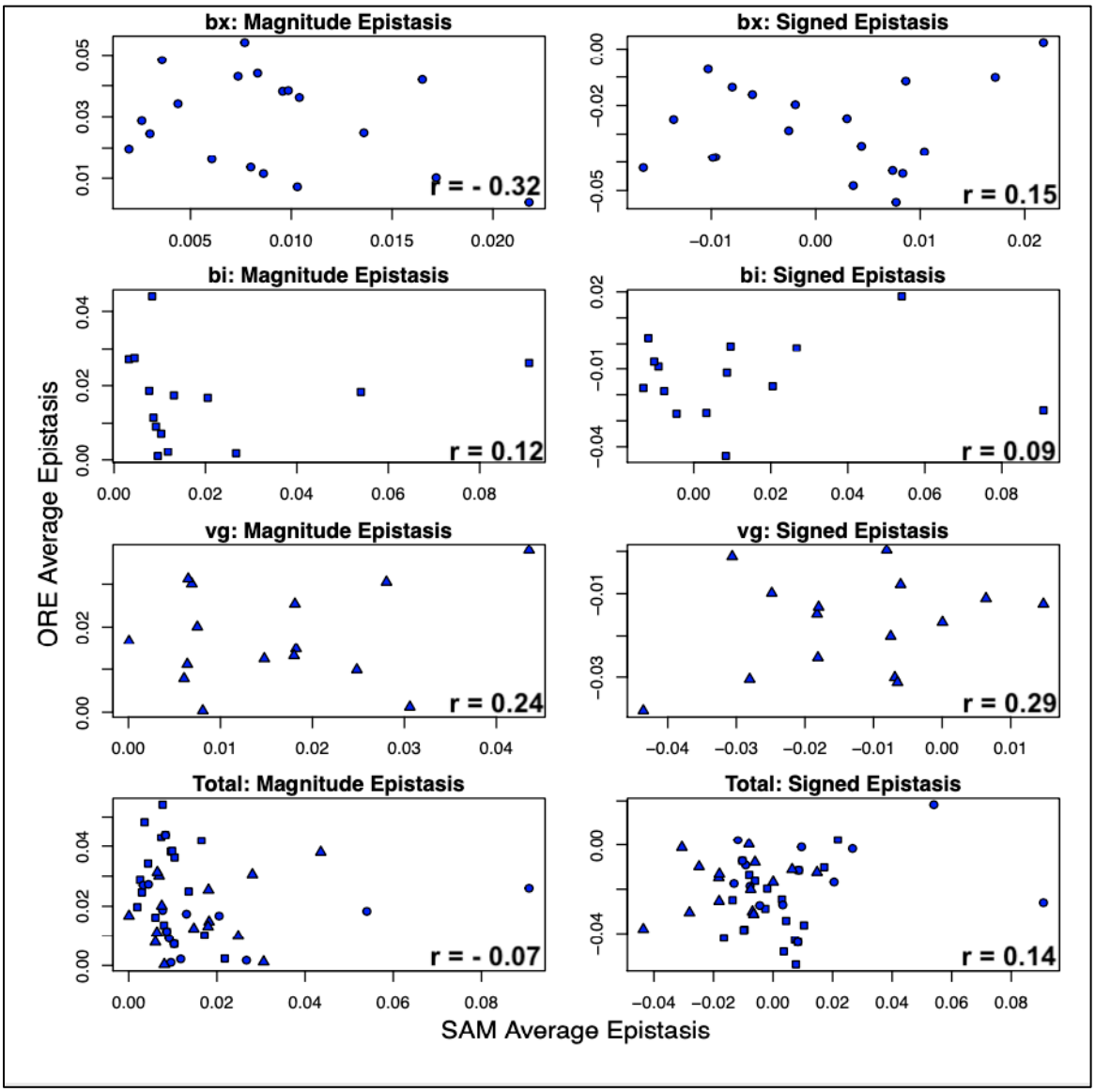

Figure 3.30: Correlation values among Samarkand and Oregon-R mutants for average magnitude and signed epistasis for each gene combination. Values represent how similar average epistasis values are across all allelic pairs between genetic backgrounds. High r values indicate a high degree of association for epistasis values between genetic backgrounds and a low r value indicates a low association. N = 5,905

Correlation of Samarkand and Oregon-R Additive–by–Additive Epistasis Among Allelic Pairs

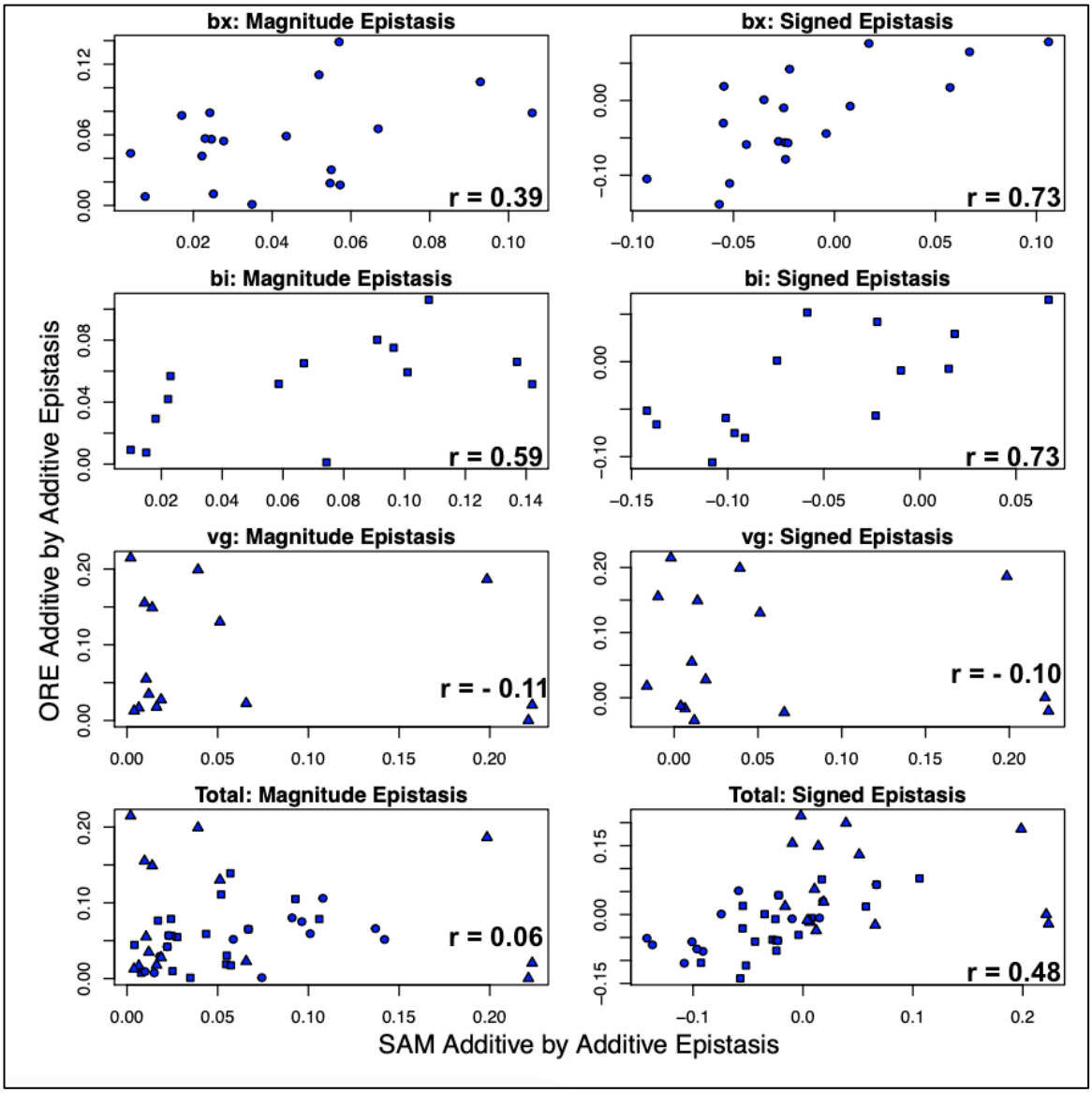

Figure 3.31: Correlation values among Samarkand and Oregon-R mutants for additive-by-additive magnitude and signed epistasis for each gene combination. Values represent how similar average epistasis values are across all allelic pairs between genetic backgrounds. High r values indicate a high degree of association for epistasis values between genetic backgrounds and a low r value indicates a low association. N = 5,905

Correlation of Samarkand and Oregon-R Additive–by–Dominance Epistasis Among Allelic Pairs

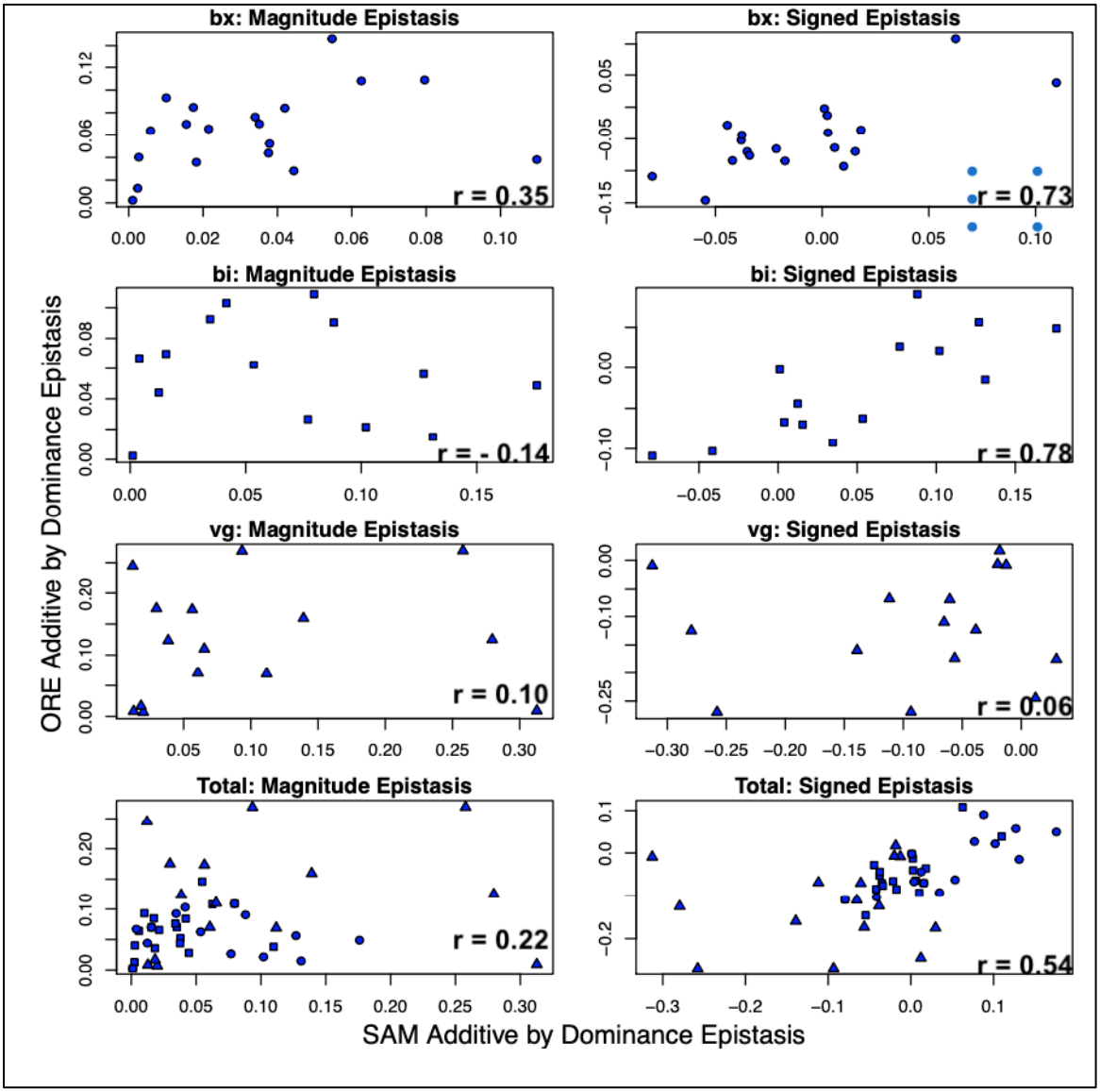

Figure 3.32: Correlation values among Samarkand and Oregon-R mutants for additive-by-dominance magnitude and signed epistasis for each gene combination. Values represent how similar average epistasis values are across all allelic pairs between genetic backgrounds. High r values indicate a high degree of association for epistasis values between genetic backgrounds and a low r value indicates a low association. N = 5,905

Correlation of Samarkand and Oregon-R Dominance–by–Additive Epistasis Among Allelic Pairs

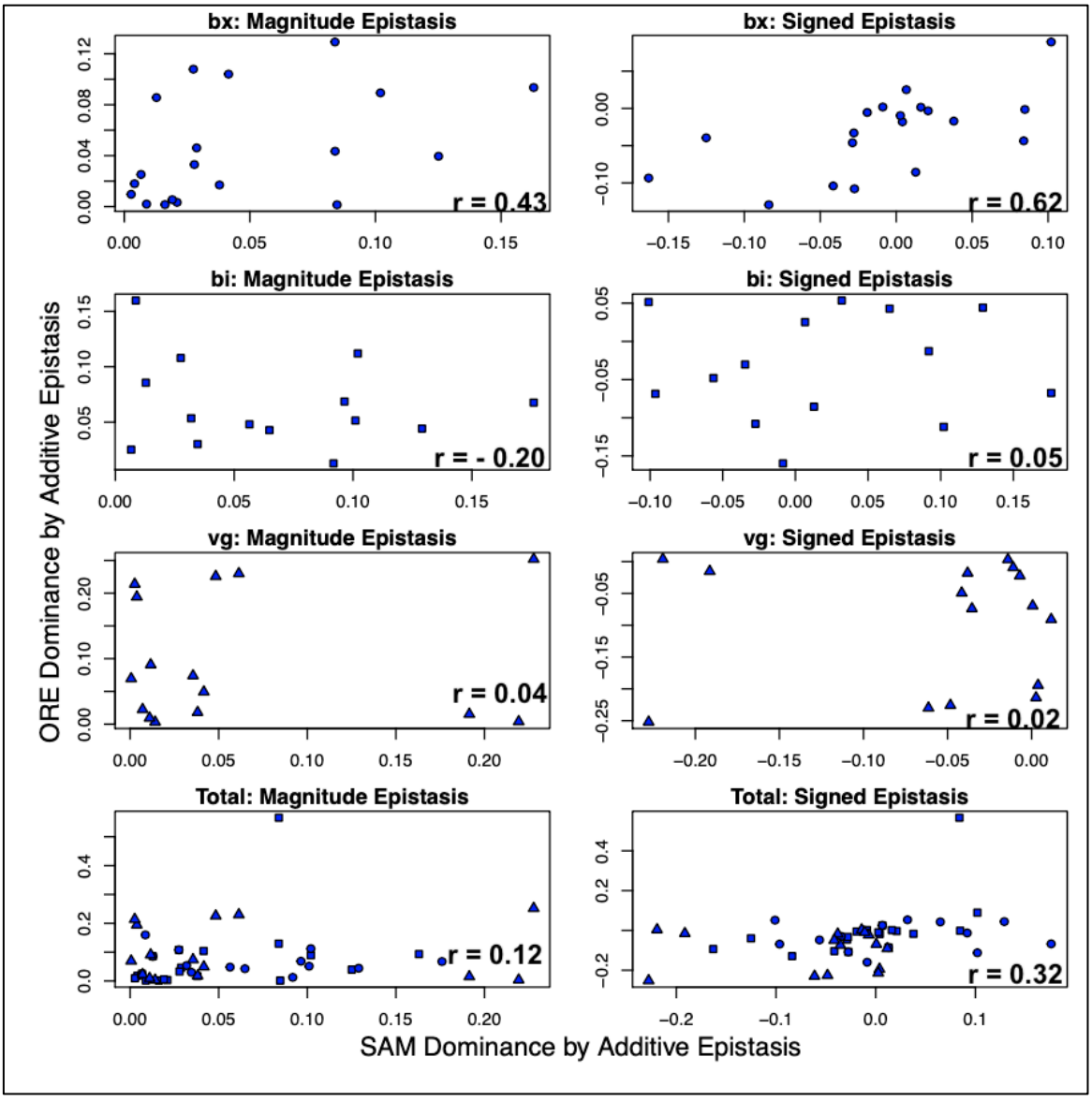

Figure 3.33: Correlation values among Samarkand and Oregon-R mutants for dominance-by-additive magnitude and signed epistasis for each gene combination. Values represent how similar average epistasis values are across all allelic pairs between genetic backgrounds. High r values indicate a high degree of association for epistasis values between genetic backgrounds and a low r value indicates a low association. N = 5,905

Correlation of Samarkand and Oregon-R Dominance–by–Dominance Epistasis Among Allelic Pairs

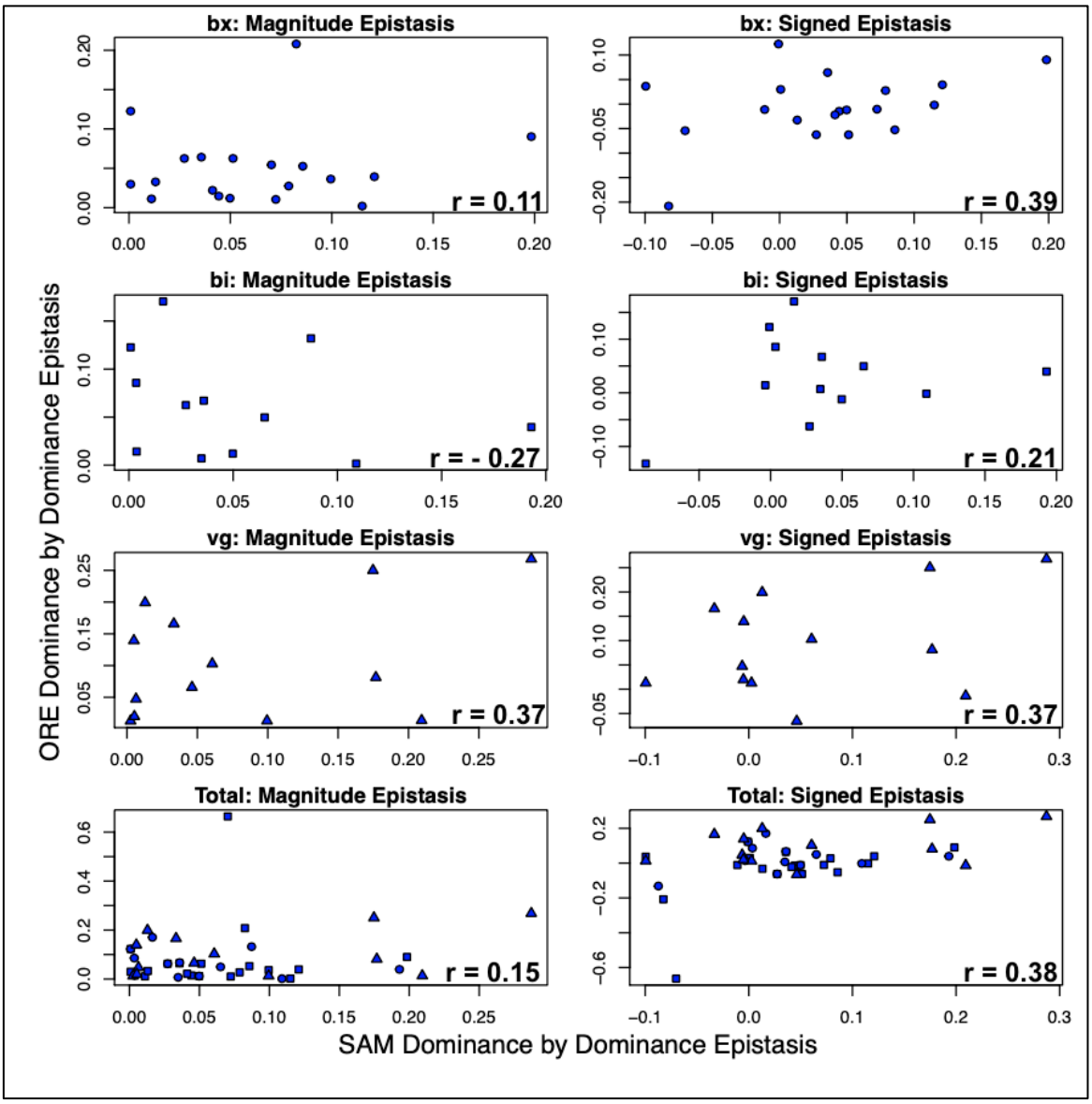

Figure 3.34: Correlation values among Samarkand and Oregon-R mutants for dominance-by-dominance magnitude and signed epistasis for each gene combination. Values represent how similar average epistasis values are across all allelic pairs between genetic backgrounds. High r values indicate a high degree of association for epistasis values between genetic backgrounds and a low r value indicates a low association. N = 5,905

How Much Does Scale Matter?

Transforming the scale of measurement can have major effects when examining epistasis. For example, an epistatic interaction seen with one scale, may be entirely additive on another scale. Therefore, it was important to verify that epistasis values observed using the square root wing area transformation are not simply scale effects. To examine this, the Pearson correlation coefficient was calculated for log transformed and square root transformed data used for epistasis estimates among allelic pairs. The correlation estimates indicate how similar the epistasis values are when using each scale for each allelic pair.

Overall, the correlation of epistasis values for the square root and log transformed data is very high. Illustrating that when we see higher values of epistasis using one scale (the linear/arithmetic scale which is the relevant scale of measure for the square root of wing area), we also see high values in on the log2 scale. This suggests the epistatic effects do not simply reflect proportional (i.e. multiplicative) changes in wing size. When looking at all gene combinations together the correlation is high for both magnitude ($r = 0.93$) and signed epistasis ($r = 0.91$). Indicating that the epistatic effects are largely invariant to such scale effects.

Correlation of Log Transformed and Square Root Transformed Data for Epistasis Estimates Among Allelic Pairs

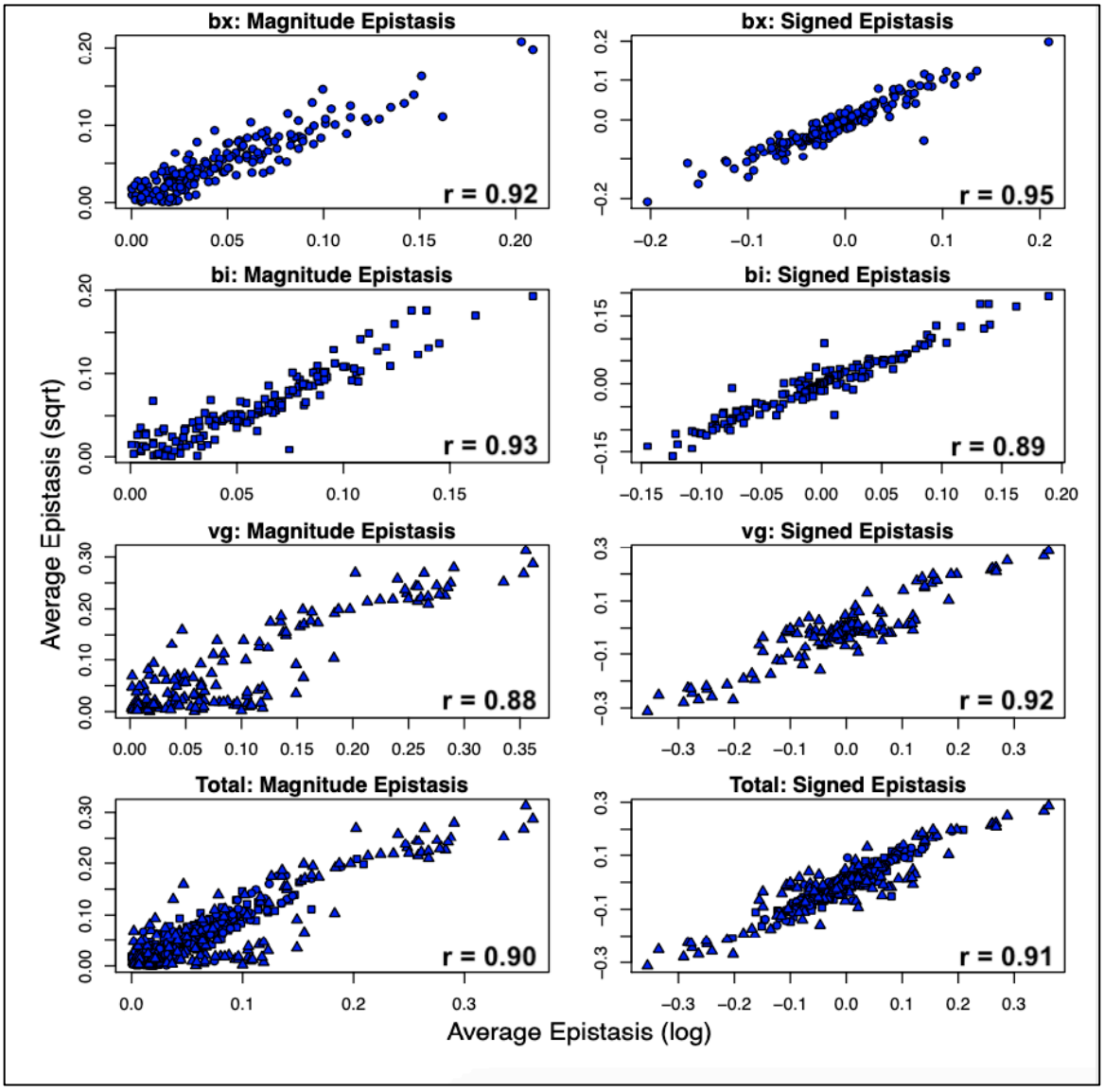

Figure 3.35: Correlation of Log Transformed and Square Root Transformed Data for Epistasis Estimates Among Allelic Pairs**.** Values represent how similar epistasis values are across allelic pairs for each data transformation. High r values indicate a high degree of association for epistasis values between log and square root data transformation and a low r value indicates a low association. N = 5,905.

Block Effects

Experimental crosses were performed over 8 blocks as the number of crosses performed was too large to conduct at one single time. Three repeat crosses (and subsequent progeny genotypes) were performed in each block so we could estimate the magnitude of block effects. While experimental design does its best to help minimize such sources of variation, it is important to consider blocking effects that happen even in the best of experimental conditions. The NOIA package used to estimate epistasis values for each allelic pair does not allow for random effects to be fitted. Therefore, any variation between blocks is not accounted for in our current estimates. To get a better idea of how this may be impacting our results we estimated the variance in wing size between blocks using the data from the three repeat crosses preformed in all 8 blocks. The variance for the block effect is 0.0249, while the residual variance is 0.0752. Therefore, the variation due to block effects model is only about 10.7% the magnitude of the unexplained variation. Suggesting that the block effect accounts for a relatively modest amount variance in our data. While this shouldn't impact the overall trends in our results, accounting for the block effects will influence individual epistasis estimates. To get a better idea of blocks effects we ran two models that estimated these effects. The first model estimated the average block effects averaged across the genotypes and backgrounds. The second model estimated the block effects for each background and genotype. This showed that block effects do not always move in the same direction for each genotype. Indicating that for some genotypes the average wing size is bigger in one

block, while for other genotypes the wing size is smaller in that block. For example, the block effect for bx^1sd^1 is -0.0318 for block 2, but for bx^2sd^{E3} it is 0.0059 for that block. The block effects also effect Samarkand and Oregon-R to varying degrees and directions. For example, the block effect for wt^+in Oregon-R is 0.0215 in block 4, while for wt^+in Samarkand the block effect is -0.0283. Despite these examples, the block effects seemed to behave similarly between genotypes and backgrounds overall. Prior to submitting this work for peer reviewed publication, additional models will be further examined to assess block effects and the extent to which they influence our epistatic estimates.

Block Effects

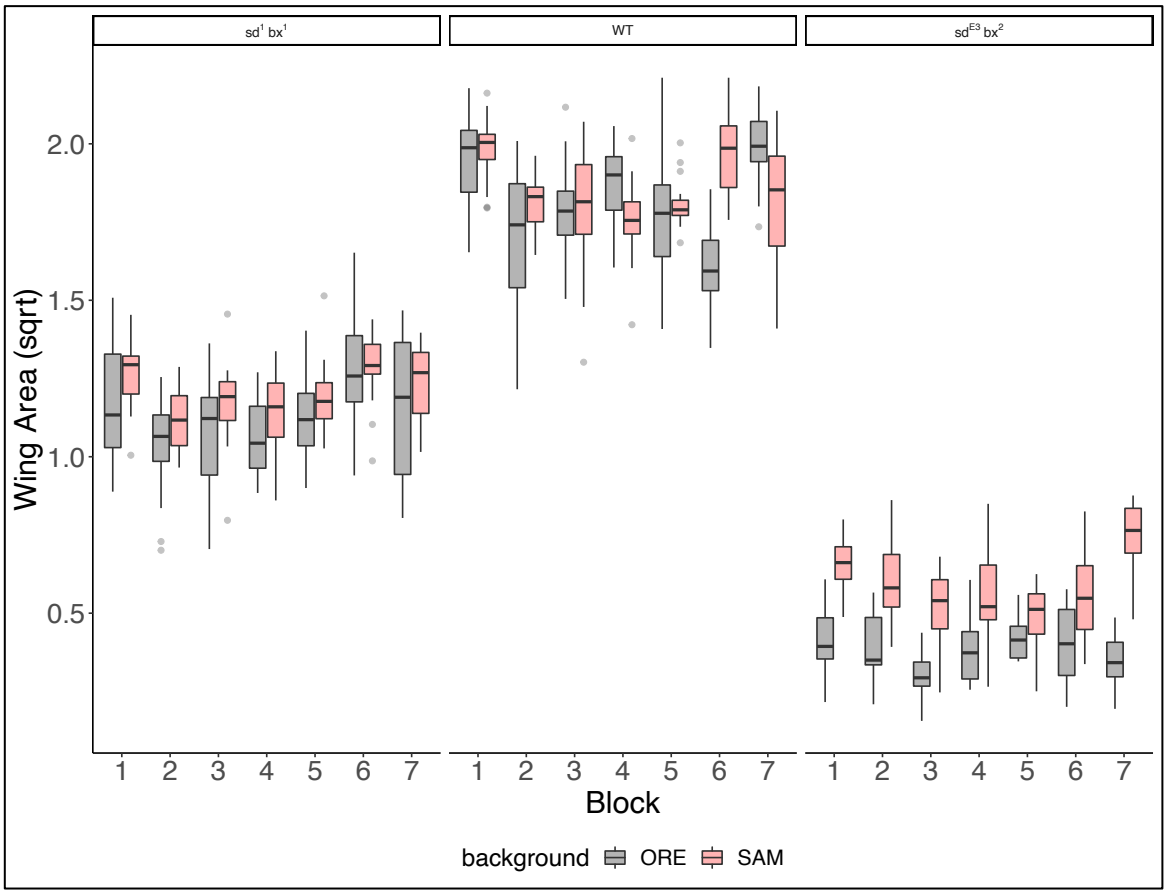

Figure 3.36: The block effects for individuals generated from 6 repeat crosses performed across all experimental blocks (1-7). N = 784.

Examining epistatic interactions between the sd allelic series and a set of previously identified modifiers

The detailed results presented in the previous section suggest that interactions between alleles of sd and bx, bi and vg suggest a fairly clear picture about the relationship between epistatic effects and magnitude of allelic effects as well as genetic background effects. However, to further confirm these results and determine the broader scope of the effects I wished to also examine an additional set of potential modifiers that are known to interact epistatically with *sd*. Using a subset of deletions that cover previously identified modifiers of the phenotypic effects of sd^{E3} identified in Chari and Dworkin (2013), I wanted to examine how background dependence changes and how the magnitude of modifier effects changes when using *scalloped* alleles differing in magnitude of phenotypic effects. The aim for this experiment was to examine how enhancer and suppressor relationships resulting from deletions with *scalloped* alleles vary as function of allelic effect and genetic background. The phenotypic effects of the *scalloped* alleles with a subset of deletion lines can be observed in a reaction norm plot (shown in Figure 3.37). These deletions can dominantly enhance or suppress the phenotypic effects of *scalloped* mutants to varying degrees, with these effects changing in magnitude and direction in different genetic backgrounds.

In order to summarize these relationships, we examined the phenotypic variability for each *scalloped* allele among all deletion lines. More variation in the phenotypic effects for a *scalloped* allele among all the deletion lines indicates a relative greater

magnitude of modifier effects (either enhancers or suppressors) either across *scalloped* alleles or wild type backgrounds.

Figure 3.38 illustrates the mean wing area for each *scalloped* allele with the control Exelixis strain (shown as solid circle) as well as the mean wing area for each *scalloped* allele with each deletion (shown as transparent circle). As expected alleles of moderate effect result in greater among (deletion) strain variation across both backgrounds than alleles of weak and severe phenotypic effect. The standard deviation among deletion lines for each allele was estimated allowing for comparisons between other alleles. sd^{ETX4} has the highest standard deviation value (stdev = 4.30E-02mm), with sd^{E3} having a close second (stdev = 4.22E-02 mm). In contrast, sd^{58} has the lowest standard deviation (stdev = 8.90E-11mm). These results suggest that the effects of modifiers are greater in magnitude for alleles of moderate effect.

Our results also indicate that the effects of modifiers are background dependent. To examine this background dependence, we estimated the standard deviation for each *scalloped* allele in each background. While the overall pattern for which alleles show the greatest variation stay consistent between genetic backgrounds, we do see differences between the phenotypic variability for each *scalloped* allele among all deletion lines between backgrounds. For instance, for sd^{ETX4} the phenotypic variation among deletion lines is approximately twice the magnitude in in Oregon-R (stdev = 5.47E-02mm) than the variation in Samarkand (std = 1.79E-02mm). Indeed, the phenotypic variability among deletion strains for *scalloped* alleles is always lower in Samarkand than in Oregon-R (Table 3.37). Suggesting that the effects of modifier alleles of scalloped are of

smaller in magnitude in Samarkand than in Oregon-R, consistent with the more limited results of Chari and Dworkin (2013).

To see how significant these background effects are we compared the two models that estimated the standard deviations among deletions (treating the deletion lines as random effects). For the first model, the standard deviations were estimated for each *scalloped* allele among genetic backgrounds. For the second model, the standard deviations were estimated for each *scalloped* allele in each genetic background. The AIC (Akaike Information Criterion) for the first model is -5756.2 and the AIC for the second model is -6109.3 (ΔAIC = 353), suggesting that the model allowing for background specific estimates is a substantially improved fit. This is consistent with estimates of variability among deletion lines for *scalloped* alleles differs across each wild type background.

Table 3.36: Statistical estimates of standard deviations for each *scalloped* allele across deletions.

sd Allele	**Std**
WT	2.69E-03
29.1	4.64E-03
1	1.83E-02
ETX4	4.30E-02
E3	4.22E-02
58d	8.90E-11

Table 3.37: Statistical estimates of standard deviations for each *scalloped* allele across deletions for Samarkand and Oregon-R.

sd Allele	**Std : ORE**	**Std : SAM**
WT	5.41E-03	1.47E-02
29.1	4.71E-03	2.47E-03
1	1.91E-02	2.89E-04
ETX4	5.47E-02	1.79E-02
E3	2.49E-02	2.65E-02
58d	9.39E-11	1.41E-12

Phenotypic Effects of *Scalloped* Alleles with a Subset of Deletion Lines

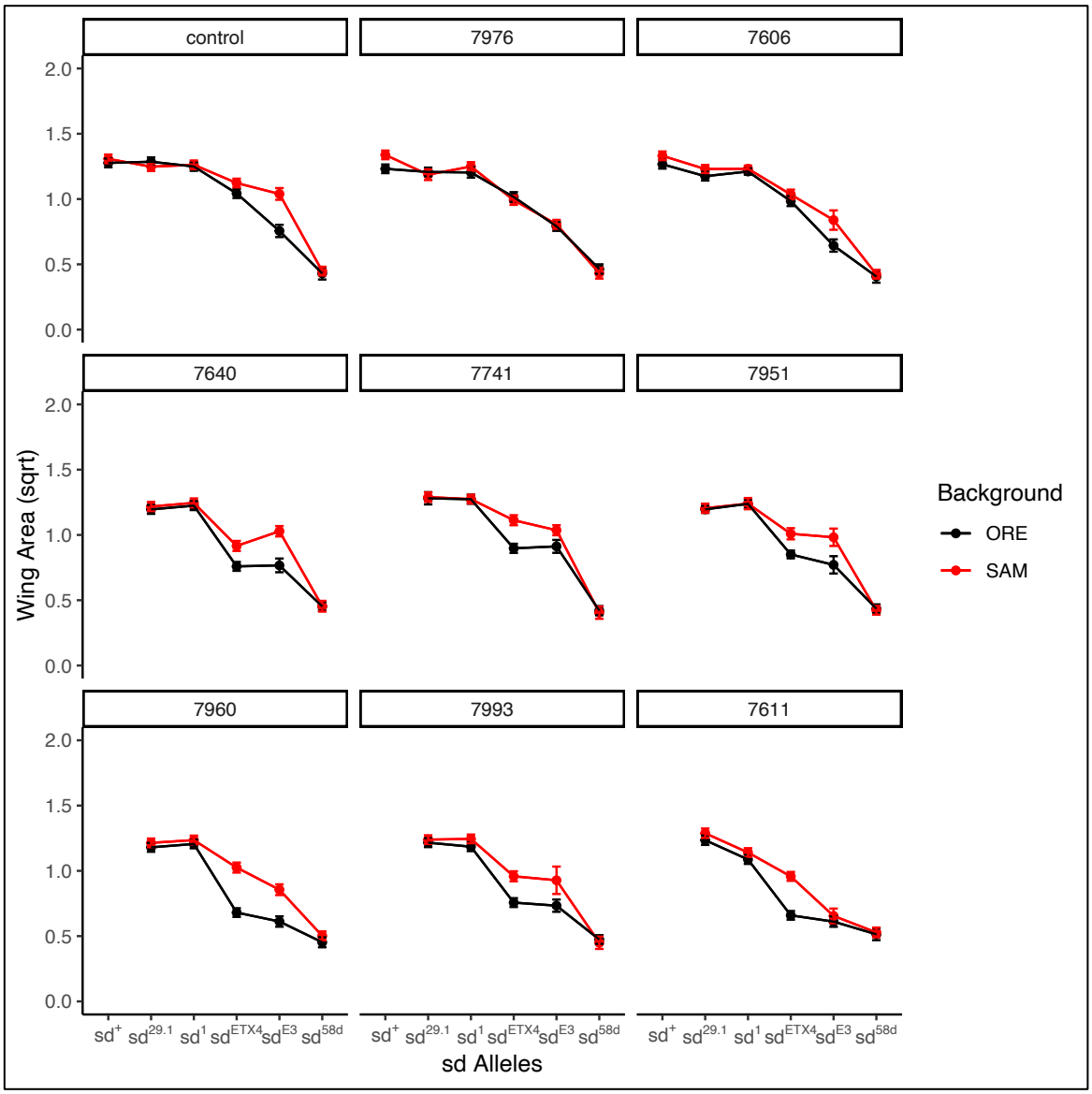

Figure 3.37: Estimates of mean phenotypic effect of each *scalloped* mutant with a subset of deletions. N = 1616.

Phenotypic Variability of *Scalloped* Alleles Across Deletion Lines in Samarkand and Oregon-R

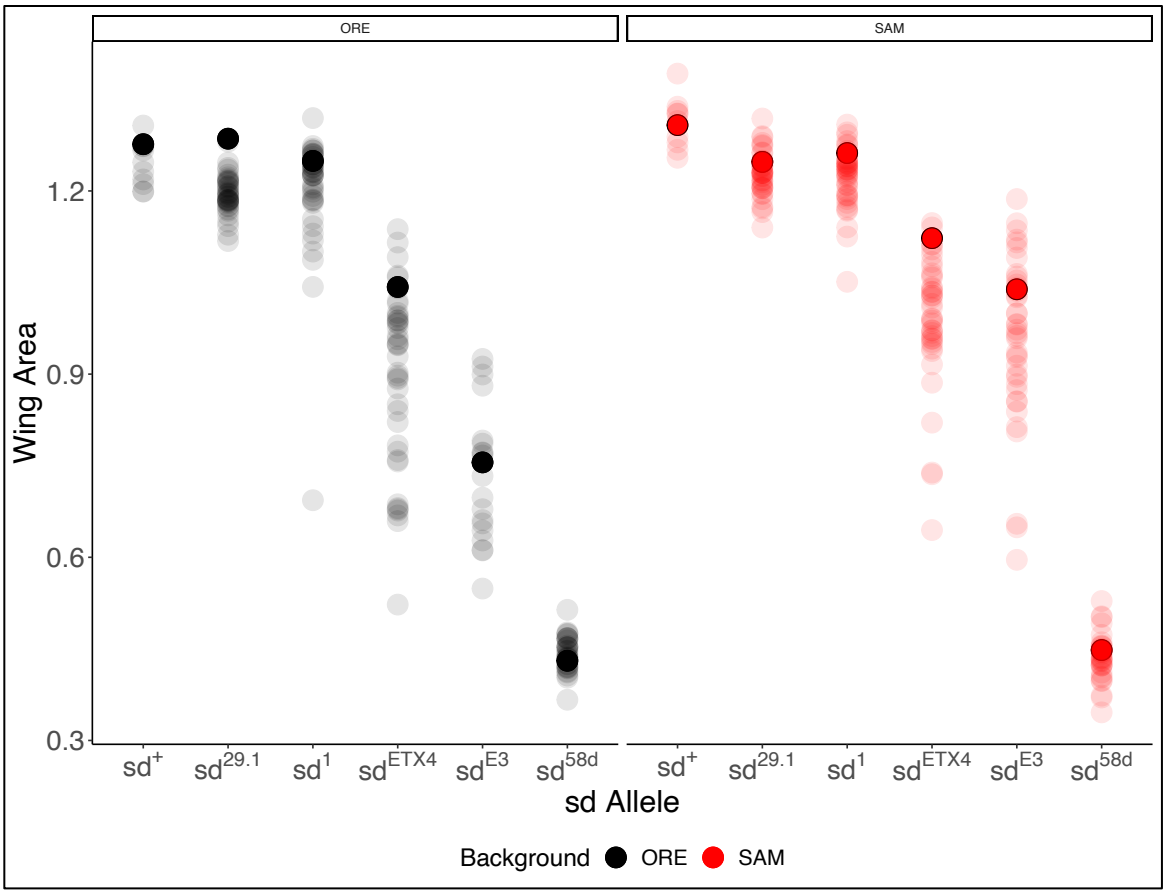

Figure 3.38: Estimates of mean wing area for each *scalloped* allele with the control Exelixis line (shown as solid circle) as well as the mean wing area for each *scalloped* allele with each deletion (shown as transparent circle). N = 6506.

Discussion

The effects of epistasis can differ significantly in both magnitude and sign, but it is not always clear why such a range is observed. Understanding what causes variation in epistatic interactions is essential to predict phenotypic effects from genotypic variation. One explanation for why genetic interactions may emerge is from the quantitative nonlinearity between gene activity and the phenotype. An example of nonlinearity was demonstrated in Green et al. (2017) where the gene dosage of a regulator of mouse development was manipulated. It was shown that variation in activity in this signalling molecule has a nonlinear relationship to phenotypic variation. Changes in gene expression have also shown to alter how mutations interact when the relationship between gene expression and phenotype is nonlinear. Li et al. (2019) introduced random mutations into the DNA binding domain of the phage lambda repressor and demonstrated that changes in gene expression can dramatically alter the effects of mutations and importantly how mutations interact. Specifically, a change in mutant expression transformed the magnitude and the direction of epistasis. While this work illustrates that the magnitude of individual allelic effects may have a strong influence on the resulting epistasis, it was not clear how changes in gene expression alone can facilitate changes in genetic interactions and if these changes are predictable.

The main goal for this project was to examine genetic interactions as a function of the magnitude of individual allelic effects and genetic background. Specifically, we sought to determine if the magnitude and direction of epistatic interactions can be predicted from the individual allelic effects. Using wing size in *Drosophila*, I examined

the phenotypic effects across a broad set of allelic combinations using four genes in the wing regulatory network, among two genetically distinct wild type genetic backgrounds (Samarkand and Oregon-R). In addition, I examined the phenotypic effects of known modifiers of sd^{E3} with the *scalloped* allelic series in both Samarkand and Oregon-R. The aim was to observe how genetic background effects and the magnitude of modifier effects changes when using *scalloped* alleles of differing magnitude of phenotypic effects. Our results indicate that the magnitude and sign of epistatic interactions can, in large part, be predicted based on the average additive effects of allele and that the genetic background can have a strong influence on epistasis (both will be discussed in more detail below).

The choice of scale can become important measuring epistasis as mutations that are additive for a phenotype measured on one scale may not be additive when a different transformed scale is used (Frankel & Schork, 1996). Epistasis estimates were calculated using square root (producing a "standard" arithmetic scale of measure) and logarithm of wing area. To verify that epistasis values observed are not the result of a scale effect we calculated the Pearson correlation coefficient for log transformed and square root transformed data used for epistasis estimates among allelic pairs. A high correlation was observed between the two transformations for both magnitude and signed epistasis for each gene combination. Suggesting that epistasis estimates are not substantially impacted whether the responses measures are on an additive (for arithmetic scale) or multiplicative (log scale). Rather, epistasis estimates reflect "real" differences in the interaction effects among mutations.

Recapitulating Genetic Background Effects For *sd*, *bx*, *bi,* and *vg* Homozygotes

Chandler et al. (2017) demonstrated the influence of genetic background on the expressivity of an allelic series in two functionally related genes in the *Drosophila* wing network. For *vestigial* and *scalloped* alleles, the extent of background dependence was predicted from the magnitude of the individual phenotypic effect (severity) of the allele. Work by Daley (2009) extended and confirmed these findings across a larger set of wild type backgrounds, more alleles and more genes that function in the wing development network. Estimates of wing size and variance confirmed that *scalloped* alleles of moderate effect (sd^{ETX4} and sd^{E3}) exhibited greater background dependence than alleles of weak and strong effect. However, the relationship between magnitude and variance was less clear for other genes. Among *beadex*, *cut* and *bifid* alleles the magnitude of phenotypic variance was largely similar among alleles of the same gene. However, a limited phenotypic range of some allelic series may explain the limited range of phenotypic variance among alleles compared to the *scalloped* alleles that had a much bigger range of effects on wing size. While both studies illustrate the impact of genetic background on individual allelic effects, it was unclear how this relationship impacts more alleles and genes with different functional relationships. Before we could begin to examine the background dependence of genetic interactions, it was necessary to examine the background dependence of the alleles and genes being used in my project. The phenotypic effects were analyzed for homozygous females for allelic series in *scalloped*, *beadex*, *bifid*, and *vestigial*, among two genetically distinct wild-type backgrounds,

Samarkand and Oregon –R. There was considerable variation in mean wing size between the two backgrounds. Genetic background effects were common across alleles, but as expected the largest effects were seen in alleles with individually moderate phenotypic effects. Interestingly, for some weak alleles of *scalloped*, mean wing size was slightly larger in Samarkand than Oregon-R. In Chandler et al. (2017), mutational effects of *scalloped* and *vestigial* were greater in Oregon-R than in Samarkand. Data from Daley (2009) illustrated that Oregon- R wings are larger than Samarkand with weaker *scalloped* knockdown, however the slope of this effect is greater in Oregon-R. This pattern is seen in the results from my project with *scalloped* alleles as well (seen in Figure 3.1). Samarkand has smaller wings for weak *scalloped* alleles ($sd^{29.1}$ and sd^{1}) but larger wings for moderate alleles (sd^{ETX4} and sd^{E3}). For *beadex*, we see switching for which background has larger wings for each allele (Figure 3.1). This switching may be due to a modest sample size (per genotype) and relatively modest phenotypic effects rather than reflecting background effects that are not consistently moving in the same direction for different alleles. Overall, our results are largely consistent with the results seen with Chandler et al. (2017) and Daley (2009). Moderate effect homozygotes showed the greatest background dependence, while alleles with weak and strong effects showed less background dependence. This suggests that the sensitivity to genetic background effects may be predictable for individual alleles. One explanation for background dependence of mutations is natural variation for robustness to mutational perturbations across wild type strains (Chari & Dworkin, 2013). Regulatory networks often exhibit nonlinear relationships between genes and gene products (Félix & Barkoulas, 2015). As such, one

strain may be more sensitive to genetic perturbations due to differences in the ability to buffer sources of variation. This proposed explanation and the predictability seen between individual allelic effects and background dependence allowed us to make predictions between the relationship of genetic background and genetic interactions (Figure 1.4 and Figure 1.5).

The Magnitude and Sign of Epistatic Interactions Can Be Predicted Based on The Average Additive Effects of Alleles.

We sought to demonstrate if differences between the magnitude and sign of epistasis can be explained solely through the distinctive effects of particular gene combinations, or if differences can be explained by the quantitative relationship between gene activity and phenotype. To examine if the magnitude and sign of epistatic interactions can be predicated based on the average additive effects of alleles, we estimated the effect of the average mutant effect on the mean magnitude and signed epistasis among all allelic pairs for each epistatic component and each gene combination. When looking at the summary of significant mutant effects for magnitude epistasis among all allelic pairs across gene combinations and types of epistasis we saw that the average mutant effect had a significant effect on magnitude and signed epistasis 60% of the time (Table 3.2). For the majority of cases where the average mutant effect is significant for magnitude epistasis, as the mutant effect increases so does the mean epistasis. Illustrating strong predictably between the magnitude of the individual mutant effects and the resulting epistasis. These results suggest that epistasis is likely to be stronger for alleles of

strong effect and weaker in magnitude when alleles of weaker effect interact. However, when examining additive-by-additive epistasis for *bifid* and *scalloped* mutants, as the magnitude of mutant effect increases, the magnitude of epistasis decreases. An opposite relationship compared to the other significant relationships between average mutant effect and magnitude of epistasis. While rare in this context, this illustrates that patterns observed can differ dramatically between different components of epistasis and gene combinations, which could lead to inaccurate predictions when assuming the magnitude of epistasis is always stronger for alleles of strong effect.

It is also apparent that the relationship between average mutant effect and signed epistasis can differ greatly between epistatic components. For example, when observing additive-by-additive signed epistasis it is very clear that as mutant effect increases the epistasis becomes increasingly more positive. However, for additive-by-dominance and dominance-by-additive we see that as mutant effect increases the epistasis becomes increasingly more negative. This demonstrates a strong predictability between average mutant effect and signed epistasis for each type of epistasis individually, but that the direction of average mutant effect is dependent on the component of epistasis. In addition, when looking at all the genes combined for all 4 individual epistatic interactions the average mutant effect is always significant for signed epistasis. These results suggest that while the average mutant effect may be a good predicator for the sign of some epistatic effects individually, it is not a good predictor for the average epistasis. This may suggest that our average epistasis measure is not capturing the epistatic components in a way that best illustrates the relationships between average allelic effect and epistasis. Displaying

that just because the average epistatic effect is a simple measure, it may not be easy to interpret biologically. This can be very misleading because by just looking at the average signed epistasis it appears that the average mutant effect does not have a relationship with epistasis, but we see this is clearly the not the case when looking at the epistasis components individually.

We examined the phenotypic variability for each *scalloped* allele among all deletion lines and illustrated that alleles of moderate effect result in more phenotypic variation than alleles of weak and strong phenotypic effect. Suggesting that the effects of modifiers are greater in magnitude for alleles of moderate effect. This matches with the predictions made for this project (Figure 1.4), and is consistent with intra-locus interactions among alleles (Chandler et al. 2017) for *sd* and *vg*. These results match the explanation that epistatic interactions emerge from the quantitative nonlinearity between gene activity and phenotype, where a fractional change in gene activity may have different consequences depending on the form of the curve. This results in modifiers having different magnitude of effects for different *scalloped* alleles. For example, our results show that modifiers do not have as strong as an effect on sd^{58d} compared to alleles of moderate phenotypic effect, as strong mutants may disrupt the system so greatly that there is little room for compensation. It is also possible that modifiers of alleles of weak phenotypic effect ($sd^{29.1}, sd^{1}$) show less magnitude of effects as they only marginally perturb the function of the regulatory network and result in little changes in mean phenotype. Lastly, modifiers of alleles of moderate effect (sd^{ETX4}, sd^{E3}) may show the greatest magnitude of allelic effects as changes in gene activity may have the most

severe consequences due to the shape of the nonlinear relationship between gene activity and phenotype. Our analysis has not allowed for us to make direct comparisons for how specific deletions affect each *scalloped* allele specifically. For example, with our analysis we cannot compare the magnitude of an enhancer effect in sd^{1} versus $sd^{29.1}$ for specific deletions. Therefore, just because the effects for moderate alleles are more variant overall, specific deletions may have larger magnitude of effects in weak or strong alleles. Despite this, these results clearly illustrate the magnitude of modifier effects may be predicable from the severity of the focal mutations in *scalloped*.

While both experiments for this project demonstrate predictive relationships, we observed key differences between them when observing genetic interactions as a function of average mutant effect. For the modifiers, moderate alleles had more phenotypic variability among all deletion lines compared to weak and strong mutants. Yet, when examining the relationship between average mutant effect and epistasis with double mutants, we did not see this same relationship. Here, when the average mutant effect increased so did epistasis. Meaning that when alleles of strong phenotypic effect interact, they are more likely to have stronger epistatic interactions for these allelic combinations. This suggests that observed patterns can change drastically when using different techniques and analyses to examine epistasis. It remains unclear why such differences were observed and what the genetic architecture is underlying these effects.

The Influence of Genetic Background on the Magnitude and Sign of Epistatic Interactions

To investigate how context dependence affects genetic interactions, we first examined estimates of mean magnitude epistasis among all allelic pairs in Samarkand and Oregon-R for the different gene combinations and types of epistasis. My results indicate that while genetic background can influence epistatic interactions, it was often a seemingly modest impact and depends a great deal on the allelic pairs under consideration, and importantly the component of epistasis under consideration (Table 3.1). The only time we see significant genetic background effects for the magnitude average epistasis (i.e the average of the four epistatic components {*aa*, *ad*, *da*, *dd*}) is for *vestigial* and *scalloped* mutants (Figure 3.6). This was unexpected as the *vestigial* homozygote phenotypes showed the least amount of variation between Samarkand and Oregon (Figure 3.1). These results suggest that if you combine individual alleles that do not have strong background dependence on their own, they may have significant background effects when combined together. This was similar to observations also seen in Chandler et al. (2017) where hetero-allelic combinations (but within a locus) showed strong genetic background effects, even when the homozygotes (for very weak or very severe alleles) did not show strong background dependence. Demonstrating that genotypic combinations for one allelic pair can have dramatically different relationships between epistasis and background effects and that it is not always obvious which allelic combinations will show strong background dependence.

When examining estimates of mean signed epistasis among all allelic pairs in Samarkand and Oregon-R for the different gene combinations and types of epistasis, the

genetic background had a significant effect 55% of the time (Table 3.1). For these cases, Oregon-R is more likely to be a negative value, meaning that the wings for these genotypes are more likely to be smaller than expected based off the individual mutants. While in Samarkand, epistatic interactions were more often slightly positive (or close to zero), indicating that these wings are close to, or slightly larger than expected based off the additive effects of individual mutants. When examining the estimates of mean magnitude epistasis among all allelic pairs in Samarkand and Oregon-R for the different gene combinations and types of epistasis, the genetic background had a significant effect in two instances (Table 3.1) This is interesting because an earlier explanation for the context dependent nature of individual alleles is that Oregon-R is less robust to genetic perturbations than Samarkand. However, these results suggest that the magnitude of epistasis may be somewhat similar in the two backgrounds when comparing mean estimates, it just tends to be a different sign.

For signed epistasis we see significant differences in estimates of mean epistasis values among all allelic pairs in Samarkand and Oregon-R for *scalloped* - *bifid* as well as *scalloped* - *beadex* mutant pairs across the different components of epistasis. Yet, there is not one instance of a significant background effect when comparing mean signed epistasis values for *vestigial* and *scalloped* mutants. Unfortunately, it not clear if these differences are due to the relationship *bifid*, *beadex* and *vestigial* have with *scalloped* or if this is due to the magnitude of mutant effects, where the *vg* alleles tended to be among the most severe as homozygotes. *scalloped* and *vestigial* form a heterodimer that functions as a transcription factor, that among other targets regulates the transcription of each other.

Specifically, *scalloped* is needed for early *vestigial* expression, while *vestigial* is needed to maintain *scalloped* expression (Bray, 1999). This direct physical relationship between *scalloped* and *vestigial* may possibly explain the distinct patterns of epistasis than the less direct relationships *scalloped* has with *bifid* and *beadex*. Another consideration is that the mutational effects are not equal between gene combinations. Alleles in *beadex* and *bifid* have weaker phenotypic effects compared to *vestigial*. The average mutant effects (in mm) for *scalloped* and *bifid* mutants range from a value of 0.004 – 0.30, *beadex* and *scalloped* range from 0.017 – 0.335, and *vestigial* and *scalloped* range from 0.228 – 0.497. Therefore, the overlap in patterns seen between *bifid* and *beadex* combinations may be due to a similar range in effects of the individual mutant alleles. While the patterns observed for *vestigial* and *scalloped* mutants may be linked to the more severe end of distributions of allelic effects. It would have been beneficial to have alleles of greater phenotypic range (for *vg*, *bx* and *bi*) to help indicate what relationships are due to mutant effects and what are due to gene differences. For example, do we see no significant background effects when comparing mean sign epistasis values for *vestigial* and *scalloped* mutants because the nature of *scalloped* and *vestigial* interaction? Or do we see less background effects for the sign of epistasis when the average mutant effect is higher? Including stronger effect *bifid* and *beadex* alleles, and weaker *vestigial* alleles would help cover a greater average mutant effect range for each gene. Unfortunately, we were limited by the alleles available and with stronger alleles the issue of lethality arises.

Despite the background dependence appearing to be weak across the set of all interactions, there were a number of cases of quite profound effects. For *bifid* and

scalloped mutants there is a significant effect from the interaction of the genetic background and average mutant effect for average, additive–by–dominance and dominance–by–additive epistasis. Meaning that the effect of the average mutant effect on epistasis differs between Samarkand and Oregon-R. In some cases, the effect of the average mutant effect is much greater in one genetic background, while in other cases the effects are in opposite directions (illustrating sign epistasis). For example, when observing *bifid* and *scalloped* mutants for dominance–by–additive epistasis, the average mutant effect is much stronger in Oregon-R than in Samarkand (indicated by differences in slopes) (Figure 3.24). In comparison, when observing *bifid* and *scalloped* mutants for additive-by-dominance magnitude epistasis we see that the average mutant effect appears to be strong in both backgrounds, but this effect moves in opposite directions between genetic backgrounds (Figure 3.19). Specifically, in Oregon-R as the mutant effect increases, so does the epistasis. Yet, in Samarkand as the mutant effect increases the mean epistasis slightly decreases. Indicating the relationship between average mutant effect and magnitude of average epistasis can be background dependent. Interesting, these interaction effects occurred only in *bifid* and *scalloped* mutants.

To further assess the relationship between genetic background and genetic interactions, the Pearson correlation coefficient was estimated using the estimated epistasis values for Samarkand and Oregon-R among all allelic pairs. While there are a few examples of moderate to strong correlation between backgrounds for signed epistasis (Figure 3.31 and Figure 3.32), we see that the epistasis estimates are generally not well correlated overall between the genetic backgrounds. This illustrates that while the genetic

backgrounds effects can appear generally modest when comparing mean epistasis estimates between genetic backgrounds, wild type genetic background does have a strong influence on epistasis. While there are significant correlations between genetic backgrounds in all 4 epistatic components for different gene combinations, there is never a significant correlation for average epistasis. Reinforcing that that our average epistasis measure is not capturing the epistatic components in a way that best illustrates the relationships between average allelic effect and epistasis across genetic backgrounds. In addition, there are instances where we see significant differences in estimates of mean sign epistasis values among all allelic pairs in Samarkand and Oregon-R, but the epistasis values are significantly correlated. For example, when examining additive by dominance sign epistasis for *bifid* and *scalloped* mutants, Oregon-R is more negative while Samarkand is more positive value (P = 2.19E-06). In this instance the backgrounds have significant differences in the overall direction of their additive by dominance epistatic effects, but the epistatic effects are still correlated (Figure 3.32). Meaning, when the epistasis value for one allelic pair in Samarkand is small it tends to also be small in Oregon-R. This demonstrates that both approaches can be necessary when evaluating the degree of genetic background effects. When examining only the mean epistasis estimates it could be misinterpreted that genetic background effects are weak, when we see the opposite when examining correlations. In comparison, when examining only the correlations we see a case where a strong correlation is seen, but the mean estimates are significantly different in genetic backgrounds across allelic pairs.

Chari and Dworkin (2013) examined whether background dependence of genetic interactions is a general property of genetic systems by performing a genome wide modifier screen for sd^{E3} in Samarkand and Oregon-R using deletions. They demonstrated that ~74% of all modifiers were background dependent. Deletions displayed enhancement or suppression for sd^{E3} in Samarkand or Oregon-R, with many showing an effect in only one genetic background. However, there were instances where deletions had opposite effects in genetic backgrounds, indicating sign epistasis. While this work illustrates the impact of higher-order effects on genetic interactions, it remained unclear how this relationship would change when using different *scalloped* alleles across an allelic series (i.e. not just an allele of moderate effect). Our aim for our second experiment was to examine how modifiers vary as function of genetic background across the full range of allelic effects. Our results indicate that the effects of modifiers are background dependent, with alleles across a spectrum of phenotypic effects. While the overall pattern for which alleles show the greatest variation stay consistent between genetic backgrounds, we do see differences between the phenotypic variability for each *scalloped* allele among all deletion lines between backgrounds. Overall the phenotypic variability for *scalloped* alleles is lower in Samarkand than in Oregon-R. Suggesting that the magnitude of effects for modifiers are smaller in magnitude in Samarkand than in Oregon-R, consistent with the more limited experimental design of Chari and Dworkin (2013). Our approach has not allowed for us to make direct comparisons for how specific deletions affect each *scalloped* allele in Samarkand and Oregon-R. For example, we have not directly assessed if deletion 7960 enhances sd^1 in Oregon-R but suppresses sd^1 in Samarkand. We have

simply observed how the deletions overall effect each *scalloped* allele in each background. Therefore, just because *scalloped* alleles in Samarkand are less variant overall, specific deletions may have larger magnitude of effects in Samarkand than in Oregon-R. Overall, our results reinforce that the genetic background can have strong influence on epistasis.

Caveats

For this project *Drosophila* wing area, measured using a custom ImageJ macro, was used to assess phenotypic effects of alleles. An important consideration is how well wing size in general (and the macro in particular) can accurately reflect weak phenotypic effects. Individuals with some of the phenotypically weaker alleles may not have strong size effects but more subtle phenotypic effects that influence bristle loss along the margin of the wing. The ImageJ macro used to estimate wing area is sensitive to subtle changes in wing size, but it is only estimating wing area, not any changes in wing shape or structure. This is particularly relevant for the weak *bifid* alleles as these mutants often display vein defects as well. Meaning the effects of mutants with weak *bifid* alleles may have larger phenotypic effects on the wing than what is captured using wing size as a measurement for phenotypic effect. Previous work (Chari and Dworkin 2013, Chandler et al. 2017, Daley 2019) have all demonstrated that while there is a strong correlation between semi-quantitative scales of wing perturbation and wing area for moderate to strong allelic effects, very subtle effects are not captured well by wing area alone.

A limitation for the experiment examining the effect modifiers with various *scalloped* alleles and between genetic backgrounds is that sd^{E3} in Oregon-R has not been examined with all possible deletions. When performing a large set of experimental crosses, crosses fail. sd^{E3} in Oregon-R is prone to bacterial infections more so than other stocks which can cause higher rates of failed crosses. Due to time constraints induced by COVID-19, there was not enough time to repeat some failed crosses. Due to this, we have less data for sd^{E3} in Oregon-R compared to other *scalloped* alleles. This may impact our interpretations as less data may result in poorer estimates of phenotypic variability among deletion strains. Despite missing data, sd^{E3} in Oregon-R still manages to have the second largest standard deviation compared to other *scalloped* alleles in Oregon-R, consistent with previous results (Chari & Dworkin, 2013). This suggests the missing data is not interfering with our conclusions about which alleles have large modifier effects. However, when comparing standard deviations (among deletions) for sd^{E3} in Oregon-R and Samarkand, we see these values are somewhat similar in the two backgrounds compared with other *sd* alleles. Adding in the data from missing crosses may increase the standard deviation for sd^{E3} in Oregon-R and cause Oregon-R to be more variable than Samarkand. Therefore, our inferences regarding the background dependence for the interactions with sd^{E3} specifically may change. Prior to submitting this work for peer reviewed publication, failed crosses will hopefully be repeated. Similarly, sd^{+} has not been examined with all possible deletion lines. Due to time constraints caused by COVID-19, there was not enough time to dissect and analyze sd^{+} with all deletion lines. A subset of ten deletion lines was chosen to represent the phenotypic effects for the wild

type *sd* allele. While adding the remaining deletion lines may increase the phenotypic variability for sd^+, this should not impact any main conclusions drawn previously regarding how modifiers vary as function of allelic effect and genetic background. Prior to submitting this work for peer reviewed publication, missing genotypes will hopefully be dissected and analyzed.

Conclusions

To conclude, we have confirmed that moderate effect homozygotes show greater background dependence compared to homozygotes with weak and strong phenotypic effect alleles for *scalloped*, *bifid*, *beadex* and *vestigial*. We also demonstrated that the average mutant effect can have a strong influence on the magnitude and sign of epistasis. This was illustrated when examining mean epistasis estimates among all allelic pairs across gene combinations and types of epistasis. In general, as the average mutant effect increases, so does the mean epistasis. While this relationship offers some predictability for how alleles may interact, it is not consistent between gene combinations and types of epistasis. When examining the phenotypic variability for each scalloped allele among various deletion lines we saw that alleles of moderate effect result in more phenotypic variation than alleles of weak and strong phenotypic effect. Clearly demonstrating that the magnitude of modifier effects may be predicable based off the severity of the focal mutation for *scalloped*.

Our results also demonstrate that the genetic background can have a strong influence on the magnitude and sign of epistasis. When comparing mean epistasis

estimates for signed epistasis there is a clear relationship between the genetic background and the sign of epistasis. Oregon-R is more likely to be a negative value, meaning that the wings for these genotypes are more likely to be smaller than expected based off the individual mutants. While in Samarkand, epistatic interactions were more often positive, indicating that these wings are bigger than expected based off the individual mutants. When comparing mean magnitude epistasis estimates the relationship between genetic background can be more subtle. Despite this, we observed cases of strong interaction effects between the genetic background and the average mutant effect in both magnitude and signed epistasis. Indicating that the genetic background can have a strong influence on the relationship between epistasis and average mutant effect. The influence of the genetic background is further reinforced as we see a generally weak correlation between genetic backgrounds when the Pearson correlation coefficient was estimated using epistasis values for Samarkand and Oregon-R among all allelic pairs. We also observed differences between the phenotypic variability for each *scalloped* allele among all deletion lines between backgrounds as the phenotypic variability for *scalloped* alleles is lower in Samarkand than in Oregon-R. Suggesting that the magnitude of effects for modifiers are smaller in magnitude in Samarkand than in Oregon-R.

While our results shed some light on the predictability of epistatic interactions, many unknowns still exist. For example, it is important to investigate these relationships with different genes in additional developmental networks. The genes in our study are all transcription factors in the *Drosophila* wing network, and it is unclear how generalizable these results are. Furthermore, understanding how genetic interactions vary as a function

of the magnitude of allelic effects and genetic background is necessary, but there is also great importance in understanding mechanistically why this variation occurs. In particular, non-additive effects that occur between mutations involved in epistatic interactions may appear in the adult phenotype (wing size), yet aspects of the gene regulatory network (such as gene expression) or aspects governing the development of the trait (such as cell proliferation and apoptosis) may appear as additive (or potentially vice versa). Thus, understanding the relationship between modes of gene action, its molecular underpinnings (or close proxies) are crucial to improve our understanding of how genotype maps to phenotype. The study of the development of the *Drosophila* wing imaginal disc is an excellent model for investigating genetic pathways, proliferation and patterning during development (Neufeld, De La Cruz, Johnston, & Edgar, 1998). Therefore, it is suggested that interesting sets of interacting pairs observed will be further examined by looking at cellular and molecular correlates during wing disc development to determine not just their effects, but associations with the phenotypic effects in the adult wing. The purpose being to determine when or where changes during development can be detected that govern the phenotypic changes we observe in the wing. I.e. can we observe non-linear relationships between genes (that we are perturbing) and in known target gene expression? Quantitative RT-PCR can quantify transcript abundance as a proxy for gene expression for both focal genes (the ones being manipulated) and downstream targets in late third instar wing imaginal discs. Lastly, the statistical approach we employed is built upon a general linear model. This assumes that the effects of mutations will act additively, with deviations for dominance and epistasis

being second order effects. However, if the fundamental relationship is nonlinear, this can result in "apparent" epistasis reflecting the difference between the linear relationship that is assumed, and the actual non-linear relationship (Cordell, 2002; Phillips, 2008). While not investigated for data like I have generated here, it has been examined for higher-order epistasis (beyond 2 way interactions) in haploids (Sailer & Harms, 2017). Therefore, the linear model framework here for the NOIA approach used could lead to different epistatic estimates that may reflect the difference between the assumptions of linear relationships between genotype and phenotype, when the reality is most likely a non-linear relationship. While my data will be very useful to explore such relationships, there are no specific methods that have been developed to examine this in detail yet. Despite the limitations of the statistical approach used, my work represents a "classical" genetic analysis, and it is clear that this "simple" approach still has a great deal to offer and teach us about the nature of genetic interactions.

References

Abecasis, G. R., Altshuler, D., Auton, A., Brooks, L. D., Durbin, R. M., Gibbs, R. A., … McVean, G. . (2011). A map of human genome variation from population-scale sequencing. *Nature*. https://doi.org/10.1038/nature09534

Algahtani, H. A., Aldarmahi, A. A., Al-Rabia, M. W., & Yar, W. N. (2013). Finding the missing heritability of complex diseases Hindorff5,. *Neurosciences*, *18*(4), 378–381. https://doi.org/10.1038/nature08494.Finding

Alvarez-Castro, J. M., & Carlborg, O. (2007). *A Unified Model for Functional and Statistical Epistasis and Its Application in Quantitative Trait Loci Analysis ′*. *1167*(June), 1151–1167. https://doi.org/10.1534/genetics.106.067348

Anderson, K. J., Davis, M. M., & Hodgetts, R. B. (2006). Novel events associated with phenotypic reversion of a P element mutant in Drosophila melanogaster. *Genome*, *49*(9), 1184–1192. https://doi.org/10.1139/G06-065

Ashworth, A., Lord, C. J., & Reis-filho, J. S. (2011). Perspective Genetic Interactions in Cancer Progression and Treatment. *Cell*, *145*(1), 30–38. https://doi.org/10.1016/j.cell.2011.03.020

Bandura, J. L., & Edgar, B. A. (2008). Yorkie and Scalloped : partners in growth activation National Center for Biotechnology Information. *Dev Cell*, 19. https://doi.org/10.1002/dvdy.23942.

Barkoulas, M., van Zon, J. S., Milloz, J., van Oudenaarden, A., & Félix, M. A. (2013). Robustness and Epistasis in the C. elegans Vulval Signaling Network Revealed by Pathway Dosage Modulation. *Developmental Cell*, *24*(1), 64–75.

https://doi.org/10.1016/j.devcel.2012.12.001

Bates, D., Maechler, M., Bolker, B., & Walker, S. (2015). Fitting Linear Mixed-Effects Models Using lme4. *Journal of Statistical Software*, *67*(1), 1–48.

Bateson, W. (1909). Mendel's Principles of Heredity. *Cambridge Univ. Press*.

Blanco-Gómez, A., Castillo-Lluva, S., del Mar Sáez-Freire, M., Hontecillas-Prieto, L., Mao, J. H., Castellanos-Martín, A., & Pérez-Losada, J. (2016). Missing heritability of complex diseases: Enlightenment by genetic variants from intermediate phenotypes. *BioEssays*, *38*(7), 664–673. https://doi.org/10.1002/bies.201600084

Boucher, B., & Jenna, S. (2013). Genetic interaction networks: Better understand to better predict. *Frontiers in Genetics*, *4*(DEC), 1–16. https://doi.org/10.3389/fgene.2013.00290

Bouwman, P., Aly, A., Escandell, J. M., Pieterse, M., Bartkova, J., Van Der Gulden, H., … Jonkers, J. (2010). 53BP1 loss rescues BRCA1 deficiency and is associated with triple-negative and BRCA-mutated breast cancers. *Nature Structural and Molecular Biology*, *17*(6), 688–695. https://doi.org/10.1038/nsmb.1831

Bray, S. (1999). Drosophila development : Scalloped and Vestigial take wing. *Current Biology*, *9*(7), R245–R247.

Brooks, M., Kristensen, K., vsn Benthem, K. J., Magnusson, A., Berg, C., Nielsen, A., … Bolker, B. M. (2017). glmmTMB Balances Speed and Flexibility Among Packages for Zero-inflated Generalized Linear Mixed Modeling. *The R Journal*.

Caicedo, A. L., Stinchcombe, J. R., Olsen, K. M., Schmitt, J., & Purugganan, M. D. (2004). Epistatic interaction between Arabidopsis FRI and FLC flowering time

genes generates a latitudinal cline in a life history trait. *Proceedings of the National Academy of Sciences*, *101*(44), 15670–15675. https://doi.org/10.1073/PNAS.0406232101

Campbell, S. D., Duttaroy, A., Katzent, A. L., & Chovnick, A. (1991). Cloning andCharacterization of the scalloped Region of Drosophila melanogaster. *Genetics Society of America*, *380*, 367–380.

Carlborg, O., Hocking, P. M., Burt, D. W., & Haley, C. S. (2004). Simultaneous mapping of epistatic QTL in chickens reveals clusters of QTL pairs with similar genetic effects on growth National Center for Biotechnology Information. *Genetic Res.*, 19. https://doi.org/10.1101/gr.528003.PMID

Chandler, C. H., Chari, S., Kowalski, A., Choi, L., Tack, D., DeNieu, M., … Dworkin, I. (2017). How well do you know your mutation? Complex effects of genetic background on expressivity, complementation, and ordering of allelic effects. *PLoS Genetics*, *13*(11), 1–25. https://doi.org/10.1371/journal.pgen.1007075

Chandler, C. H., Chari, S., Tack, D., & Dworkin, I. (2014). Causes and Consequences of Genetic Background. *Genetics*, *196*(April), 1321–1336. https://doi.org/10.5061/dryad.1375s.

Chari, S., & Dworkin, I. (2013). The Conditional Nature of Genetic Interactions: The Consequences of Wild-Type Backgrounds on Mutational Interactions in a Genome-Wide Modifier Screen. *PLoS Genetics*, *9*(8). https://doi.org/10.1371/journal.pgen.1003661

Chen, Rong and Shi, Lisong and Hakenberg, Jörg and Naughton, Brian and Sklar, Pamela

and Zhang, Jianguo and Zhou, Hanlin and Tian, Lifeng and Prakash, Om and Lemire, Mathieu and Sleiman, Patrick and Cheng, Wei-yi and Chen, Wanting and Shah, Hardik and She, S. H. (2016). Analysis of 589,306 genomes identifies individuals resilient to severe Mendelian childhood diseases. *Nature Biotechnology*, *34*, 531.

Cheverud, J. M., & Routman, E. J. (1995). Epistasis and Its Contribution to Genetic Variance Components. *Genetic Society of America*, *139*(3), 1455–1461.

Clark, A. G., & Wang, L. (1997). Epistasis in measured genotypes: Drosophila P-element insertions. *Genetics*, *147*(1), 157–163.

Cohen, B., Mcguffin, M. E., Pfeifle, C., Segal, D., & Cohen, S. M. (1992). apterous , a gene required for imaginal disc development in Drosophila encodes a member of the LIM family of developmental regulatory proteins National Center for Biotechnology Information. *Genes Dev*, 19. https://doi.org/10.1101/gad.6.5.715

Combarros, O., Cortina-borja, M., Smith, A. D., & Lehmann, D. J. (2009). Epistasis in sporadic Alzheimer ' s disease. *Neurpbiol Aging*, *30*(9), 1333–1349.

Connahs, H., Rhen, T., & Simmons, R. B. (2016). Transcriptome analysis of the painted lady butterfly, Vanessa cardui during wing color pattern development. *BMC Genomics*, *17*(1), 1–16. https://doi.org/10.1186/s12864-016-2586-5

Cordell, H. (2002). Epistasis: what it means, what it doesn't mean, and statistical methods to detect it in humans. *Human Molecular Genetics*, *11*(20), 2463–2468.

Costanzo M, VanderSluis B, Koch EN, Baryshnikova A, Pons C, Tan G, Wang W, Usaj M, Hanchard J, Lee SD, Pelechano V, Styles EB, Billmann M, van Leeuwen J, van

Dyk N, Lin ZY, Kuzmin E, Nelson J, Piotrowski JS, Srikumar T, Bahr S, Chen Y, Deshpande R, Kurat, B. C. (2016). A global interaction network maps a wiring diagram of cellular function. *Science*, *353(6306)*.

Daley, C. (2009). *Examining The Predictability of Genetic Background Effects in The Drosophila Wing*. McMaster.

Delanoue, R., Legent, K., Godefroy, N., & Flagiello, D. (2004). The Drosophila wing differentiation factor Vestigial – Scalloped is required for cell proliferation and cell survival at the dorso-ventral boundary of the wing imaginal disc. *Cell Death & Differentiation*, 110–122. https://doi.org/10.1038/sj.cdd.4401321

Diss, G., Lehner, B., & Morgunova, E. (2018). The genetic landscape of a physical interaction. *Elife.* https://doi.org/10.7554/eLife.32472

Domingo, J., Baeza-Centurion, P., & Lehner, B. (2019). The Causes and Consequences of Genetic Interactions (Epistasis). *Annual Review of Genomics and Human Genetics*, *20*(1), 1–28. https://doi.org/10.1146/annurev-genom-083118-014857

Dowell, R. D., Ryan, O., Jansen, A., Cheung, D., Agarwala, S., Danford, T., … Boone, C. (2010). Genotype to phenotype: a complex problem - Supplementary. *Science*, *328*(5977), 469. https://doi.org/10.1126/science.1189015.Genotype

Dworkin, I., Kennerly, E., Tack, D., Hutchinson, J., Brown, J., Mahaffey, J., & Gibson, G. (2009). Genomic consequences of background effects on scalloped mutant expressivity in the wing of drosophila melamogaster. *Genetics*, *181*(3), 1065–1076. https://doi.org/10.1534/genetics.108.096453

Elena, S. F., & Lenski, R. E. (1997). Test of synergistic interactions among deleterious

mutations in bacteria. *Nature*, *390*(6658), 395–398. https://doi.org/10.1038/37108

Enerly, E., Larsson, J., & Lambertsson, A. (2002). Reverse genetics in Drosophila: from sequence to phenotype using UAS-RNAi transgenic flies. *Genesis*.

Entchev, E., Schwabedissen, A., & Gonzalez-Gaitan, M. (2000). Gradient Formation of the TGF- β Homolog Dpp. *Cell*, *103*(6), 981–992.

Félix, M., & Barkoulas, M. (2015). Pervasive robustness in biological systems. *Nat Rev Genet*, *16*(July), 483–496. Retrieved from https://doi.org/10.1038/nrg3949

Fisher, R. (1918). The correlations between relatives on the supposition of Mendelian inheritance. *Trans. Roy. Soc. Edinb*, 399–433.

Ford, E. . (1907). The Theory of Dominance. *Press, Chicago Society, The American*, *41*(492), 781–784.

Forsberg, S. K. G., Bloom, J. S., Sadhu, M. J., Kruglyak, L., & Carlborg, Ö. (2017). Accounting for genetic interactions improves modeling of individual quantitative trait phenotypes in yeast quantitative traits. *Nature Genetics*, 3–5. https://doi.org/10.1038/ng.3800

Frank, T. D., Cavadas, M. A. S, Nguyen, L. K. & Cheong, A. (2016). Non-linear dynamics in transcriptional regulation: Biological logic gates. *Nonlinear Dynamics in Biological Systems*, *7*, 43–62. Retrieved from https://doi.org/10.1007/978-3-319-33054-9_3

Frankel, W. N., & Schork, N. J. (1996). Who ’ s afraid of epistasis ? *Nature*, *14*(december), 371–373.

Gaertner, B. E., Parmenter, M. D., Rockman, M. V., Kruglyak, L., & Phillips, P. C.

(2012). More than the sum of its parts: A complex epistatic network underlies natural variation in thermal preference behavior in Caenorhabditis elegans. *Genetics*, *192*(4), 1533–1542. https://doi.org/10.1534/genetics.112.142877

Gerke, J., Lorenz, K., Ramnarine, S., & Cohen, B. (2010). Gene – Environment Interactions at Nucleotide Resolution. *PLoS Genetics*, *6*(9). https://doi.org/10.1371/journal.pgen.1001144

Gilchrist, A. S., & Partridge, L. (2001). The contrasting genetic architecture of wing size and shape in Drosophila melanogaster. *Heredity*, *86*(2), 144–152. https://doi.org/10.1046/j.1365-2540.2001.00779.x

Gjuvsland, A. B., Hayes, B. J., Omholt, S. W., & Carlborg, Ö. (2007). Statistical Epistasis Is a Generic Feature of Gene Regulatory Networks. *Genetics*, *175*(1), 411–420.

Gjuvsland, A. B., Plahte, E., & Omholt, S. W. (2007). Threshold-dominated regulation hides genetic variation in gene expression networks. *Bmc, Syst*, *1*(57). https://doi.org/10.1186/1752-0509-1-57

Gonze, D., & Abou-Jaoudé, W. (2013). The Goodwin Model: Behind the Hill Function. *PLoS ONE*, *8*(8). https://doi.org/10.1371/journal.pone.0069573

Goulev, Y., Fauny, J. D., Gonzalez-marti, B., Flagiello, D., & Silber, J. (2008). SCALLOPED interacts with YORKIE , the nuclear effector of the hippo tumor-suppressor pathway in Drosophila National Center for Biotechnology Information. *Current Biology*, 19. https://doi.org/10.4161/cc.22486.

Green, R. M., Fish, J. L., Young, N. M., Smith, F. J., Roberts, B., Dolan, K., … Hallgrímsson, B. (2017). Developmental nonlinearity drives phenotypic robustness.

Nature Communications, *8*(1). https://doi.org/10.1038/s41467-017-02037-7

Grimm, S., & Pflugfelder, G. (1996). Control of the Gene optomotor-blind in Drosophila Wing Development by decapentaplegic and wingless. *Science*, (March). https://doi.org/10.1126/science.271.5255.1601

Guss, K., Benson, M., Gubitosi, N., Brondell, K., Broadie, K., & Skeath, J. (2014). Expression and Function of Scalloped During Drosophila Development. *Dev Dyn*, *242*(7), 1–19. https://doi.org/10.1002/dvdy.23942.Expression

Handsaker, R. E., Korn, J. M., Nemesh, J., & Mccarroll, S. A. (2011). Discovery and genotyping of genome structural polymorphism by sequencing on a population scale. *Nature Genetics*, *43*(3). https://doi.org/10.1038/ng.768

Hartman, J. L., Garvik, B., & Hartwell, L. (2016). *Principles for the Buffering of Genetic Variation*. *291*(March 2001), 1001–1004. https://doi.org/10.1126/science.1056072

Hodgetts, R. B., & Keefe, S. L. O. (2001). The Mutant Phenotype Associated With P -Element Alleles of the vestigial Locus in Drosophila melanogaster May Be Caused by a Readthrough Transcript Initiated at the P -Element Promoter. *Genetics*, *4*(157), 1665–1672.

Inamdar, M., Vijayraghavan, K., & Veronica, R. (2009). The Drosophila Homolog of the Human Transcription Factor TEF-1, Scalloped, is Essential for Normal Taste Behavior. *Journal of Neurogenetics*, *9*(2), 123–139. https://doi.org/10.3109/01677069309083454

Jarvis, J. P., & Cheverud, J. M. (2011). Mapping the epistatic network underlying murine reproductive fatpad variation. *Genetics*, *187*(2), 597–610.

https://doi.org/10.1534/genetics.110.123505

Johnston, D. S. (2002). THE ART AND DESIGN OF GENETIC SCREENS : DROSOPHILA MELANOGASTER. *Nature Reviews Genetics*, *3*(March), 176–188. https://doi.org/10.1038/nrg751

Jorgensen, E. M., & Mango, S. E. (2002). The art and design of genetic screens: Caenorhabditis elegans. *Nature Reviews Genetics*, *3*(5), 356–369. https://doi.org/10.1038/nrg794

Kacser, H., & Burns, J. A. (1981). The molecular basis of dominance. *Genetics*, *97*(3–4), 639–666.

Kraft, P., Yen, Y., Stram, D., Morrison, J., & Gauderman, W. (2007). Exploiting gene-environment interaction to detect genetic associations. *Hum Hered*, *63*(2), 111–119. https://doi.org/10.1159/000099183

Le Rouzic, A., Gjuvsland, A., & Ariste, O. (2015). *noia: Implementation of the Natural and Orthogonal InterAction (NOIA) model.* Retrieved from https://cran.r-project.org/package=noia

Lecuit, T., Brook, W., Ng, M., Calleja, M., Sun, H., & Cohen, S. (1996). Two distinct mechanisms for long-range patterning by Decapentaplegic in the Drosophila wing. *Nature*, (381), 387–393. Retrieved from https://doi.org/10.1038/381387a0

Li, X., Lalic, J., Baeza-centurion, P., Dhar, R., & Lehner, B. (2019). Changes in gene expression predictably shift and switch genetic interactions. *Nature Communications*. https://doi.org/10.1038/s41467-019-11735-3

Li, Y., Cho, H., Wang, F., Canela-Xandra, O., & Luo, C. (n.d.). *Statistical and Functional*

Studies Identify Epistasis of Cardiovascular Risk Genomic Variants From Genome - Wide Association Studies. *3807865*, 17465637.

Lunde, K., Trimble, J. L., Guichard, A., Guss, K. A., Nauber, U., & Bier, E. (2003). Activation of the knirps locus links patterning to morphogenesis of the second wing vein in Drosophila. *Dev*, 235–248. https://doi.org/10.1242/dev.00207

Macarthur, D. G., Balasubramanian, S., Frankish, A., Huang, N., Morris, J., Walter, K., & Luke, J. (2012). A Systematic Survey of Loss-of-Function Variants in Human Protein-Coding Genes More options Gene Losses in the Human Genome Read the Latest Issue of Science. *Science*, 9203. https://doi.org/10.1126/science.1215040

Mafhukar, N., Elemento, O., & Pandey, G. (2015). Prediction of genetic interactions using machine learning and network properties. *Frontiers in Bioengineering and Biotechnology*, *3*(October), 1–12. https://doi.org/10.3389/fbioe.2015.00172

Melamed, D., Young, D. L., Gamble, C. E., Miller, C. R., & Fields, S. (2013). Deep mutational scanning of an RRM domain of the Saccharomyces cerevisiae poly (A) - binding protein. *RNA*, *1*, 1537–1551. https://doi.org/10.1261/rna.040709.113.

Milan, M., Diaz-benjumea, F. J., & Cohen, S. M. (1998). Beadex encodes an LMO protein that regulates Apterous LIM – homeodomain activity in Drosophila wing development : a model for LMO oncogene function. *Genes Dev*, (Dv), 2912–2920.

Mitra, I., Yeh, E., & Tsang, K. (2017). Reverse Pathway Genetic Approach Identifies Epistasis in Autism Spectrum Disorders National Center for Biotechnology Information. *PLoS Genetics*, 19. https://doi.org/10.3390/genes11030239.PMID

Monnahan, P. J., & Kelly, J. K. (2015). Epistasis Is a Major Determinant of the Additive

Genetic Variance in Mimulus guttatus. *PLoS Genetics*, *11*(5), 1–21. https://doi.org/10.1371/journal.pgen.1005201

Moore, J. (2003). The ubiquitous nature of epistasis in determining susceptibility to common human diseases. *Hum Hered*, *1*(3), 73–82. https://doi.org/10.1159/000073735.

Morcillo, P., Rosen, C., Baylies, M. K., & Dorsett, D. (1997). Chip , a widely expressed chromosomal protein required for segmentation and activity of a remote wing margin enhancer in Drosophila. *Genes Dev*, 2729–2740.

Moscona, A. (2009). Global Transmission of Oseltamivir-Global Transmission of Oseltamivir-Resistant Influenza. *N Engl J Med*, (360), 953–956. https://doi.org/10.1056/NEJMp0900648

Musso, G., Costanzo, M., Huangfu, M., Smith, A. M., Paw, J., Luis, B. S., … Zhang, Z. (2008). The extensive and condition-dependent nature of epistasis among whole-genome duplicates in yeast. *Genome Res.*, 1092–1099. https://doi.org/10.1101/gr.076174.108.1

Nellen, D., Burke, R., Struhl, G., & Basler, K. (1996). *Direct and Long-Range Action of a DPP Morphogen Gradient*. *85*, 357–368.

Neufeld, T. P., De La Cruz, A. F. A., Johnston, L. A., & Edgar, B. A. (1998). Coordination of growth and cell division in the Drosophila wing. *Cell*, *93*(7), 1183–1193. https://doi.org/10.1016/S0092-8674(00)81462-2

Nica, A. C., Parts, L., Glass, D., Nisbet, J., Barrett, A., Sekowska, M., … Mark, I. (2011). The Architecture of Gene Regulatory Variation across Multiple Human Tissues :

The MuTHER Study. *PLoS Genetics*, *7*(2), 1–9. https://doi.org/10.1371/journal.pgen.1002003

Nijman, S. M. B., & Friend, S. H. (2013). Potential of the Synthetic Lethality Principle. *Science*, *342*(6161), 809–811. https://doi.org/10.1126/science.1244669

Ortlund, E., Bridgham, J., Redinbo, M., & Thornton, J. (2007). Crystal structure of an ancient protein. *Science*, *sep 14*(317), 20894. https://doi.org/10.1126/science.1142819

Parks, A. L., Cook, K. R., Belvin, M., Dompe, N. A., Fawcett, R., Huppert, K., … Francis-lang, H. L. (2004). Systematic generation of high-resolution deletion coverage of the Drosophila melanogaster genome. *Nature Genetics*, *36*(3), 288–292. https://doi.org/10.1038/ng1312

Paumard-Rigal, S., Zider, A., Vaudin, P., & Silber, J. (1998). Specific interactions between vestigial and scalloped are required to promote wing tissue proliferation in Drosophila melanogaster. *Development Genes and Evolution*, *208*(8), 440–446. https://doi.org/10.1007/s004270050201

Phillips, P. C. (1998). The language of gene interaction. *Genetics*, *149*(3), 1167–1171.

Phillips, P. C. (2007). Epistasis—the essential role of gene interactions in the structure and evolution of genetic systems. *Nat Rev Genet*, *78*(1), 855–867. https://doi.org/10.1038/nrg2452.Epistasis

Phillips, P. C. (2008). Epistasis - The essential role of gene interactions in the structure and evolution of genetic systems. *Nature Reviews Genetics*, *9*(11), 855–867. https://doi.org/10.1038/nrg2452

Rabinow, L., Chian, S. L., & Birchler, J. A. (1993). Mutations at the Darkener. *Genetics Society of America*, *185*, 1175–1185.

Remold, S. K., & Lenski, R. E. (2004a). Pervasive joint influence of epistasis and plasticity on mutational effects in Escherichia coli. *Nature Genetics*, *36*(4), 423–426. https://doi.org/10.1038/ng1324

Remold, S. K., & Lenski, R. E. (2004b). Pervasive joint influence of epistasis and plasticity on mutational effects in Escherichia coli. *Nature Genetics*, *36*(4), 423–426. https://doi.org/10.1038/ng1324

Resino, J., Salama-cohen, P., & Garcı, A. (2002). Determining the role of patterned cell proliferation in the shape and size of the Drosophila wing. *Developmental Biology*, *99*(11), 7502–7507.

Robinson, M., Wray, N., & Visscher, P. (2015). Explaining additional genetic variation in complex traits. *Trends in Genetics*, *30*(4), 124–132. https://doi.org/10.1016/j.tig.2014.02.003.Explaining

Roch, F., Baonza, A., Martin-Blanco, E., & Garcia-Bellido, A. (1998). Genetic interactions and cell behaviour in blistered mutants during proliferation and differentiation of the Drosophila wing. *Development (Cambridge, England)*, *125*(10), 1823–1832.

Rogriguz, Felix, & Diaz-Benjumea. (2001). The role of the T-box gene optomotor-blind in patterning the Drosophila wing. *Developmental Biology*, *268*(2), 481–492. https://doi.org/10.1016/j.ydbio.2004.01.005

Rutledge, B. J., Mortin, M. A., Schwarz, E., Thierry-Mieg, D., & Meselson, M. (1988).

Genetic interactions of modifier genes and modifiable alleles in Drosophila melanogaster. *Genetics*, *119*(2), 391–397.

Sailer, Z. R., & Harms, M. J. (2017). *Detecting High-Order Epistasis in Nonlinear Genotype-Phenotype Maps*. *205*(March), 1079–1088. https://doi.org/10.1534/genetics.116.195214

Segrè, D., DeLuna, A., Church, G. M., & Kishony, R. (2005). Modular epistasis in yeast metabolism. *Nature Genetics*, *37*(1), 77–83. https://doi.org/10.1038/ng1489

Shen, J., Dorner, C., Bahlo, A., & Pflugfelder, G. O. (2005). optomotor-blind suppresses instability at the A / P compartment boundary of the Drosophila wing. *Mechanisms of Development*.

Shoresh, M., Orgad, S., Shmueli, O., Werczberger, R., Gelbaum, D., Abiri, S., & Segal, D. (1998). Overexpression Beadex Mutations and Loss-of- Function heldup-a Mutations in Drosophila Affect the 3 ′ Regulatory and Coding Components , Respectively , of the Dlmo Gene. *Genetics*, *150*(Figure 7), 283–299.

Shyamala, B. V, & Chopra, A. (1999). Drosophila melanogaster chemosensory and muscle development: Identification and properties of a novel allele ofscalloped and of a new locus, SG18.1, in a Gal4 enhancer trap screen. *Journal of Genetics*, *78*(87). https://doi.org/10.1007/BF02924560

Silber, J., Menn, A., Chevillard, S., Zider, A., & Paumard, S. (1993). No The vestigial locus of Drosophila melanogaster is involved in resistance to inhibitors of dTMP synthesis. *Molecular and General Genetic Mgg*.

Simmonds, A. J., Liu, X., Soanes, K. H., Krause, H. M., Irvine, K. D., & Bell, J. B.

(1998). *Molecular interactions between Vestigial and Scalloped promote wing formation in Drosophila*. (403), 3815–3820.

Sorrosal, G., Bejarano, F., & Luque, C. M. (2008). A Gain-of-Function Suppressor Screen for Genes Involved in Dorsal–Ventral Boundary Formation in the Drosophila Wing ′. *Genetics Society of America*, *323*(January), 307–323. https://doi.org/10.1534/genetics.107.081869

Sturtevant, M. A., Roark, M., & Bier, E. (1993). The Drosophila rhomboid gene mediates the localized formation of wing veins and interacts genetically with components of the EGF-R signaling pathway. *Genes and Development*, *7*(6), 961–973. https://doi.org/10.1101/gad.7.6.961

Stylianou, I. M., Korstanje, R., Li, R., Sheehan, S., Paigen, B., & Churchill, G. A. (2006). Quantitative trait locus analysis for obesity reveals multiple networks of interacting loci National Center for Biotechnology Information. *Mamm Genome*, 19. https://doi.org/10.1038/nrg3627.

Tabata, T. (2001). GENETICS OF MORPHOGEN GRADIENTS. *Nature Reviews Genetics*, *2*(August), 620–630.

Timpson, N. J., Greenwood, C. M. T., Soranzo, N., & Lawson, D. J. (2017). Genetic architecture : the shape of the genetic contribution to human traits and disease. *Nature Publishing Group*, *19*(2), 110–124. https://doi.org/10.1038/nrg.2017.101

Toivonen, J. M., Walker, G. A., Martinez-diaz, P., Bjedov, I., Driege, Y., Jacobs, H. T., … Partridge, L. (2007). No Influence of Indy on Lifespan in Drosophila after Correction for Genetic and Cytoplasmic Background Effects. *PLoS Genetics*, *3*(6).

https://doi.org/10.1371/journal.pgen.0030095

Tokuriki, N., & Tawfik, D. S. (2009). Stability effects of mutations and protein evolvability Slow Folding of a Helical Protein : Large Barriers , Strong Internal Friction , or a Shallow , National Center for Biotechnology Information. *Current Opinion in Genetics and Development*, 19. https://doi.org/10.1002/pro.3966.

Trudy F. C. Mackay. (2014). Epistasis and Quantitative Traits: Using Model Organisms to Study Gene-Gene Interactions. *Nat Rev Genet.*, *15*(1), 22–33. https://doi.org/10.1038/nrg3627.Epistasis

Tsai, L. T., Bainton, R. J., Blau, J., & Heberlein, U. (2004). Lmo Mutants Reveal a Novel Role for Circadian Pacemaker Neurons in Cocaine-Induced Behaviors. *PLoS Biol*, *2*(12). https://doi.org/10.1371/journal.pbio.0020408

Uppu, S., Krishna, A., & Gopalan, R. (2018). A Review on Methods for Detecting SNP Interactions in High-Dimensional Genomic Data. *IEE/ACm*.

Verheyen, E. M., Purcell, K. J., Fortini, M. E., & Artavanis-Tsakonas, S. (1996). Analysis of dominant enhancers and suppressors of activated Notch in Drosophila. *Genetics*, *144*(3), 1127–1141.

Vieira, A. R. (2008). Unraveling human cleft lip and palate research National Center for Biotechnology Information. *Journal of Dental Research*, 19. https://doi.org/10.1002/mgg3.714.

Wagner, G. (2015). Two Rules for the Detection and Quantification of Epistasis and Other Interaction Effects. In *Epistasis: Methods and Protocols* (pp. 145–157).

Wang, X., Fu, A. Q., Mcnerney, M. E., & White, K. P. (2014). Widespread genetic

epistasis among cancer genes. *Nature Communications*, 1–10. https://doi.org/10.1038/ncomms5828

Wang, Y., Díaz Arenas, C., Stoebel, D. M., & Cooper, T. F. (2013). Genetic background affects epistatic interactions between two beneficial mutations. *Biology Letters*, *9*(1). https://doi.org/10.1098/rsbl.2012.0328

Weihe, U., Milán, M., & Cohen, S. M. (2001). Regulation of Apterous activity in Drosophila wing development. *Development*, *4622*, 4615–4622.

Weinreich, D., Watson, R., & Chao, L. (2005). PERSPECTIVE: SIGN EPISTASIS AND GENETIC COSTRAINT ON EVOLUTIONARY TRAJECTORIES. *Evolution*, *59*(6), 1165–1174.

Williams, J., Bell, J., & Carroll, S. (1991). Drosophilawing, Control of Product, and haltere developmentby the nuclear vestigial gene. *Genes Dev*. https://doi.org/10.1101/gad.5.12b.2481

Wiltshire, S., Bell, J. T., Groves, C. J., Dina, C., Hattersley, A. T., Frayling, T. M., … Mccarthy, M. I. (2006). Epistasis between type 2 diabetes susceptibility Loci on chromosomes 1q21-25 and 10q23-26 in northern Europeans National Center for Biotechnology Information. *Ann Hum Genet*, 19. https://doi.org/10.1086/323249.

Wright, S. (1934). Physiological and Evolutionary Theories of Dominance. *Society, The American Press, Chicago*, *68*(714), 24–53.

Xu, G., Chapman, J. R., Brandsma, I., Yuan, J., Mistrik, M., Bartkova, J., … Nieuwland, M. (2015). *Europe PMC Funders Group REV7 counteracts DNA double-strand break resection and impacts PARP inhibition* (Vol. 521).

https://doi.org/10.1038/nature14328.REV7

Yamamoto, A., Zwarts, L., Callaerts, P., Norga, K., Mackay, T. F. C., & Anholt, R. R. H. (2007). Neurogenetic networks for startle-induced locomotion in Drosophila melanogaster. *PNAS*, *105*(34), 12393–12398.

You, L., & Yin, J. (2002). Dependence of Epistasis on Environment and Mutation Severity as Revealed by in Silico Mutagenesis of Phage T7. *Genetics Society of America*, *1281*(April), 1273–1281.

Zecca, M., Basler, K., & Struhl, G. (1996). *Direct and Long-Range Action of a Wingless Morphogen Gradient*. *87*, 833–844.

Zeng, Z., Wang, T., & Zou, W. (2005). Modeling Quantitative Trait Loci and Interpretation of Models. *Genetics Society of America*, *1725*(March), 1711–1725. https://doi.org/10.1534/genetics.104.035857

Zuk, O., Hechter, E., Sunyaev, S. R., & Lander, E. S. (2012). The mystery of missing heritability: Genetic interactions create phantom heritability. *Proceedings of the National Academy of Sciences*, *109*(4), 1193–1198. https://doi.org/10.1073/PNAS.1119675109